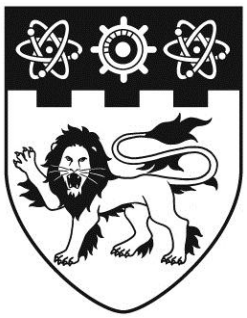

NANYANG TECHNOLOGICAL UNIVERSITY

TRANSPARENT EXOPOLYMER PARTICLES (TEP) FORMATION FROM ALGINATE BLOCKS AND THEIR EFFECTS ON MEMBRANE FOULING

MENG SHUJUAN

SCHOOL OF CIVIL AND ENVIRONMENTAL ENGINEERING

2016

TRANSPARENT EXOPOLYMER PARTICLES (TEP) FORMATION FROM ALGINATE BLOCKS AND THEIR EFFECTS ON MEMBRANE FOULING

MENG SHUJUAN

School of Civil and Environmental Engineering

A thesis submitted to the Nanyang Technological University

in partial fulfilment of the requirements for the degree of

Doctor of Philosophy

2016

ACKNOWLEDGEMENTS

I would like to express the most sincere gratitude to my supervisor, Professor Liu Yu. The research could not be carried out without his prudent supervision and insightful guidance. When I was confused, he always provided valuable advice and clarified the research direction for me. When I was depressed, he always shared his experience with me and encouraged me to move on. I was always highly motivated each time after meeting with him. He also granted me the permission to pursue my curiosity in the established direction of the research group. Besides, he was always available to discuss with me and provide me instructive suggestions, even over the weekends. His teachings about conducting novel and deep research inspired me to think differently and deeply. I will always be very thankful to him for being a great advisor both in research and in my life. I cordially thank for his encouragement, support and supervision throughout my graduate study.

I also express my sincere appreciation to my co-supervisor Professor Harvey Winters, for his support.

I greatly express my thanks to Dr. Miles Edward Rzechowicz, Dr. Xu Huijuan, and Dr. Ashutosh Agarwal for their kind help during my PhD study. Thanks a lot to my good friends, Ms. Cai Weiwei, Ms. Yang Qin, Mr. Gu Jun, Mr. Wu Weiyi and some other classmates for their care and love. It was a great pleasure to share my studies and life with wonderful people like them.

I also express my appreciation to those technicians in the environmental laboratory, especially Mr. Tan Han Khiang. Without their professional assistance and kindly help, my work in the lab would be impossible.

I also appreciate the School of Civil and Environmental Engineering, Nanyang Technological University to award me the research scholarship, which could enable me to focus myself on my study and research.

I also appreciate the Visiting Professor Program funded by the Environment and

Water Industry Programme Office of Singapore.

Last but not least, my special appreciation and thanks would go to my family. Thank my parents for their everlasting love, care and understanding when I stay far away from home. Thank to my husband, Mr. Wei Zhongbao for his love, continuous understanding, trust, accompany and encouragement during this exciting period time of my life.

TABLE OF CONTENTS

ABSTRACT

Transparent exopolymer particles (TEP) are known as a class of transparent particulate acidic polysaccharides that can be stained by alcian blue. Although the involvement of TEP in membrane fouling development has been reported, the formation mechanisms of TEP in various water chemistry conditions have not yet been understood. Therefore, this study aimed to investigate the TEP formation from alginate blocks under different chemistry conditions and the specific role of TEP in membrane fouling development.

In the first phase of study, alginate blocks and their effect on membrane fouling was investigated. Alginate as a common and widespread polysaccharide has been reported to generate TEP-like particles that can be stained by alcian blue. Alginate is composed of two different monomers, namely M ((1→4) linked β-D-mannopyranuronic acid) and G ((1→4) linked α-L-gulopyranuronic acid) which are randomly arranged into MG-, MM- and GG-blocks. Results showed the severest fouling in the filtration of MG-block, and the least flux decline in the filtration of MM-block. The initial pore blocking was found to be responsible for the fouling observed in MG-block filtration, while the cake layer formed on membrane surface during the MM-block filtration could serve as a pre-filter that prevented membrane from further pore blocking. TEP were found to form through aggregation or cross-link of alginate blocks. It was observed that more TEP were produced from MM-blocks than from MG-blocks in solutions. As TEP were bigger than original alginate blocks, they could facilitate the formation of cake layer on membrane surface, which explained why cake resistance was dominant in the filtration of MM-blocks as compared to MG-blocks. The analysis by the extended Derjaguin-Landau-Verwey-Overbeek (XDLVO) theory further revealed that MM-blocks had lowest cohesive interaction energy among all three alginate blocks, which favoured aggregation of MM-blocks, and ultimately leading to the formation of more TEP. This study provided insights into the TEP formation from different alginate blocks and revealed the role of TEP in microfiltration.

The importance of calcium ion in TEP formation has been reported before. In this phase of study, the TEP formation from alginate blocks was investigated with various calcium concentrations and the effect of TEP on membrane fouling development was further studied. Results showed that calcium ion had the most serious effects on GG-blocks and significantly promotes the formation of TEP from GG-blocks which in turn led to rapid formation of thick cake layer on membrane surface during the filtration of GG-blocks. In addition, results further revealed that the TEP formation from GG-blocks was subject to the Ca^{2+} concentration of bulk solution. As for MM-blocks, it was found that the formation of TEP was proportional to the Ca^{2+} concentration in MM-blocks solution studied, while the membrane fouling was enhanced by Ca^{2+} in the filtration of MM-blocks solution. Unlike MM- and GG-blocks, MG-blocks were nearly not affected by addition of calcium ion, as the result, there was no significant increase in TEP. The initial fouling rates and the mass of foulants deposed on the membrane surfaces further revealed a close correlation between the TEP concentration and the membrane fouling propensity. Tracking the cake layer development process on membrane surface with FE-SEM and AFM techniques indicated that TEP accumulation directly led to the cake layer formation. This study offers deep insights into the development of membrane fouling by different alginate blocks in the presence of calcium ion, and suggests that TEP formed from alginate blocks played a very significant role in the fouling development.

TEP formation at various sodium ion concentrations with a fixed calcium ion concentration was investigated in this phase study. Results showed that increasing sodium ion concentration largely reduces the TEP production in all three types of alginate blocks, which further prevented the cake layer development on the membrane surface. Competition between calcium ions and sodium ions is likely responsible for the reduction of TEP formation from alginate blocks. At high sodium ion concentration, the bonding opportunity of alginate blocks to calcium ions is out-competed by sodium ions, thus decreasing the formation of TEP. These results suggest that a more abundant TEP could be expected in freshwater than in seawater at the same level of precursor materials. Thus, TEP-associated biofilm

development and membrane fouling would be more significant in membrane filtration of freshwater than seawater.

In conclusion, this study clearly showed the formation of TEP from alginate blocks at diverse chemistry conditions as well as the role of TEP in membrane fouling development, providing insights into the TEP-associated fouling problems.

LIST OF TABLES

LIST OF FIGURES

LIST OF ABBREVIATIONS

ΔP	transmembrane pressure
μ	solution viscosity
A_{eff}	effective membrane surface area
AFM	atomic force microscope
d_0	contact distance between two solid
DOM	dissolved organic matter
e	electron charge
EfOM	effluent organic matter
EPS	extracellular polymeric substance
FE-SEM	field emission scanning electron microscope
G	(1→4) linked α-L-gulopyranuronic acid
GG	homopolymeric alginate blocks composed of α-l-guluronic acids
G^{AB}	Lewis Acid-Base interaction component of surface free energy
G^{EL}	electrostatic double layer component of surface free energy
G^{LW}	Lifshitz-van der Waals component of surface free energy
G^{XDLVO}	total interaction free energy between two solid surfaces
J	permeate flux
k	Boltzmann's constant
K_a	blocked membrane surface per unit of the total volume permeated through the membrane
K_c	area of the cake per unit of permeate volume
K_s	Hermia's parameter, the decrease in the cross-section area of the pores per unit of permeate volume

LC-OCD	liquid chromatography-organic carbon detection
M	(1→4) linked β-D-mannopyranuronic acid
MF	microfiltration
MG	heteropolymeric alginate blocks composed of β-d-mannuronic acids and α-l-guluronic acids
MM	homopolymeric alginate blocks composed of β-d-mannuronic acids
MWCO	molecular weight cut off
n	so-called blocking index (0, 1, 1.5 or 2)
N_A	Avogadro constant
NOM	natural organic matter
PES	polyethersulfone
R^2	square of correlation coefficient
R_c	cake layer resistance
R_f	internal resistance
R_m	intrinsic membrane resistance
R_p	pore blocking resistance
R_r	the ratio of the cake resistance to the clean membrane resistance
R_t	total filtration resistance
RO	reverse osmosis
SDI	silt density index
T	absolute temperature
$t_{1/2}$	the filtration time when permeate flux is reduced to half of the initial flux
TEP	transparent exopolymer particles
TOC	total organic carbon

UF	ultrafiltration
XDLVO	extended Derjaguin-Landau-Verwey-Overbeek
γ^-	electron donor parameter
γ^+	electron acceptor parameter
γ^{AB}	Lewis Acid-Base interaction component of surface tension
γ^{LW}	Lifshitz-van der Waals component of surface tension
γ^{TOT}	the total surface tension
ε_0	absolute dielectric constant
ε_r	permittivity of the liquid
ζ	surface potential of solid
θ	contact angle
κ	inverse Debye screening length

LIST OF PUBLICATIONS

Journal Papers:

1. Meng, S., Rzechowicz, M., Winters, H., Fane, A. and Liu, Y. (2013) Transparent exopolymer particles (TEP) and their potential effect on membrane biofouling. **Applied Microbiology and Biotechnology** 97(13), 5705-5710.

2. Meng, S. and Liu, Y. (2013) Alginate block fractions and their effects on membrane fouling. **Water Research** 47(17), 6618-6627.

3. Meng, S., Winters, H., & Liu, Y. (2015). Ultrafiltration behaviors of alginate blocks at various calcium concentrations. **Water Research**, 83, 248-257.

4. Meng, S. and Liu, Y. (2016). New insights into transparent exopolymer particles (TEP) formation from precursor materials at various Na^{+}/Ca^{2+} ratios. **Scientific Reports** 6, 19747.

5. Meng, S. and Liu, Y. Transparent exopolymer particles (TEP)-associated membrane fouling at various Na^{+} concentrations. Submitted to **Environmental Science & Technology** (under review).

Conference Paper:

1. Meng, S., Yang, Q. and Liu, Y. Fouling Propensities of Alginate Blocks Derived from Seaweeds in the Membrane Filtration. 2015 International Congress on Chemical, Biological and Environmental Sciences **(ICCBES)**. Osaka, Japan. May, 2015.

CHAPTER 1 INTRODUCTION

1.1 BACKGROUND

Water scarcity is one of the most serious global crises. To cope with such situation, scientists and engineers have been developing many water and wastewater reclamation technologies, one of which is membrane technology. In fact, membrane technology has been widely employed for more than 30 years for its advantage, e.g. of less complexity, easier to operate, less man power needed, smaller footprints and less chemical usage (Daigger et al. 2006). However, a major obstacle to the wider applications of membrane technology is membrane fouling which leads to reduced membrane performance and permeate flux (Shannon et al. 2008).

Transparent exopolymer particles (TEP) are considered as a potential foulant towards membrane fouling development (Berman and Holenberg 2005, Bar-Zeev et al. 2012). TEP represents a class of particulate acidic polysaccharides which are large, transparent organic particles and can be stained by alcian blue, and they have been commonly found in surface water, seawater and wastewater (Alldredge et al. 1993). These gel-like particles are deformable, highly sticky and appear in various forms, e.g. amorphous blobs, strings, films, sheets, clouds, or clumps. As surface active acidic polysaccharides, TEP can attach onto or be easily adsorbed onto other solid surfaces including membranes. Besides, TEP can also serve as “carriers” of microbial attachment in seawater and freshwater, i.e. they are often colonized by bacteria (Passow 2002). As such, bacteria colonized TEP may be brought to membrane surface through the deposition of TEP. This in turn suggests a possible mechanism of membrane biofouling may be initiated. However, it should be pointed out that little information is available so far about the formation mechanisms of TEP in various water environments. Obviously, such information is essential for better elucidate TEP-associated membrane fouling.

In natural water environment, TEP may be generated from different precursors, among which alginate has similar characteristics to TEP in terms of richness in

acidic polysaccharides and gelling ability (Passow and Alldredge 1995, Thornton et al. 2007). Due to such reason, alginate has commonly used a model organic foulant in many studies of membrane fouling. In fact, alginates are unbranched binary copolymers consisting of (1→4) linked β-D-mannopyranuronic acid (M) and (1→4) linked α-L-gulopyranuronic acid (G) monomers, which are randomly arranged along the alginate chain in two kinds of homopolymeric blocks (MM-blocks, GG-blocks) and one kind of heteropolymeric block (MG-blocks) (Smidsrød 1974, Draget et al. 2005, Lee and Mooney 2012). Therefore, this study investigated the formation of TEP from different alginate blocks as precursors under various water conditions and their effect on membrane fouling development.

1.2 OBJECTIVES AND SCOPE

The main objectives of this study are:

(1) To examine the fouling propensities of alginate blocks i.e. MG-, MM- and GG-blocks; further to explore the fouling mechanisms behind them. The TEP formation from MG-, MM- and GG-blocks and their effects on membrane fouling as well as the cohesive interaction energy of MG-, MM- and GG-blocks were also studied.

(2) To study the influence of calcium ion on the formation of TEP from MG-, MM- and GG-blocks, and to explore the crosslink mechanism between calcium and each type of alginate blocks, further to look into the filtration behaviors of MG-, MM- and GG-blocks at different calcium concentrations. The process of cake layer development on membrane surface was tracked and the role of TEP in the fouling development was studied.

(3) To investigate the TEP formation at various sodium ion concentrations with a fixed calcium ion concentration. The quantity, morphology and viscoelasticity properties of TEP were determined. The effects of sodium ion on the fouling propensities of MG-, MM- and GG-blocks and the effect of TEP formation on membrane fouling were also studied.

1.3 ORGANIZATION OF THE THESIS

The thesis includes the following six chapters:

(1) Chapter 1 is a brief introduction to the background and objectives of this study.

(2) Chapter 2 presents a comprehensive literature review, covering (i) the applications of membrane technology in water and wastewater treatment; (ii) the definition, formation pathways, determination methods and characteristics of TEP; (iii) the general properties of alginate.

(3) Chapter 3 demonstrates the effect of alginate blocks on membrane fouling. Fractionation of alginate was performed to obtain MG-, MM- and GG-blocks and subsequently their filtration behaviors were examined. The effect of TEP on membrane fouling was revealed with fouling mechanism analysis and XDLVO theory further explained the difference lying in TEP formation abilities of alginate blocks. This study suggests that the membrane fouling would be related to molecular structure of alginate.

(4) Chapter 4 focuses on the effect of calcium ions on the alginate blocks, including their TEP formation and filtration behaviors. For this purpose, TEP formation from MG-, MM- and GG-blocks were determined in different calcium ion levels. The role of TEP in membrane fouling was analyzed by calculating the initial fouling rate and foulant mass deposition on membrane. TEP accumulation on membrane surface was visualized directly by employing FE-SEM and AFM techniques.

(5) Chapter 5 investigated the TEP formation at various sodium ion concentrations. It was found that increasing sodium ion reduced the TEP production in all three types of alginate blocks, which further prevented the cake layer development on the membrane surface. Competition between calcium ions and sodium ions was likely responsible for the reduction of TEP formation from alginate blocks. These results suggest that a more abundant TEP could be expected in freshwater

than in seawater at the same level of precursor materials. Thus, TEP-associated biofilm development and membrane fouling would be more significant in membrane filtration of freshwater than seawater.

(6) Chapter 6 summarizes the major findings of this study and recommendations for future investigation.

CHAPTER 2 LITERATURE REVIEW

2.1 INTRODUCTION

Nowadays, water scarcity is one of the most serious challenges around the world (Elimelech and Phillip 2011). To alleviate the stresses on water supply, membrane separation technology is considered as a promising method. However, membrane fouling still remains as a major obstacle to the broad applications of membrane filtration utilizing pressure-driven membrane technologies, especially when it leads to flux losses that cleaning cannot restore (Shannon et al. 2008). Membrane fouling is a process whereby a solution or a particle is deposited on a membrane surface or in membrane pores (Meng et al. 2008), resulting with permeate flux reduction. Considerable effort has been invested into fundamental studies of membrane fouling problems in diverse membrane systems. Berman and Holenberg (2005) first reported the potential role of TEP in membrane fouling and considered them as "major initiators" of biofilm formation. TEP have attained such important attention because they possess some properties which are prone to foul membrane, such as high stickiness, deformability, heavy colonization by microorganisms in natural water systems. Since several recent studies have attributed membrane fouling to the presence of TEP, there is a considerable need for further work to gain an understanding of the formation of TEP in diverse aquatic environmental conditions and the fundamental interactions between TEP and the membrane fouling phenomenon. Alginate is an ideal model to model TEP in laboratory conditions due to its richness in acid polysaccharides and ability of gelling. Concurrently, TEP formation from different alginate blocks also provides insight of the effect of molecule composition of alginate on its fouling propensity.

Part of this chapter has been published as: Meng, S., Rzechowicz, M., Winters, H., Fane, A. and Liu, Y. (2013) Transparent exopolymer particles (TEP) and their potential effect on membrane biofouling. Applied Microbiology and Biotechnology 97(13), 5705-5710.

2.2 MEMBRANE TECHNOLOGY IN WATER INDUSTRY

2.2.1 Membrane Types and Properties

Membrane filtration technology has been commonly used for producing high-quality water for water reuse and recycle due to its advantages of small footprint, extremely high solid-liquid separation efficiency and easy maintenance (Watanabe and Kimura 2011). According to the driving force, the membrane technologies can be grouped into four clusters: pressure, electric potential, concentration gradient and temperature gradient driven membrane operations. The membrane separation is based on different permeability of membranes to the solvent and solutes or particles. The pressure-driven membrane processes for water treatment can be further classified into four categories: microfiltration (MF), ultrafiltration (UF), nanofiltration (NF) and reverse osmosis (RO) membranes, as summarized in Table 2.1.

Table 2.1 Typical properties of pressure-driven membranes (Fane et al. 2011, Wachinski 2013)

	Microfiltration (MF)	Ultrafiltration (UF)	Nanofiltration (NF)	Reverse Osmosis (RO)
Separation mechanism	Sieve	Sieve	Sieve, solution/diffusion +exclusion	Solution/diffusion
Pore size (apprx.) (μm)	0.05–10	0.001–0.1	~0.002	<0.002
MWCO (Da)	Not applicable	1,000–300,000	>100	>10
Water permeability ($L^{-1}m^{-2}h^{-1}bar^{-1}$)$^{-1}$)	>500	20–500	5.0–50	0.5–10
Operating pressure (bars)	0.1–2.0	1.0–5.0	2.0–10	10–100
Rejection layer	Porous	Porous	Between tight UF and loose RO	Nonporous
Removes	Bacteria/algae, suspended solids, turbidity	Bacteria, virus, colloids, macromolecules	Di-/multivalent ions, natural organic matter, small organic molecules	Dissolved ions, small molecules
Membrane materials	Ceramic (various materials), polypropylene, polysulfone (pvdf), polyethan sulfane	Aromatic, polyamides, ceramic (various materials), cellulose acetate, polypropylene, polysulfone, polyethersulfone (PES), polyvinylidene fluoride (PVDF)	Cellulosic, aromatic polyamide, polysulfone, polyvinylidene fluoride (PVDF), thin film composite	Cellulosic, aromatic polyamide, thin film composite

MF and UF membranes are porous membrane that can be operated at low pressures,

and often referred to as low-pressure membranes (Fane et al. 2011). The typical pore size of MF membranes is in the range of 0.05 to 10 μm. Separation by MF membranes is achieved via mechanical sieving of substances in water. UF membranes can retain large organic macromolecules, thus the pore structure of UF membrane is historically characterized by molecular weight cut off (MWCO) instead of a specific pore size (Wachinski 2013). The rejection of UF membranes is determined by the size and shape of the solutes relative to the pore size of the membranes (Peinemann and Nunes 2010). In water industry, MF and UF processes have been widely employed for removing microorganisms, suspended solids, turbidity, virus, colloids and macromolecules. As such, they may serve as a pretreatment step for RO and NF processes.

RO membranes essentially are nonporous membranes without visible pore structure (Fane et al. 2011). Both RO and NF membrane filtrations are operated under high pressure as summarized in Table 2.1. NF known as membrane softening has been widely applied for removing divalent and multivalent ions as well as some organic matters (Childress and Elimelech 2000, Wachinski 2013). RO membranes are able to reject small organic molecules and dissolved ions, including monovalent ions, such as NaCl, thus they are commonly used for desalinating seawater and brackish water.

2.2.2 Membrane Operation Modes

In general, a membrane module may be operated in two different modes: i.e. dead-end and cross-flow as illustrated in Figure 2.1. In the dead end filtration, all the feed was forced to pass through the membrane (Tchobanoglous et al. 2003). Substances in feed water that are too large to pass through the membrane accumulate at the membrane surface or deposit in the membrane pores (Wachinski 2013), leading to the build-up of the cake layer on membrane. In contrast, in cross-flow filtration mode, the feed water is pumped with a cross flow tangential to the membrane surface and a concentrate and a permeate streams are obtained (Tchobanoglous et al. 2003). During cross-flow filtration, only a portion of feed water is harvested as permeate.

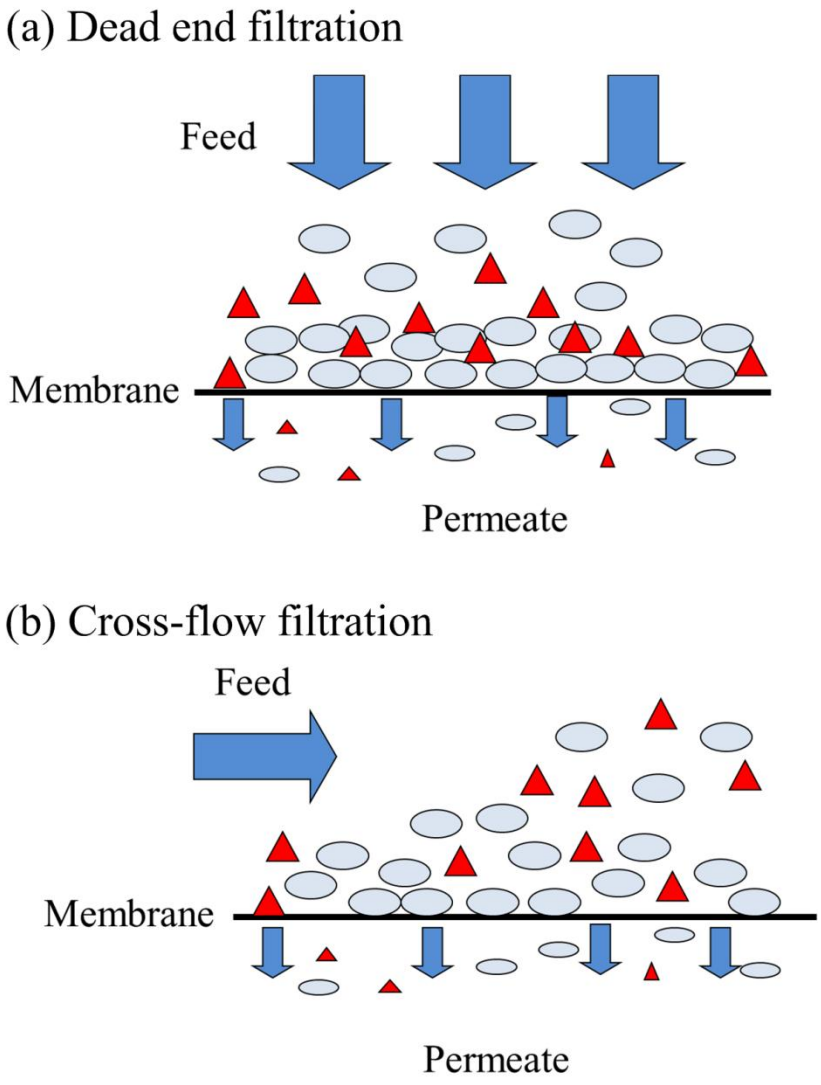

Figure 2.1 Membrane operation modes. (a) dead-end filtration mode and (b) cross-flow filtration mode.

2.2.3 Membrane Fouling

Membrane fouling is the biggest challenge encountered in nearly all membrane processes. Membrane fouling is a process in which solute or particles deposit onto a membrane surface or into the membrane pores which result in the poor membrane performance (Koros et al. 1996, Baker 2004). As the result, membrane fouling may cause severe flux decline and further affect the quality of the product water. Moreover, severe fouling may require intense chemical cleaning or frequent

membrane replacement leading to increased operating costs (Baker 2004). The main mechanisms of membrane fouling include adsorption of substances, pore clogging, particles deposition and gel-layer formation (Goosen et al. 2005, Peinemann and Nunes 2010). Adsorption occurs due to specific interactions between the solutes or particles in feed water and the membrane. Pore clogging is the result of deposition or accumulation of solutes and particles inside membrane pore.

2.2.3.1 Types of Fouling

Feed water often contains a wide spectrum of foulants according to which membrane fouling can be classified into four basic categories as illustrated in Figure 2.2 (Baker 2004, Goosen et al. 2005).

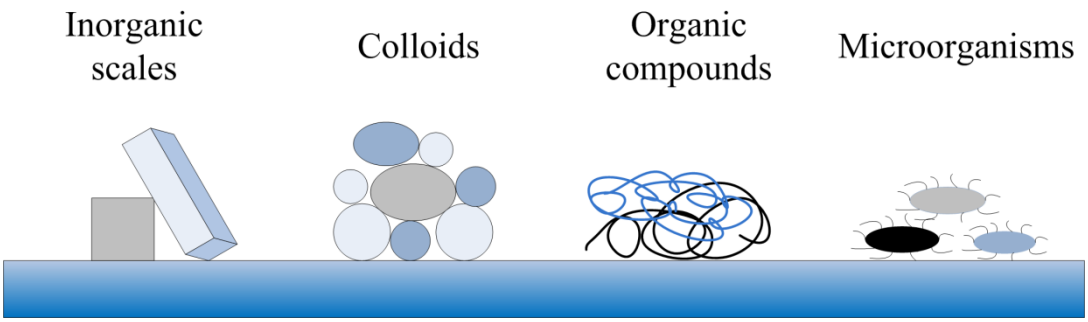

Figure 2.2 The common types of foulants present in feed water to membrane systems.

(1) Scaling

Scaling is caused by the precipitation of soluble inorganic compounds in feed water on the membrane surface. Precipitation or scale formation on the membrane surface occurs when the salts in raw feed water are concentrated beyond their solubility. Scaling is an important consideration for the operation of RO and NF (Mallevialle et al. 1996). Since the RO permeate is nearly salt-free, the inorganic compounds in feed water should be concentrated according to the production yield. One their solubility limits are exceeded, the inorganic compounds start to form precipitates on the membrane surface, known as scaling (Bremere et al. 1998, Bremere et al. 1999, van de Lisdonk et al. 2000), e.g. calcium carbonate ($CaCO_3$), barium sulfate (BaSO4), silica (SiO2), and calcium sulfate (CaSO4) (Baker 2004, Bartels et al.

2005).

(2) Colloidal fouling

Colloidal particles in feed water can lead to severe fouling due to the formation of a dense cake layer on the membrane surface. Generally, the sources of colloids in feed water are organic colloid, iron corrosion products, precipitated iron hydroxide, algae, and so on (Cohen and Probstein 1986, Baker 2004). The silt density index (SDI) is a good predictor of the possibility of the feed water to produce colloidal fouling (Baker 2004, Alhadidi et al. 2011, Wei et al. 2012, Habib et al. 2013).

(3) Organic fouling

Organic fouling occurs when natural organic matter (NOM) and effluent organic matter (EfOM), existing in natural water and waste water respectively, accumulate on membrane surfaces. Organic fouling accidently happens in drinking water but commonly occur in wastewater treatment plants. Typical organic compounds involved in the organic fouling may include humic acids (Hong and Elimelech 1997, Seidel and Elimelech 2002, Tang et al. 2007, Peeva et al. 2011), polysaccharides (Broeckmann et al. 2005, Saha et al. 2007, Susanto et al. 2008, Ulbricht et al. 2009, Kimura et al. 2012), proteins (Chan and Chen 2004, Li et al. 2007, Kanani et al. 2008, Susanto et al. 2008, Boributh et al. 2009, Yao et al. 2010, Hao et al. 2013) and fatty acids (Brinck et al. 2000, Ang and Elimelech 2008, Amin et al. 2010, Li et al. 2011). The properties of organic materials determine their relative propensities to foul the membranes, such as the affinity for the membrane employed, molecule weight of the organic materials, function groups they have and molecule conformation (Mallevialle et al. 1996).

(4) Biofouling

Biofouling is the formation of a biofilm on the membrane surface, leading to severe flux decline (Flemming 1997, Herzberg and Elimelech 2007, Al-Juboori and Yusaf 2012). Biofouling is often defined in terms of interactions between the microorganism and the membrane surface (Mallevialle et al. 1996). It is caused by the accumulated living microorganism on the membrane surfaces and the biofilm is difficult to be removed even with chemical cleaning. Membrane fouling caused by

organic and inorganic materials may also occur synergistically with the onset of biofilm formation (Mallevialle et al. 1996). Currently, many studies have been reported on extracellular polymeric substance (EPS)-associated biofouling (Kim et al. 2006, Tansel et al. 2006, Cogan and Chellam 2009, Sweity et al. 2011, Guezennec et al. 2012, Taimur Khan et al. 2013).

2.2.3.2 Fouling Mechanism

In general, the mechanism of membrane fouling can be classified into three types: pore closure, pore plugging and cake formation (Figure 2.3), depending on the relative size of solute in feed water to the membrane pore size (Schäfer et al. 2005). When the dimension of solute is much smaller than the pore size of membrane, pore closure induced by the penetration of solute into the membrane pores may occur, causing serious flux decline. If the solute has a dimension similar to the membrane pore size, pores may be plugged by the solute. Finally, solute bigger than membrane pore may eventually accumulate on membrane surface, resulting in the formation of a cake layer. Pore closure or plugging is insignificant for non-porous NF and RO membranes.

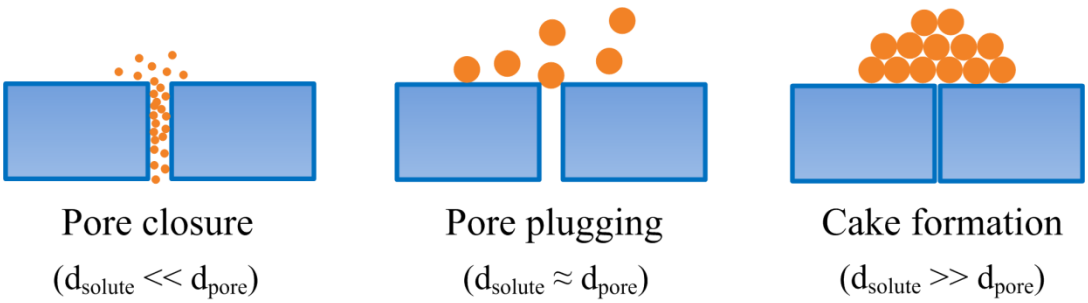

Figure 2.3 The mechanisms of membrane fouling (Schäfer et al. 2005).

The active areas for porous membranes are their pores. Hence, most fouling mechanisms are related to the processes which lead to a reduction in the number of active pores. Based on this, in general, membrane fouling can be quantitatively described according to the following four fouling mechanism models (Hermia 1985, Bowen et al. 1995, Field 2010).

(A) Complete blocking

This mechanism assumes that particles are larger than the pore size and each particle in feed water arriving to the membrane surface will participate in membrane pore blocking, blocking one pore or some pores. There is no superposition of particles that arrive on membrane surface. Therefore, the blocked area of membrane surface depends on the filtrated volume of feed water. Furthermore, in this phenomenon, it is assumed that the areas of the membrane whose pores are blocked are impermeable. As a consequent, the filtration resistance is inversely proportional to the ratio of free pores.

(B) Standard blocking

In standard blocking, it is assumed that particles are smaller than pore size and all particles arriving on membrane settle inside the membrane pores resulting in decrease in the pore radius and pore volume. Hence, the occupied pore volume is proportional to the volume of feed water that is filtrated.

(C) Intermediate blocking

The intermediate blocking law is based on the assumption that particles are possible to settle on both previously deposited particles and clean membrane surface. That is to say each location of the membrane surface has an equal probability of being occupied by particles in feed water.

(D) Cake filtration

Finally, by presuming that all particles are accumulated in a cake layer on membrane surface, the resulting model corresponds to the so called “cake filtration” model. Furthermore, in this model it is assumed that the cake resistance is proportional to the thickness of the cake layer formed.

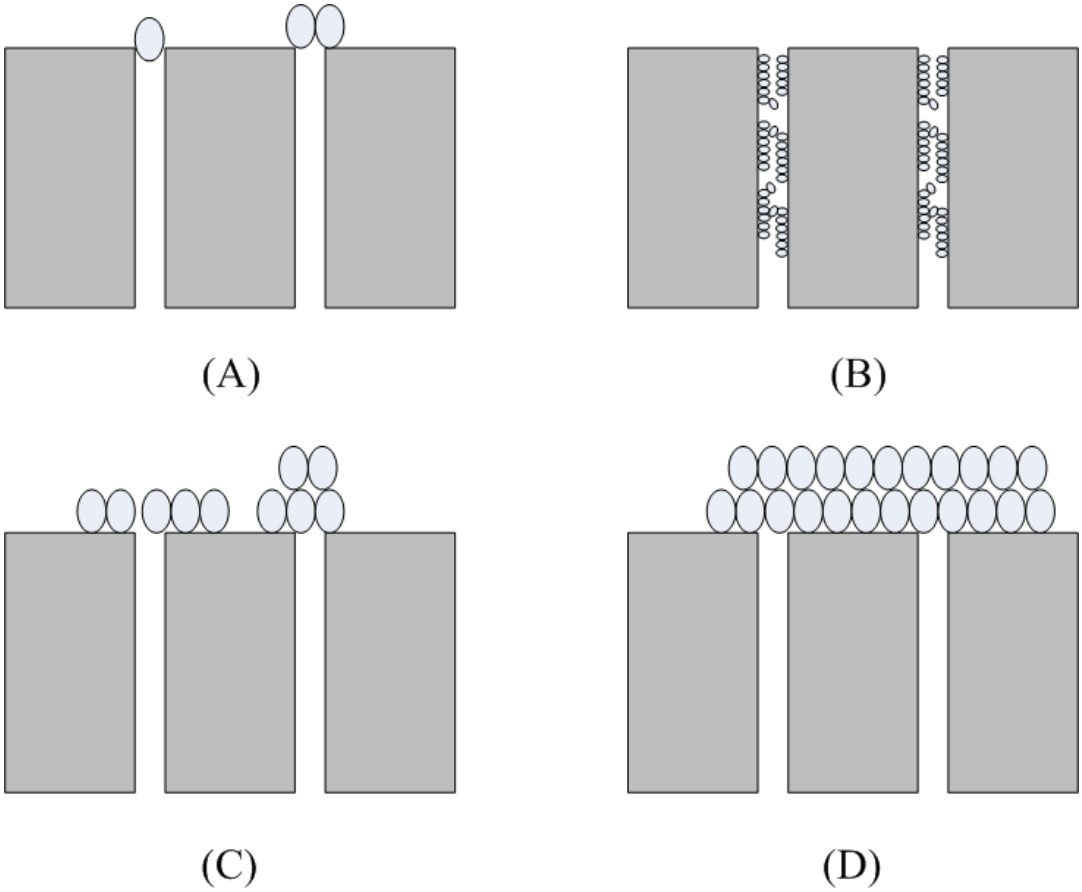

Figure 2.4 Four fouling mechanism models for porous membranes: (A) complete blocking, (B) standard blocking, (C) intermediate blocking and (D) cake filtration.

2.2.3.3 Characterization of Mechanical Properties of Cake Layer Developed on Membrane Surface

AFM technique has been widely used for measuring surface roughness of foulant layer formed on membrane, while these measurements are usually operated on dry surface (Lee et al. 2001, Lin et al. 2009). In fact, AFM can be operated in liquid and it has been used for measuring the elastic properties of thin polymer gelation film to investigate the degree of swelling and the softness of the gelatin (Domke and Radmacher 1998). Besides, AFM was also employed to measure the elastic properties of living cells in the field of cell biology (Radmacher 2002). However, few studies have applied the AFM in characterizing the mechanical properties of cake layer developed on membrane surface *in-situ*.

As shown in Figure 2.5, the differences lying in the AFM force curves of the still and soft samples are described (Radmacher 2002). The elastic properties of a sample could be corroborated from the slope of the force curve. For a stiff surface, when the tip of cantilever touching the surface, the deflection of the tip is proportional to the distance between the tip and sample surface (Domke and Radmacher 1998, Radmacher 2002). However, as for soft surface, the tip of the cantilever tends to indent the sample, resulting in a force curve with a smaller slope (Domke and Radmacher 1998, Radmacher 2002).

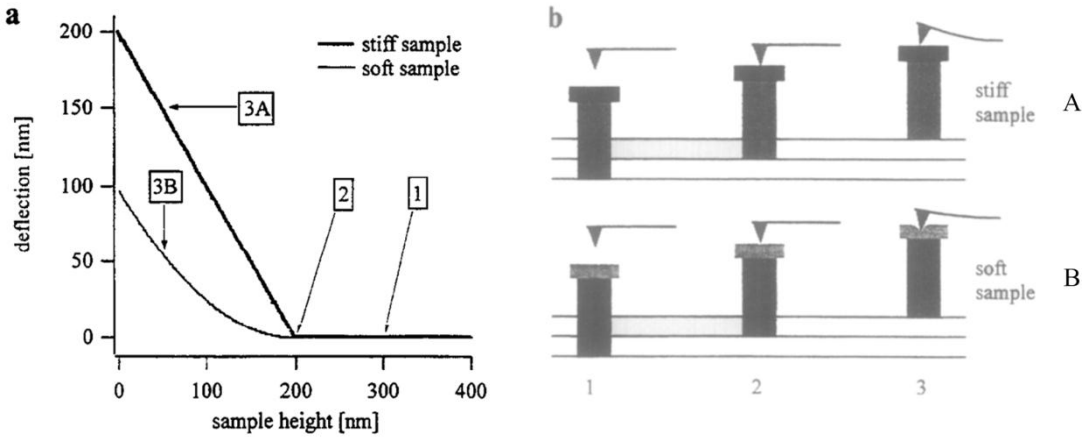

Figure 2.5 The differences in AFM force curves of the stiff and soft samples. Figures are adopted from literature (Radmacher 2002).

2.3 TRANSPARENT EXOPOLYMER PARTICLES (TEP)

2.3.1 Introduction

Transparent exopolymer particles (TEP) have been commonly found in surface water, seawater and wastewater, and have been described as a class of particulate acidic polysaccharides, which are large, transparent organic particles and can be stained by alcian blue (Alldredge et al. 1993). These gel-like particles are deformable, highly sticky and appear in various forms, e.g. amorphous blobs, strings, films, sheets, clouds, or clumps. TEP and other microgles are parts of the size continuum of organic matter in aquatic environments (Passow 2002, Bar-Zeev et al. 2012). Membrane technology has been widely employed for seawater

desalination, water and wastewater reclamation, while membrane fouling, especially biofouling, remains a big challenge (Xu and Liu 2011). TEP have been considered as a potential foulant in various membrane systems, such as MF, UF and RO, especially at the early stage of biofilm formation on membrane surfaces due to their wide existence in aquatic environments (Berman and Holenberg 2005, Berman and Passow 2007, Berman 2010, Komlenic 2010, Bar-Zeev et al. 2012).

The extensive involvement of TEP in membrane fouling is probably due to the unique physicochemical properties of TEP: (i) TEP are typically stickier than other particles in water (Passow 2002), leading to their easy deposition/accumulation on, while difficult to remove from the membrane surfaces; (ii) TEP are highly deformable, meaning that they may pass through membrane with a pore size even smaller than their dimensions; (iii) TEP are often colonized by microbes in the water environment, i.e. TEP may serve as a carrier to transport bacteria from water phase to membrane surface through adhesion. This in turn may accelerate the formation of biofilm on the membrane surface (Bar-Zeev et al. 2012) and (iv) TEP are the materials that can flex easily, fragment and disperse through the MF and UF membranes, and then reassemble in the filtrate to form large size network before reaching the RO membrane modules (Bar-Zeev et al. 2015).

2.3.2 Formation and Characteristics of TEP

Extensive effort has been dedicated to understanding of TEP formation mechanisms in water environment. As illustrated in Figure 2.6, two pathways may lead to the formation of TEP from dissolved organic matters (DOM) in aquatic environments (Passow 2002): (i) some phytoplankton and bacteria can generate TEP directly, i.e. TEP may form from mucus, cell coating surfaces, particulate materials and organic detritus produced by phytoplankton and bacteria; (ii) TEP can form from precursor substances under specific environmental conditions, e.g. turbulence, ion strength, concentrations of inorganic colloids etc. It has been believed that the second pathway dominates TEP production in marine environments (Passow 2002). The precursors, such as polysaccharide fibrils with a diameter of 1-3 nm and 100 nm long, are secreted by microorganisms (e.g. phytoplankton and bacteria) or produced

through lysis or breakage of cells (Leppard et al. 1977). The produced polysaccharides fibrils are then transformed into submicron gel-like substances through coagulation (Wells and Goldberg 1993), gelation and annealing (Chin et al. 1998). Coagulation or agglomeration of the submicron gels would eventually lead to the formation of TEP. In this sense, TEP may be regarded as a kind of suspended EPS which are present in the form of discrete particles instead of surface-attached or dissolved EPS (Alldredge et al. 1993, Passow 2002, Berman and Passow 2007, Berman 2010, de la Torre et al. 2010, Berman 2012).

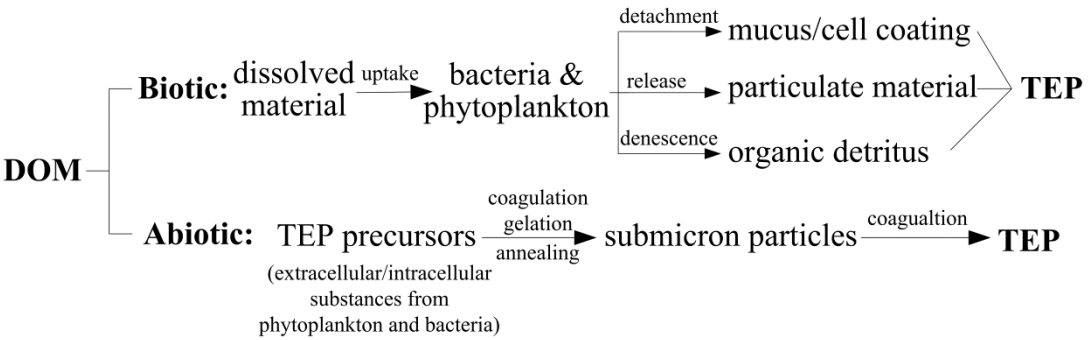

Figure 2.6 Two possible pathways leading to the TEP formation from DOM in aquatic environments (Passow 2002).

TEP have been known as transparent, expolymeric particles formed from acid polysaccharides, while are stainable with alcian blue, a dye specific for mucopolysaccharides (Passow 2002). Alcian blue is a hydrophilic cationic dye that stains both carboxylated and sulfated polysaccharides at pH 2.5 (Passow and Alldredge 1995). As TEP form from dissolved exopolysaccharides as precursors, they should be distinguished from soluble acid polysaccharides by their size. Operationally, TEP are defined as particles stainable by alcian blue, while separated through filtration for further quantification (Passow and Alldredge 1995). Filters with 0.4 μm pore size have been commonly used for TEP separation. However, different views exist in the literature with regard to the size and size distribution of TEP. Alldredge et al. (1993) first reported that the length of TEP was in the range of 3 to 100 μm, whereas particles as small as 0.05 μm had also been considered as TEP in studies of membrane fouling (Schippers et al. 2009; Villacorte et al. 2009; Schippers et al. 2010; Van Nevel et al. 2012). These in turn suggest that TEP should

be fractionated into different size ranges by filtration for quantification.

Compared with other particles (e.g. phytoplankton, bacteria, detritus and organic particles), TEP are surface-active substances and have greater stickiness, i.e. they can adsorb or be adsorbed easily by other particles (Dam and Drapeau 1995, Engel 2000). As TEP may also contain proteins, lipids, amino acids etc., they may serve as a pool of both nutrients and attachment sites for microorganisms, thus can be regarded as a bacterial "hot spot" (Passow 2002, Bar-Zeev et al. 2012). In addition, due to their deformable nature, TEP may easily pass through membranes though their 'apparent' size is greater than the membrane pore size. As the consequence, part of TEP may escape from low-pressure membrane pretreatment, and consequently would have a higher chance to foul the RO unit during seawater desalination and water reclamation.

2.3.3 Determination of TEP

TEP has been widely studied for many years in the fields of oceanography and limnology. Some determination methods for TEP are already available, all of which are based on staining with alcian blue. Alcian blue actually refers to any member of a family of polyvalent basic dyes, of which the alcian blue 8GX is the most common and reliable member (Hayat 1993). This dye has been widely used in biological and medical research to stain acidic polysaccharides such as intracellular polysaccharides in seaweed and extracellular polysaccharides in colony matrices or capsules of algae and bacteria as well as mucous layers, glycosamines in blood or urine (Parker and Diboll 1966, Whiteman 1973, Ramus 1977). Alcian blue consists of copper-phtalocyanin with four methylene-tetramethyl-isothiouronium-chloride side chains (Scott 1973). To date, several analytical methods have been developed for determination of TEP as presented below.

2.3.3.1 Microscopic Enumeration Method

The microscopic enumeration method was developed for determination of abundance and size distribution of TEP (Alldredge et al. 1993, Passow and

Alldredge 1994). In this method, the water sample is first filtered through a 0.2 μm or 0.4 μm filter. Particles retained on the filter are stained for less than 2 seconds with an aqueous solution made up by 0.06% acetic acid and 0.02% alcian blue. After stained, the filter-transfer-freeze technique proposed by Hewes and Holm-Hansen (1983) may be used for quantitative transfer of particles from the filter to a glass slide. Harvested stained particles are then observed and counted under a microscope. Alternatively, particles can be observed directly on filters if they are transferred onto clearing slides (Logan et al. 1994). The TEP concentration is finally expressed as the number of particles or total surface area covered by TEP per milliliter of water sample.

This method allows for direct visualization of TEP and has been used to determine the abundance of TEP in seawaters (Kiørboe and Hansen 1993, Kiørboe et al. 1994, Passow and Alldredge 1995). However, it should be realized that this method has some inherent shortcomings. (i) Stained particles usually do not have contrast high enough for subsequent image analysis (Passow and Alldredge 1995), whereas it is labor-intensive, time-consuming and difficult to be applied when large number samples need to be measured. (ii) Theoretically, all TEP particles bigger than 0.2 μm or 0.4 μm can be captured. However, the mass concentration and quantity of TEP in a given water sample may not directly be correlated to number of particles due to a wide size distribution of TEP. (iii) It is almost impossible to ensure that harvested TEP particles for microscopic examination are all present in a monolayer, leading to underestimation of TEP. Nevertheless, the method sill can be used for the observation of TEP.

2.3.3.2 Spectrophotometric Method

The spectrophotometric method was first developed for determination of TEP by Passow and Alldredge (1995b). In this method, the water sample is filtered gently through a 0.4 μm filter at a low and constant pressure to avoid deformable TEP being pushed through the filter. TEP retained on the filter are then stained with pre-filtered (0.2 μm) alcian blue solution made up from acetic acid (pH 2.5). After the filter has been gently rinsed with clean water to remove excess dye, it is soaked

in80% of sulphuric acid solution for 2 hours to re-dissolve the dye bound to the TEP particles. Finally, absorbance of alcian blue in the sulphuric acid solution is measured at 787 nm. Pre-filtration of alcian blue solution before its use is necessary as alclian blue can undergo self-coagulation. In this method, gum xanthan is used as a standard chemical of TEP for calibration. The TEP concentration is finally expressed as μg gum xanthan equivalent per liter of water.

Although this method has been most commonly used for determination of TEP, some challenges still need to be addressed. In this method, the size cutoff for TEP was originally set to be 0.4 μm. However, filters with pore size of 0.05 μm had also been employed for TEP determination. Evidence shows that colloidal TEP that pass through 0.4 μm filter, but retained by 0.05 μm filter are more abundant than particulate TEP bigger than 0.4 μm in various water samples (e.g. fresh and saline water) (Schippers et al. 2009, 2010; Villacorte et al. 2009; Van Nevel et al. 2012). It appears that this method is only valid for determination of TEP larger than 0.4 μm, while a large portion of colloidal TEP may be ignored unreasonably. To tackle this problem, before staining by alcian blue, TEP should be fractioned through a series of filtrations with different membrane pore sizes.

2.3.3.3 Centrifugation Method

In this method, a 70 μm nylon mesh net is used to remove large particles (e.g. zooplankton and phytoplankton). Tangential filtration with 0.45 μm nominal pore is employed to concentrate TEP. The reaction between acidic group of polysaccharides and alcian blue leads to the formation of insoluble non-ionic pigments, thus the alcian blue solution is directly added into harvested TEP sample, and insoluble pigments produced can be separated by centrifugation (Arruda Fatibello et al. 2004). After centrifugation, excess alcian blue remaining in the sample is measured at 602 nm. The difference between total alcian blue added to sample and that left over after centrifugation represents the quantity of TEP in the sample. Again, xanthan gum is used as a calibration standard and TEP concentration is expressed as μg gum xanthan equivalent per milliliter. According to Berman and Passow (2007), TEP have a mean size of 2-200 μm. However, TEP

larger than 70 μm would be removed during the pretreatment of water sample in this method.

2.3.3.4 Fractionation Method

This method is a variant of the spectrophotometric method developed by Passow and Alldredge (Passow and Alldredge 1995), which was further modified by Villacorte et al. (Villacorte et al. 2009, Villacorte et al. 2009) in order to fractionate TEP in terms of size using a series of filters with different pore sizes. Villacorte et al. (2009a) suggested that TEP smaller than 0.4 μm should be classified as colloidal TEP according to the definition of colloids (0.001-1 μm) by the International Union of Pure and Applied Chemistry (IUPAC). In fact, 65-92% of the total TEP in surface water were found to be colloidal TEP (Villacorte et al. 2009).

Table 2.2 Comparisons of various TEP determination methods (Discart et al. 2015)

	Microscopic enumeration method	Spectrophotometric method	Centrifugation method	Fractionation method
Detection limit	1 particle/filtered amount	around 2 µg xanthan gum/L	0.10×10^{3} µg xanthan gum/L	around 50 µg xanthan gum/L
Precision	~ 50% (800 particles/mL)	~ 5%	<1%	~ 5%
Sample pretreatment	No pretreatment necessary, fixation with formalin possible	No pretreatment necessary, fixation with formalin possible	Removal of salts for seawater samples, fixation with formalin is possible	No pretreatment necessary, fixation with formalin possible
Alcian blue solution	0.02% alcian blue, 0.06% acetic acid	0.02% alcian blue, 0.06% acetic acid	0.003% alcian blue, 0.2 mol/L acetate buffer solution (pH 4)	0.02% alcian blue, 0.06% acetic acid
Filter used	Polycarbonate 0.4 µm	Polycarbonate 0.4 µm	No filter	Polycarbonate 0.05-0.4 µm
Interferences by salts	None	None	Yes	None
Interferences by humic substances, amino acids	None	None	?	None
Interferences by intracellular compounds	No/Yes	No/Yes	?	No/Yes
Simplicity	Labor intensive	Medium	Simple	Medium
Implementation	Medium	Medium	Easy	Medium
Cost	Medium	Medium	Low	Medium
Variability of the results	(no calibration)	High	Low	Unknown

2.3.4 Effect of TEP on Membrane Fouling

2.3.4.1 Characteristics of TEP Relevant to Membrane Fouling

Different from other organic substances in water, TEP possess some unique physicochemical characteristics that facilitate their involvement in membrane fouling.

(1) High Stickiness

In aquatic environments, TEP are involved in many processes due to their high stickiness. TEP consist a high fraction of active function groups, such as sulfate half-ester groups ($R\text{-}OSO_3\text{-}$) and uronic acids ($R\text{-}COO^-$), which facilitate the formation of metal ion bridges and hydrogen bonds making TEP very surface-active (Mopper et al. 1995). However, it is difficult to measure the absolute stickiness of TEP because it is almost impossible to isolate natural TEP from other substances. The stickiness of TEP may be estimated by measuring the combined stickiness coefficient (α) of natural particles through evaluating the relative contribution of TEP to the overall stickiness (Passow 2002). Couette flocculator test is commonly adopted for determination of the combined stickiness coefficient of a sample with various particles, such as TEP, phytoplankton, bacteria and detritus. In this method, the aggregation rate and the size frequency distribution of all particles are measured (Passow 2002). It had been reported that the stickiness of TEP estimated by this method was greater than 0.1 during diatom blooms (Dam and Drapeau 1995, Engel 2000). Stickiness of most solid particles, such as the detritus, sediment and phytoplankton, has been reported in the range of 0.01-0.0001 (Passow 2002). These suggest that TEP has a much higher stickiness than other particles in water, implying that TEP can easily absorb or be absorbed by other particles or attach onto solid surface, e.g. membrane surface.

(2) Deformability

Although the size of TEP is usually larger than the pore sizes of MF and UF membranes, TEP have been detected in their permeates (Villacorte et al. 2009,

Villacorte et al. 2010, Gasia-Bruch et al. 2011, Van Nevel et al. 2012). It seems that under applied pressure, TEP can pass through the membrane pores due to water streaming through the membrane as well as the deformability of TEP (Bar-Zeev et al. 2015). As micro-gels, TEP share similar property of gels in terms of flexibility. A possible mechanism for the prevalence of TEP found in MF and UF filtrates has been proposed, but yet experimentally verified (Bar-Zeev et al. 2015). At the inlets of the MF or UF membrane modules, TEP and their precursors (e.g. nano-gels) are pressurized over the membrane pores. Under applied pressure, the hydrogel polymer structure of TEP may flex, fragment and disperse through the membrane pores as nano-scale TEP precursors. Subsequently, TEP precursors in the filtrates of MF and UF can reassemble to form TEP again before reaching the RO membrane modules. This re-organization process of TEP could be accelerated by the presence of divalent cations, such as calcium ions which is typically found in wastewater and seawater. Consequently, the high deformability of TEP may facilitate the survival, prevalence and difficult-removal of TEP in the membrane systems, posing a big challenge for RO desalination.

(3) Extensive microbial colonization

As particles with large surface area, TEP provide attachment sites for microorganisms, while serve as the nutrient pool for attached microorganisms as TEP are often proteinaceous particles, lipid droplets, amino acids etc.(Long and Azam 1996, Engel and Passow 2001, Passow 2002), About 0.5-25% of all bacteria present in seawater and freshwater were attached onto TEP (Passow 2002). Moreover, the bacterial density on TEP is a function of the size of TEP:

$$N = \alpha d^{-\beta} \tag{2.1}$$

where N is the bacterial density attached on TEP (number μm^{-2} TEP), and d is the equivalent spherical diameter of TEP in μm (Passow 2002). Some data pertaining to Eq. 2.1 are presented in Table 2.3.

Table 2.3 The bacterial density on TEP. Data are from Passow (2002).

Locations	α	β	Bacterial density (μm^{-2})		References
			5 µm TEP	100 µm TEP	
Coastal Pacific	1.36	0.78	0.39	0.04	(Passow and Alldredge 1994)
Adriatic	0.28	0.70	0.09	0.01	(Schuster and Herndl 1995)
Adriatic	0.30	0.82	0.08	0.007	(Schuster and Herndl 1995)
Kattegat (time series)	0.25-1.68	0.35-1.00			(Mari and Kiørboe 1996)
Pre-bloom	0.26	0.38	0.14	0.05	(Mari and Kiørboe 1996)
Post-bloom	1.53	0.72	0.48	0.06	(Mari and Kiørboe 1996)
River Danube	NV	NV	0.70	NV	(Berger et al. 1996)
Experimental	0.58	1.06	0.1	0.004	(Schuster and Herndl 1995)

Visualization of TEP and associated bacteria by dual-staining with alcian blue and SYBR green revealed that TEP were significantly colonized by microorganisms in freshwater, coastal seawater, recycled secondary treated wastewater and sulfide and iron rich groundwater (Figure 2.7) (Berman and Parparova 2010). These in turn indicate the likelihood of TEP as active agents to be involved in the development of membrane biofouling.

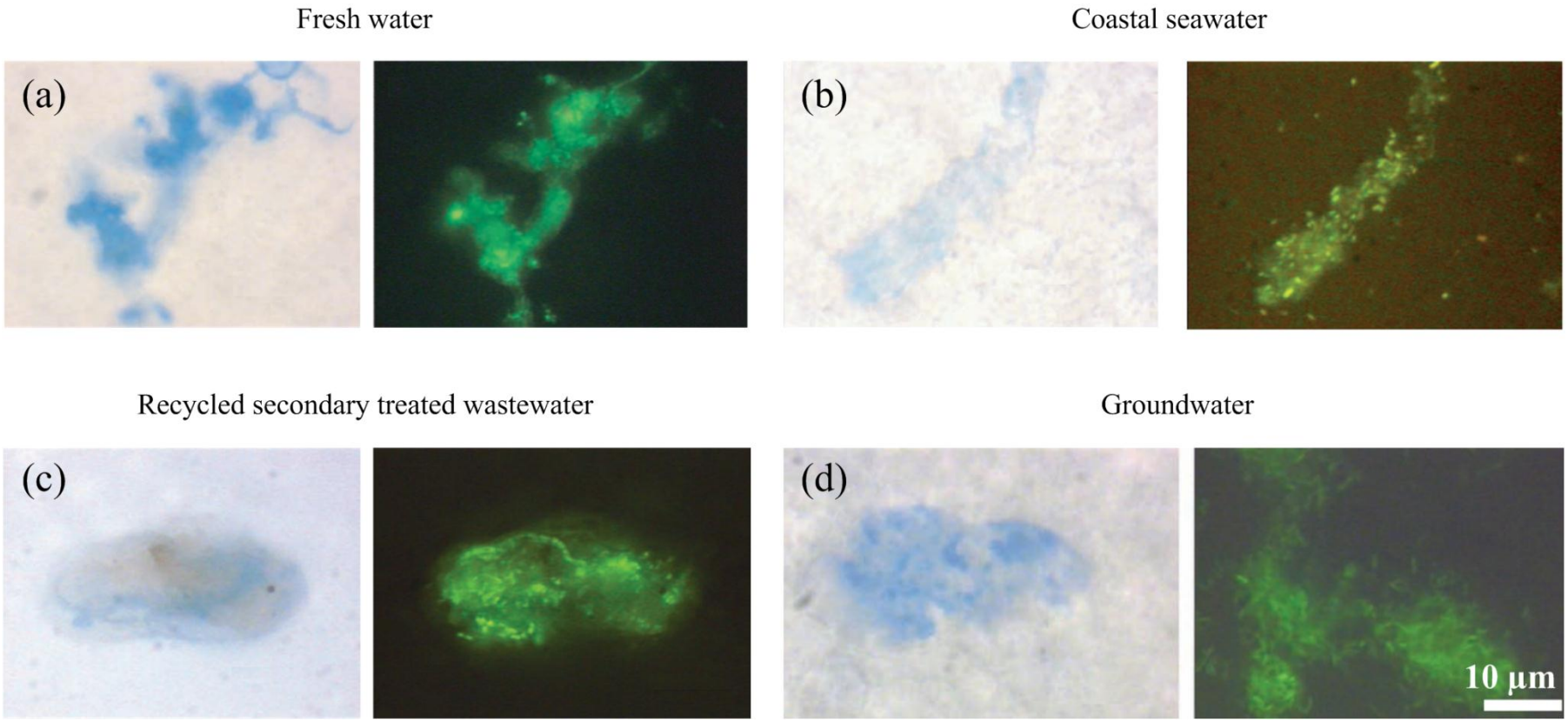

Figure 2.7 TEP and associated bacteria in fresh water (a), coastal seawater (b), recycled secondary treated wastewater (c) and ground water (d). Images are adapted from Berman and Parparova (2010). Water samples were stained by alcian blue combined with SYBR green.

2.3.4.2 Existence of TEP in Feed Water for Membrane Systems

TEP have an abundant presence in fresh water and seawater (Table 2.4). The concentration of TEP in aquatic environments is dependent on the location, season and species of phytoplankton, implying that the TEP levels in the aquatic environments are highly variable, ranging from micrograms to milligrams xanthan gum equivalent per liter (Passow 2002, Bar-Zeev et al. 2015). In natural waters, the peak of TEP concentration usually occurs during the period the bloom of phytoplankton (Passow 2002). Higher TEP concentration was observed in the euphotic zone as well as in the coastal areas than in the open sea (Passow and Alldredge 1994, Engel and Passow 2001). In the coastal and estuarial areas, there are more environmental changes compared to the open sea region:, such as (i) anthropogenic eutrophication due to runoff or river input (Rabalais et al. 2009, Sarma et al. 2009); (ii) phytoplankton bloom in the nutrient-rich coastal areas fueling intense microbial activity (Paerl 1988, Riemann et al. 2000, Armbrust 2009, Kim et al. 2009, Fouilland and Mostajir 2010, Sintes et al. 2010) and (iii) extensive organic matter release due to large-scale jellyfish swarms (Condon et al. 2011). These environmental changes drastically affect the formation and then concentration of TEP in coasts and estuaries. It should be noted that seawater for RO desalination is usually taken from the estuary or/and coastal areas. This means that abundant TEP present in these areas will pose a challenge in seawater desalination by RO. In addition, MBR has been widely employed for water and wastewater purification. In general, TEP concentration in wastewater ranges from 20 mg X_{eq} L^{-1} to 100 mg X_{eq} L^{-1}. Table 2.4 summarizes the typical TEP concentrations in various aquatic environments.

Table 2.4 TEP concentrations in various aquatic environments (Bar-Zeev et al. 2015).

Water environments	Region	Concentrations ($\mu g\ X_{eq}\ L^{-1}$)	References	Remarks
Open sea	Atlantic	27-279	(Engel 2004)	[a]Waste water secondary effluent
Seawater	Pacific	40-310	(Passow and Alldredge 1995, Boyd et al. 2005)	[b]No pretreatment
Coastal *Seawater*	Singapore	129-1073	(Wurl and Holmes 2008)	[c]Feedwater origin: seawater
	France	26-3604	(Klein et al. 2011)	[d]Feedwater origin: estuary
Estuary *Brackish water*	Brazil	13-1199	(José Juan et al. 2012)	Role of TEP in engineering systems:
	Singapore	281-8026	(Wurl and Holmes 2008)	1. Form initial conditioning layer
Lakes *Fresh water*	Spain	66-9038	(De Vicente et al. 2010)	2. Change surface properties
	Israel	759-2385	(Berman and Parparova 2010)	3. Facilitate biofilm formation through protobiofilm attachments
Wastewater treatment *Brackish water*	Israel[a]	746-4157	(Berman and Parparova 2010)	4. Reinforce existing biofilm structures
	Germany[b]	20000-100000	(de la Torre et al. 2008)	
Desalination RO inlet	Israel[c]	78-197	(Bar-Zeev et al. 2009)	
	Netherlands[d]	300	(Villacorte et al. 2009)	

2.3.4.3 TEP-associated Membrane Fouling

Due to their surface active property, TEP can attach onto or be easily adsorbed by other solid surfaces including membranes, whereas they may also serve as a nutrient source for the microbial growth in seawater and freshwater (Passow 2002). Bacteria attached onto can be brought to solid surfaces through attachment of TEP due to their high stickiness. This in turn suggests a possible mechanism by which TEP may initiate membrane biofouling. The TEP-associated membrane biofouling has been reported in membrane filtration of seawater, surface water and wastewater (Schippers et al. 2009, Villacorte et al. 2009, Bar-Zeev et al. 2012, Valladares Linares et al. 2012, Van Nevel et al. 2012). For example, a positive correlation was established found between TEP level in feed water and membrane fouling propensity (Berman et al. 2011). Autopsy of fouled RO membranes further confirmed existence of significant amount alcian blue-stainable substances on membrane surfaces (Villacorte et al. 2009). Consequently, all these clearly suggest the involvement of TEP in membrane fouling development.

2.3.4.4 TEP-facilitated Biofilm Formation

Bar-Zeev et al. (2009) reported that a relatively large alcian blue stained area was observed on glass slides immersed in seawater after 18 hour contact, suggesting that the alcian blue stained substances might not be produced by attached bacteria, but they originated from TEP presence in seawater. Such a view was supported by the observations that biofilms were developed on a membrane surface after 50 hours operation irrespective of whether feed water was disinfected or not (Berman et al. 2011). It is a reasonable assumption that TEP present in the feed water could play a critical role at the early stage of biofilm development onto a membrane surface. Thanks to with real time bright field and epifluorescence microscope technique, adhesion of TEP and protobiofilm (extensive colonized TEP) onto immersed surfaces were observed inside the flow cells upon exposure to overlying untreated seawater (Bar-Zeev et al. 2012). On the other hand, biofilm development was significantly inhibited in the experiment with seawater filtered through 0.7 μm membrane in which both TEP and protobiofilm were removed significantly. These

results indicate that highly sticky TEP and TEP-associated protobiofilm may favor microbial attachment onto a solid surface, including membrane as schematically illustrated in Figure 2.8.

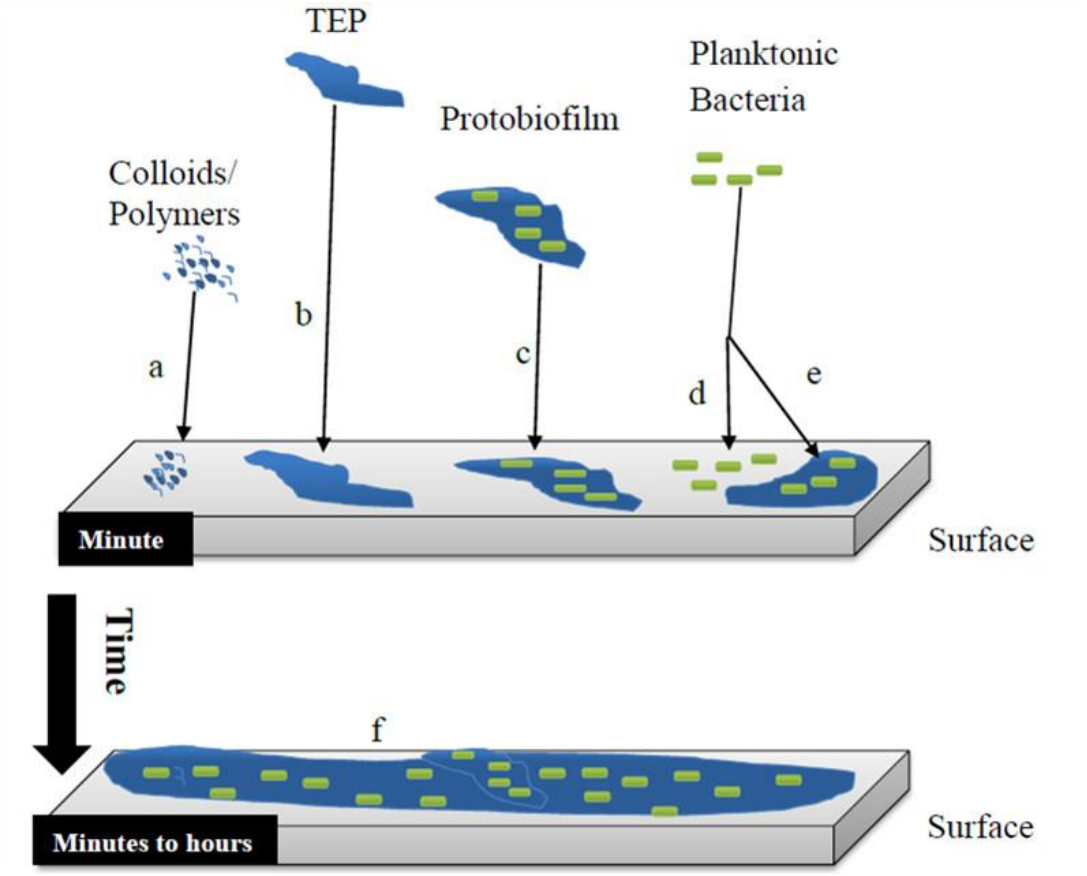

Figure 2.8 Schematic illustration of the initial stages of biofilm formation. a: Polymers and colloids; b: Uncolonized TEP; c: Protobiofilm; d: Reversible attachment of bacteria; e: Irreversible attachment of bacteria; f: mature biofilm (Bar-Zeev et al. 2012)

2.3.4.5 Removal of TEP

The removal of TEP from water treatment systems has also been investigated. Evidence suggests that particulate TEP (>0.4 μm) can be readily removed by low pressure membranes (Schippers et al. 2009, Villacorte et al. 2009). However, in the study by Villacorte et al. (2009a), it was found that colloidal TEP (0.05μm<TEP<0.4μm) in feed could not be completely removed by microfiltration,

ultrafiltration and combined coagulation-sedimentation-rapid sand filtration. As a result, a significant amount of TEP still can reach RO membranes after various feed water pretreatments (Figure 2.9). For example, it was shown in a RO desalination plant that 90% of chlorophyll was removed and silting density index (SDI) was significantly lowered through flocculation, sand filtration and microfiltration, yet TEP level was reduced only by 30% (Bar-Zeev et al. 2009). It should be noted that the concentration of TEP in seawater (in oligotrophic seawater TEP concentrations are often <100 μg $X_{eq}.L^{-1}$) is often lower than other types of naturally occurring particles and DOM. This in turn poses a new challenge on how to efficiently remove such low-concentration TEP at the pretreatment stage in order to prevent TEP-induced RO membrane fouling.

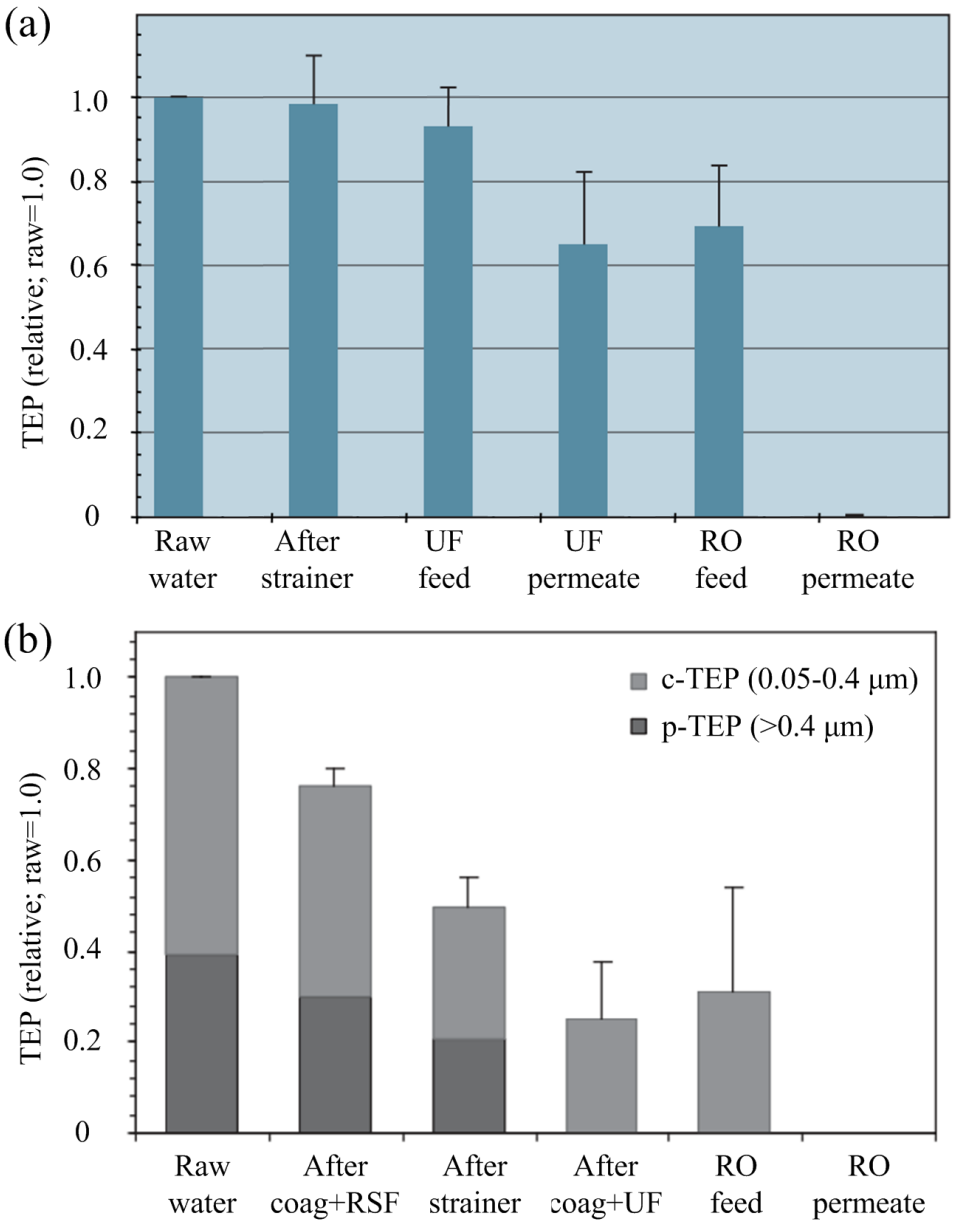

Figure 2.9 The removal of TEP through treatment processes in two integrated membrane systems. (a) A seawater UF-RO pilot desalination plant in Zeeland Province, the Netherlands (Villacorte et al. 2010). (b) A RO plant located in the Netherlands with river water as source water (Villacorte et al. 2009).

2.3.5 Remarks

Although TEP has not yet been clearly defined in terms of their size distribution, TEP should be distinguished from dissolved EPS. For example, colloidal TEP

instead of particulate TEP have been shown to be dominant in various water environments. It appears from the above that instead of using a membrane with a fixed pore size, TEP should be fractionated through a series of membrane filtrations with various pore sizes.

2.4 ALGINATE

Alginate has been commonly used as a model foulant of EPS in the study of membrane fouling.

2.4.1 Source of Alginate

Alginates are abundant in nature environments since they are not only the major structural polysaccharide present in all brown seaweeds, but also exist as the capsular polysaccharides in soil bacteria (Draget et al. 2005). Commercial alginates are produced mainly from *Laminaria hyperborea, Macrocystis pyrifera, Laminaria digitata, Ascophylum nodosum, Laminaria japonica, Eclonia maxima, Lessonia nigrescens, Durvillea Antarctica*, and *Sargassum spp* (Smidsrød and Skja˚k-Br˙k 1990, Draget et al. 2005, Donati and Paoletti 2009). Alginates are usually extracted from these algae by treatment with aqueous alkaline solutions, e.g. NaOH (Lee and Mooney 2012). Apart from being present in natural seaweeds, alginates are also synthesized as capsular polysaccharides by two types of soil bacteria, *Pseudomonas aeruginosa* and *Azotobacter vinelandii* (Pendarvis 1998, Draget et al. 2005). It should be noted that all commercial alginates are extracted from algal sources.

2.4.2 Chemical Structure of Alginate

Alginates are unbranched binary copolymers consisting of (1→4) linked β-D-mannopyranuronic acid (M) and (1→4) linked α-L-gulopyranuronic acid (G) residues (Figure 2.10a.) in varying proportions (Draget et al. 2005). In alginates, the monomers M and G are randomly arranged along the chain in two kinds of homopolymeric blocks (MM-block, GG-block) and one kind of heteropolymeric block (MG-block) (Figure 2.10b and Figure 2.10c) (Smidsrød 1974, Draget et al.

2005, Lee and Mooney 2012). The composition and sequential structure of these blocks in alginates may vary widely with the source algal species, tissue types, growth status and seasons (Table 2.5) (Draget et al. 2005, Leal et al. 2008). For example, the GG-block content of alginates extracted from L. hyperborean stems is about 60%, whereas the percentage of GG-block in other commercially available alginates falls into the range of 14.0% to 31.0% (Lee and Mooney 2012). It should be noted that the proportion, distribution and length of the three blocks may largely affect chemical and physical properties of alginates (Draget et al. 2005, Lee and Mooney 2012). In general, GG-block is responsible for the gel formation of alginates, while MM-block and MG-block provide flexibility for chains (Draget et al. 2005, Lin et al. 2010, Lee and Mooney 2012). It has been reported that the intrinsic flexibility of the blocks decrease in the order MG > MM > GG (Donati and Paoletti 2009).

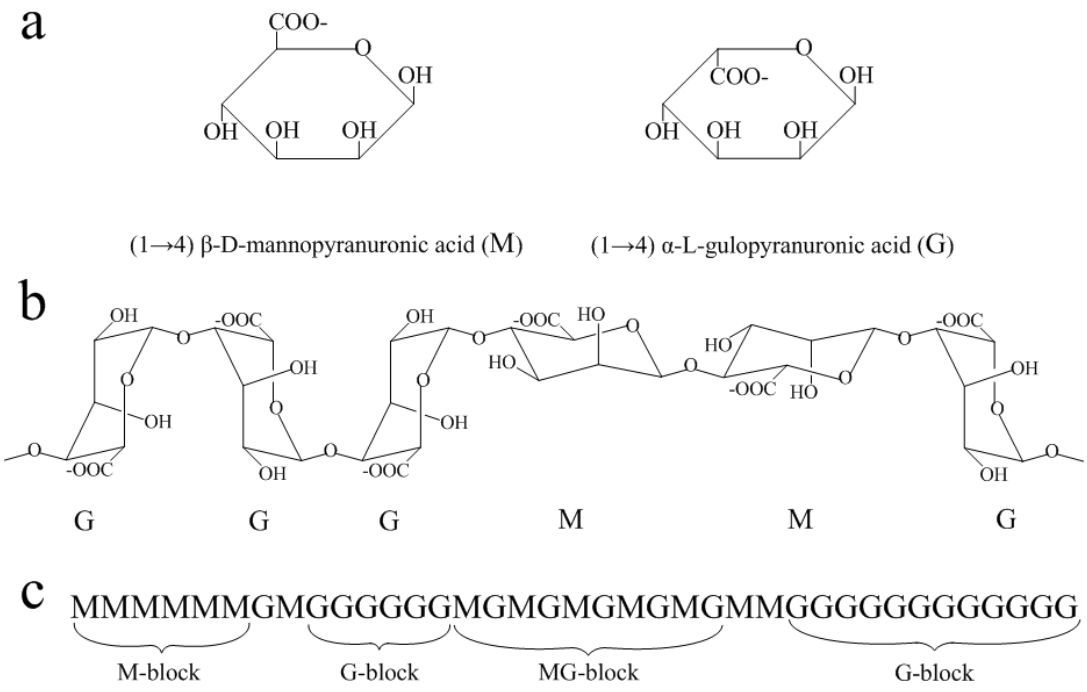

Figure 2.10 Structural characteristics of alginate molecule: (a) alginate monomer (b) alginate chain conformation (c) alginate blocks distribution.

Table 2.5 Molecular composition of alginates extracted from various sources (Smidsrød and Draget 1996, Draget et al. 2005).

Algae sources	Percentage of				
	G	M	GG-block	MM-block	MG-block
Laminaria japonica	0.35	0.65	0.18	0.48	0.17
Laminaria digitata	0.41	0.59	0.25	0.43	0.16
Laminaria hyperborea, blade	0.55	0.45	0.38	0.28	0.17
Laminaria hyperborea, stipe	0.68	0.32	0.56	0.20	0.12
Laminaria hyperborea, outer cortex	0.75	0.25	0.66	0.16	0.09
Lessonia nigrescens	0.38	0.62	0.19	0.43	0.19
Ecklonia maxima	0.45	0.55	0.22	0.32	0.32
Macrocystis pyrifera	0.39	0.61	0.16	0.38	0.23
Durvillea Antarctica	0.29	0.71	0.15	0.57	0.14
Ascophyllum nodosum, fruiting body	0.10	0.90	0.04	0.84	0.06
Ascophyllum nodosum, old tissue	0.36	0.64	0.16	0.44	0.20

2.4.3 Physical Properties of Alginate

In general, the molecular weights of commercially available sodium alginates range from 32 kDa to 400 kDa (Lee and Mooney 2012). Besides, alginates are dissolvable in water , while their solubility is related to solution conditions including pH, alginate concentration, ionic strength and the presence of divalent cations (Draget et al. 2005). In addition, the viscosity of alginates solutions is mainly determined by the solution pH, e.g. it tends to increase with decreasing pH and the highest viscosity is reached atpH 3-3.5 (Lee and Mooney 2012).

CHAPTER 3 ALGINATE BLOCKS AND THEIR EFFECTS ON MEMBRANE FOULING

3.1 INTRODUCTION

Membrane technology has been widely employed for water and wastewater reclamation around the world, while membrane fouling still remains as a big challenge. Organic fouling occurs when natural organic matters (NOM) and effluent organic matters (EfOM) accumulate on membrane surfaces. In the past few decades, to study organic fouling of membrane, alginate has been commonly used as a model foulant due to its abundance in nature environments (Lee and Elimelech 2006, Katsoufidou et al. 2007, van den Brink et al. 2009, Sioutopoulos et al. 2013).

Alginates are unbranched binary copolymers consisting of (1→4) linked β-D-mannopyranuronic acid (M) and (1→4) linked α-L-gulopyranuronic acid (G) (Fig. 1a.) in varying proportions (Draget et al. 2005). In alginates, the monomers M and G are randomly arranged along the chain in two kinds of homopolymeric blocks (MM-block, GG-block) and one kind of heteropolymeric block (MG-block) (Figs. 1b and 1c) (Smidsrød 1974, Draget et al. 2005, Lee and Mooney 2012). Composition and sequential structure of these blocks in alginates vary widely with the source algal species, tissue types, growth status and seasons (Draget et al. 2005, Leal et al. 2008). For example, the GG-block content of alginates extracted from L. hyperborean stems is 60% and for other commercially available alginates, the GG-block percent is between 14.0% and 31.0% (Lee and Mooney 2012). It should be noticed that the proportion, distribution and length of the three blocks are important characteristics of alginates because they determine the chemical and physical properties of alginates (Draget et al. 2005, Lee and Mooney 2012). Generally, GG-block is responsible for the gel formation capacity of alginates, while MM-block and MG-block provide flexibility for chains (Draget et al. 2005, Lin et al. 2010, Lee

This chapter has been published as: Meng, S. and Liu, Y. (2013) Alginate block fractions and their effects on membrane fouling. Water Research 47(17), 6618-6627.

and Mooney 2012).

Although alginate has been commonly used in membrane fouling studies, surprisingly, no attention has been given to the effects of various alginate blocks on membrane fouling development. Depending on their sources, alginates may have different chemical and physical properties, which in turn lead to uncertainty and poor repeatability of filtration experiments with alginate. Therefore, the main objective of this study is to investigate the effects of different blocks of alginate on membrane fouling. For this purpose, alginate was first fractionated into MG-, MM- and GG-block by the method of partial acid hydrolysis (Leal et al. 2008), and their respective filtration behaviors were then examined using a dead-end microfiltration system. Membrane fouling caused by MG-, MM- and GG-blocks were further analyzed by various filtration models including resistance-in-series model, complete blocking model, standard blocking model, intermediate blocking model and cake filtration model. In addition, the formation of transparent exopolymer particles (TEP) by MG-, MM- and GG-blocks and their effects on membrane fouling were also investigated. Meanwhile, the extended Derjaguin-Landau-Verwey-Overbeek (XDLVO) theory was employed to calculate the interfacial cohesion energy among alginate blocks which is related to the formation of TEP by different alginate blocks.

3.2 MATERIALS AND METHODS

3.2.1 Fractionation of Alginate

Sodium alginate (Wako, Japan) was fractionated according to the method by Leal et al. (2008). As illustrated in Figure 3.1, in this method, 10 g/L of sodium alginate solution was stirred for 2 hours at 1,000 rpm for complete dissolution. 3 M of HCl solution was then slowly added into the above alginate solution to reach a final concentration of 0.3 M HCl, and the later was heated at 100°C in oil bath for 30 min with slow stirring. The cooled solution was centrifuged at 13,420 g-force for 30 min. The supernatant was harvested and neutralized with 1 M NaOH solution and then poured into the equal-volume ethanol solution, yielding a white precipitate.

This precipitate was collected by centrifugation at 13,420 g-force for 30 min and was finally freeze-dried to obtain the MG-blocks. The insoluble fraction from the first centrifugation was re-dissolved in 1 M of NaOH solution under rapid vortex condition. The pH of this solution was then readjusted to 2.85 by addition of 1M of HCl solution. At pH 2.85, a precipitate appeared and was further separated out by centrifugation. After neutralization by 1 M of NaOH solution, the remaining soluble fraction was precipitated out by adding ethanol, and resulting precipitate was harvested by centrifugation and freeze-dried to obtain the MM-blocks. Again, the insoluble fraction was similarly dissolved in 1M NaOH solution, then neutralized by 1M HCl and finally was precipitated out by addition of ethanol to obtain the GG-blocks. All the freeze dried alginate blocks were grinded into powder form in an agate mortar and were then stored in a copper sulfate dryer to prevent them from being exposed to the damp room condition. All the solutions used were prepared with ultrapure Milli-Q water. The above fractionation was repeated three times.

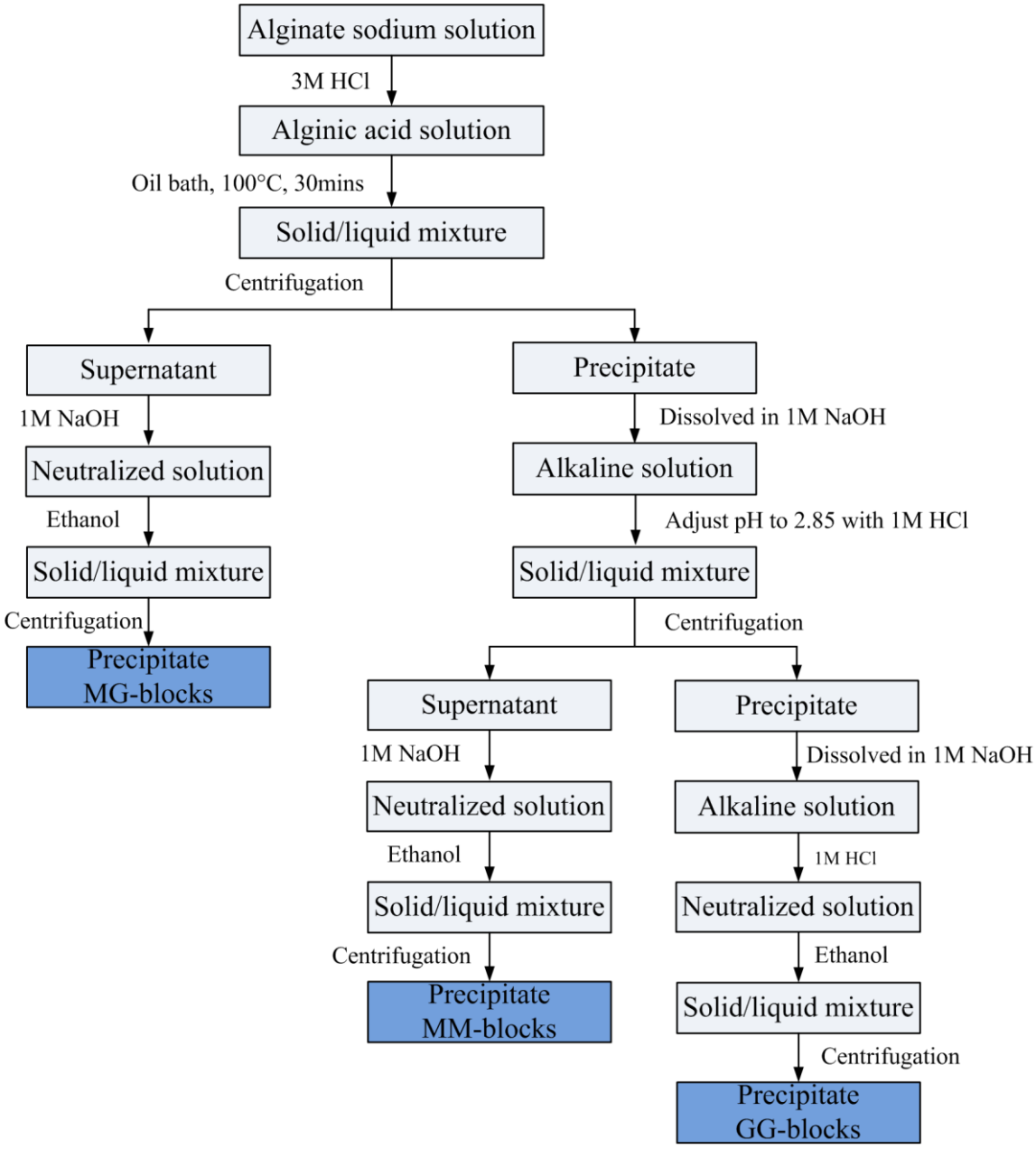

Figure 3.1 Fractionation procedure of alginate based on the partial acid hydrolysis method.

In order to characterize the alginate blocks, respective fourier transform infrared spectroscopy (FTIR) spectra of the MG-, MM- and GG-blocks fractionated from alginate were also measured. Samples were prepared with the FTIR start Kit and KBr was used to establish the baseline. 2-4 mg of prepared sample was mixed with 295 mg KBr and ground thoroughly. The pure KBr and mixed-sample pellets were transferred to the disc holder which was subsequently inserted into the spectrometer.

The FTIR spectra were recorded using a PerkinElmer FTIR Spectrum GX 50905. 60 scans were taken for both background establishment and sample measurements.

3.2.2 Filtration Tests and Membrane Fouling Analysis

3.2.2.1 Dead-end Microfiltration Test

Standard dead-end microfiltration module equipped with a 3-L feed vessel and a 50 mL stainless steel membrane cell was employed to examine the fouling potentials of the alginate blocks, i.e. MG-, MM- and GG-blocks (Figure 3.2). 0.2 μm flat-sheet nylon membrane (contact angle: 22.6±0.7° at 20°C) with an effective surface area of 11.94 cm^2 (FilTrex, Singapore) was used in this study. The microfiltration module was operated at 1 bar provided by compressed nitrogen gas, and filtrate was collected in a beaker placed on an electronic balance. The weight change of filtrate was recorded at the time interval of 5 s by a data-logger connected to a computer. All feed solutions were prepared with 0.01 M NaCl and 0.05 g/L of three alginate blocks, respectively.

Contact angle of the membrane surface was determined by an OCA contact angle system (DataPhysics Instruments GmbH, Germany). The reported contact angle is the average of at least 20 measurements. Membrane zeta potential was determined by an eletrokinetic analyser (EKA, SurPASS, Anton Paar GmbH, Austria) in 10 mM NaCl.

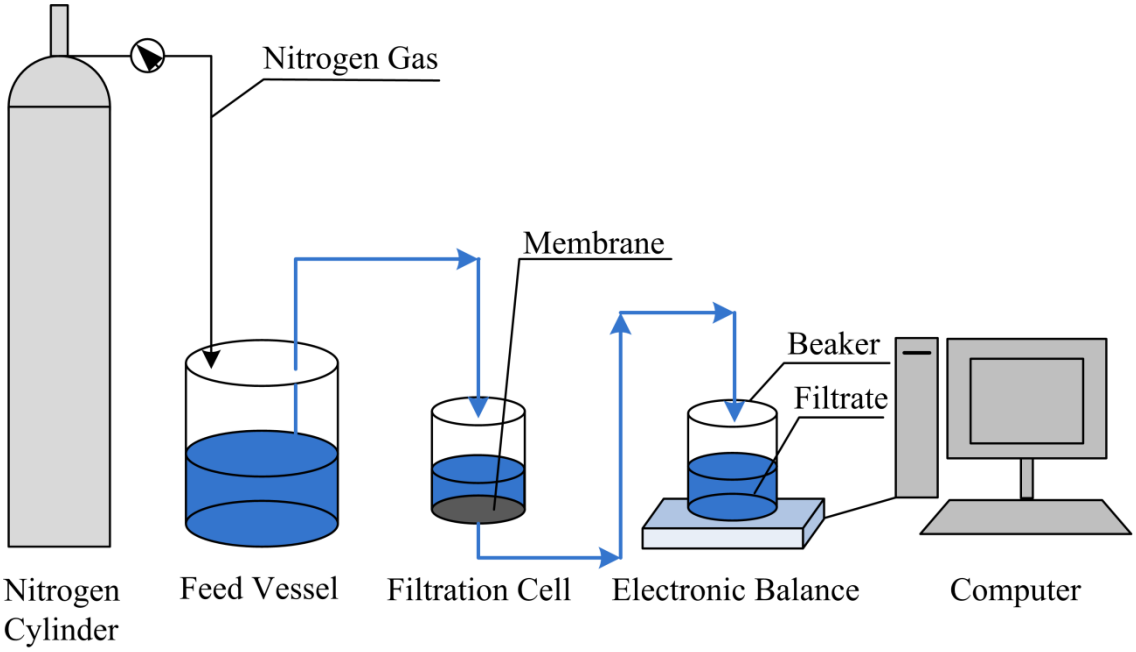

Figure 3.2 Schematic of the microfiltration system used in the study.

3.2.2.2 Determination of Membrane Resistance

The resistance-in-series model (Cheryan 1998) was used to determine the intrinsic membrane resistance (R_m), pore blocking resistance (R_p), and cake layer resistance (R_c):

$$J = \frac{\Delta P}{\mu R_t} \tag{3.1}$$

$$R_t = R_m + R_p + R_c \tag{3.2}$$

where J is permeate flux ($m^3m^{-2}s^{-1}$); R_t is total filtration resistance (m^{-1}); ΔP is applied pressure (Pa); and μ is solution viscosity (Pa•s). R_m is estimated from Eq. (3.1) by filtering ultrapure water through virgin membrane, while R_t can be calculated from filtration flux at steady state. In this study, respective fluxes at 200 min of filtration of MG-, MM- and GG-blocks were used for calculation. After fouled membranes were gently wiped with a sponge and rinsed with ultrapure water to remove the cake layer, the internal resistance R_f was calculated from ultrapure water flux through wiped membrane. Finally, R_p can be obtained from Eq. (3.3).

$$R_f = R_m + R_p \tag{3.3}$$

3.2.2.3 Analysis of Fouling Mechanism

To look into the possible mechanisms of membrane fouling by MG-, MM- and GG-blocks, complete blocking model, standard blocking model, intermediate blocking model and cake filtration model were employed in this study (Hermia 1985, Bowen et al. 1995):

Complete blocking model:

$$J / J_0 = e^{-Kt} = e^{-K_a J_o t} \tag{3.4}$$

Standard blocking model:

$$J / J_0 = (1 + 2K_s A_{eff}^2 J_0^{0.5} t)^{-2} \tag{3.5}$$

Intermediate blocking model:

$$J / J_0 = (1 + KA_{eff} J_0 t)^{-1} = (1 + K_a J_o t)^{-1} \tag{3.6}$$

Cake filtration model:

$$J / J_0 = (1 + 2KA_{eff}^2 J_0^2 t)^{-0.5} = (1 + 2K_c R_r J_o t)^{-0.5} \tag{3.7}$$

where K_a is the blocked membrane surface per unit of the total volume permeated through the membrane (1/m); K_s is Hermia's parameter which is the decrease in the cross-section area of the pores per unit of permeate volume (1/m); K_c is area of the cake per unit of permeate volume (1/m); R_r is the ratio of the cake resistance to the clean membrane resistance (dimensionless). In this study, the J/J_0 data of MG-, MM- and GG-blocks were fitted to Eqs. (3.4)-(3.7), respectively, and the curve fittings were evaluated by relative goodness f which is defined as follows (Liu and Wang 2008):

$$f = \frac{(\sigma^2)_{\min}}{\sigma^2} \tag{3.8}$$

where σ^2 is the prediction error square, and $(\sigma^2)_{min}$ is the minimum value among all σ^2 determined by Eqs. (3.4)-(3.7).

The term σ^2 is given by:

$$\sigma^2 = \frac{\sum (Y_k - \hat{Y}_k)^2}{n - p} \tag{3.9}$$

where Y_k and $\hat{Y}_k$ are experimental data and regressed values, n-p is called the residual degrees of freedom (Montgomery and Runger 2003).

3.2.3 Determination of TEP

The concentrations of TEP in three alginate blocks solutions were determined according to the method proposed by Passow and Alldredge (1995) (Figure 3.3). Water samples were first filtered through a series of polycarbonate filters (Whatman, United Kingdom) with different pore sizes (0.05 μm, 0.1 μm and 0.2 μm). An adjustable pump was used to maintain a stable vacuum of 0.2 bars. The TEP retained on the filters were further stained with 1 mL of pre-filtered staining solution which was prepared with 0.02% of alcian blue 8 GX (Sigma, USA) in 0.06% acetic acid solution (pH 2.5), and was stored in a 4°C refrigerator. Alcian blue was made contact with TEP for 5s, after then excess stain was removed by filtering 1mL of ultrapure water (Milli-Q) through the filter under low vacuum (≤0.2 bar). Subsequently, the filter was transferred into a beaker and then soaked in 5 mL of 80% H_2SO_4 solution for 2h to elute alcian blue that were bound to TEP. The beaker should be gently swirled 3-5 times during this period. At the end of 2h, absorbance of the H_2SO_4 solution with eluted alcian blue was measured using a UV spectrophotometer (Shimadzu, Japan) at the wavelength of 787 nm, while ultrapure water was used as reference. Six to ten measurements were performed for each sample. Gum xanthan was used as a standard of TEP for calibration purpose (Kennedy et al. 2009). The TEP concentration is finally expressed as mg gum xanthan equivalent per liter of water (mg X_{eq} L^{-1}). In this study, all water samples were freshly prepared and analyzed with the same batch of alcian blue solution

within one week. The calibration factor was found to be 0.181 mg Xeq per unit absorbance at 787 nm wavelength.

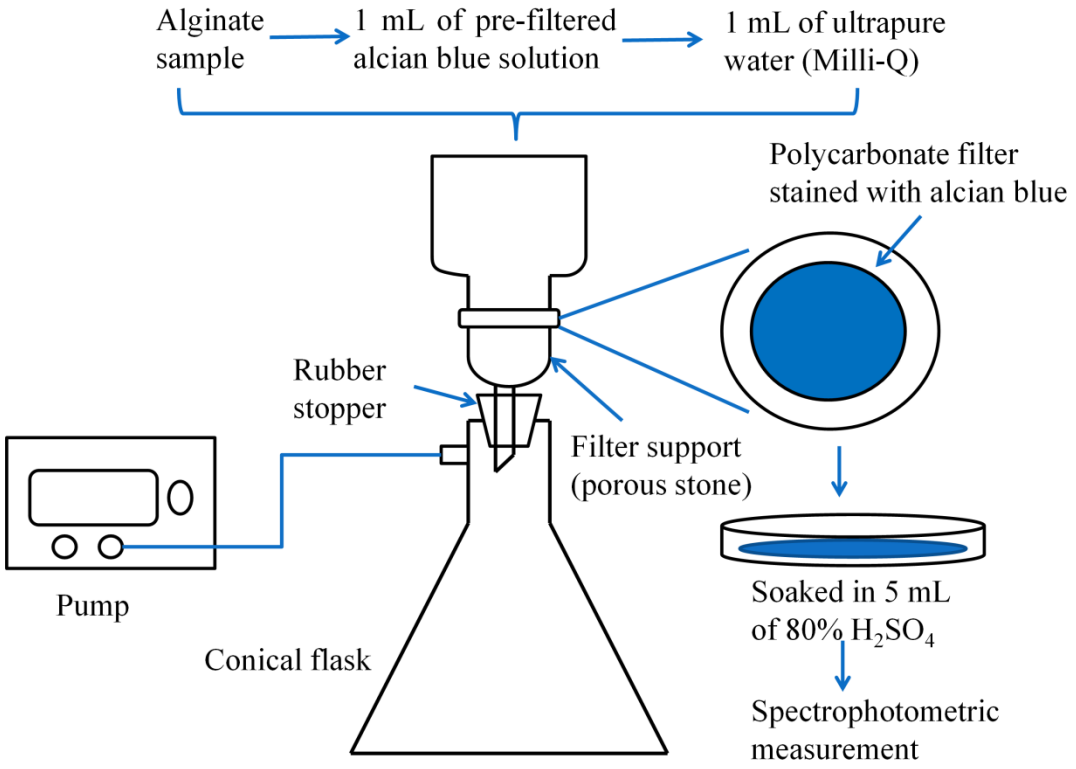

Figure 3.3 Schematic of the TEP determination system.

3.2.4 Interfacial Free Energy Analyses

In order to explore the mechanisms of TEP formation by various alginate blocks, the interfacial cohesion energy among alginate blocks was calculated according to the XDLVO theory. Cohesion energy describes the energetic favorability of a solid substance interacting through a liquid media with itself, and it offers insights into stability and aggregation ability of alginate blocks as well as their potentials of deposition onto solid surfaces covered by alginate blocks. Thus, the potentials of alginate blocks to aggregate together and further to form TEP can be evaluated.

3.2.4.1 Contact Angle

To determine the surface tension components of alginate blocks, contact angles

were measured with three probe liquids, out of which two must be polar, and the third one must be apolar (van Oss 1993). In this study, ultrapure water (Milli-Q), glycerol (Promega, USA) were chosen as polar liquids, while diiodomethane (Acros, USA) as an apolar liquid.

In measurement of the contact angles of different alginate blocks, glass slides were carefully cleaned with pure ethanol for 20 min, rinsed with ultrapure water and then dried in 60°C oven. The smooth flat surface of each alginate blocks was prepared by deposition of 1 g/L of its solution on the cleaned glass slides (Van Oss 2006). Subsequently, the coated glass slides were dried in a 60°C oven for 24h, allowing complete removal of water. A drop of 1.0 μL probe liquid was placed on the prepared glass slides, and contact angle was then measured using a goniometer (Dataphysics, USA), equipped with a video camera/computer and image analysis software. At least ten measurements were performed for each sample, and the mean values of ten measurements were reported.

3.2.4.2 Zeta Potential

Zeta potentials of alginate and alginate blocks were measured using a Malvern ZetaSizer Nano ZS. Freshly prepared sample solutions were used with 0.01 M NaCl as background electrolyte. Right before the zeta potential measurement, the pH was measured and kept stable. Each measurement was repeated at least 5 times.

3.2.4.3 Determination of Surface Tension Parameters of Alginate Blocks

The surface tension components of alginate blocks (γ_s^{LW}, γ_s^+, γ_s^-) can be calculated from contact angles (Table 3.1) (van Oss 1993) by using the extended Young equation (van Oss 1993, Brant and Childress 2002):

$$\left(1+\cos\theta\right)\gamma_l^{TOT} = 2\left(\sqrt{\gamma_s^{LW}\gamma_l^{LW}} + \sqrt{\gamma_s^+\gamma_l^-} + \sqrt{\gamma_s^-\gamma_l^+}\right) \tag{3.10}$$

where θ is the contact angle (°) and subscript *s, l* represents solid surfaces and probe liquids respectively. γ^{TOT} is the total surface tension (mJ/m^2), while γ^{LW} and γ^{AB} are the Lifshitz-van der Waals and the Lewis Acid-Base interaction components

(mJ/m^2) of surface tension respectively. According to Oss et al. (1986), γ^{TOT} can be calculated from Eq.(3.11):

$$\gamma^{TOT} = \gamma^{LW} + \gamma^{AB} \tag{3.11}$$

The Lewis Acid-Base interaction component is calculated from Eq.(3.12) (Oss and Good 1988, M. Greiveldinger and Shanahan 1999):

$$\gamma^{AB} = 2\sqrt{\gamma^{+}\gamma^{-}} \tag{3.12}$$

where γ^{+} is the electron acceptor parameter and γ^{-} is the electron donor parameter.

Table 3.1 Surface tension properties (mJ/m^2) of probe liquids at 20°C.

	γ^{LW}	γ^{+}	γ^{-}	γ^{AB}	γ^{TOT}
Ultrapure water	21.8	25.5	25.5	51.0	72.8
Glycerol	34.0	3.92	57.4	30.0	64.0
Diiodomethane	50.8	0.0	0.0	0.0	50.8

Data taken from van Oss (1993).

3.2.4.4 Calculation of Interfacial Cohesion Energy of Alginate Blocks

According to van Oss (1993), the interaction energy balance for aqueous systems is expressed as follows:

$$G_{s_1 l s_2}^{XDLVO} = G_{s_1 l s_2}^{LW} + G_{s_1 l s_2}^{AB} + G_{s_1 l s_2}^{EL} \tag{3.13}$$

where G^{XDLVO} is the total interaction energy between two solid surfaces (s_1 and s_2) immersed in water environments and G^{LW}, G^{AB}, G^{EL} are the Lifshitz-van der Waals, Lewis acid-base interaction and electrostatic double layer terms respectively.

Surface tension components calculated from above and the zeta potentials can be further used to evaluate the free energies per unit area between alginate blocks, e.g. ΔG_{d0}^{LW}, ΔG_{d0}^{AB} and ΔG_{d0}^{EL} can be calculated as follows (Hogg et al. 1966, van Oss 1993, Brant and Childress 2002):

$$\Delta G_{d_0}^{LW} = 2(\sqrt{\gamma_l^{LW}} - \sqrt{\gamma_{s1}^{LW}})(\sqrt{\gamma_{s2}^{LW}} - \sqrt{\gamma_l^{LW}}) \tag{3.14}$$

$$\begin{aligned}\Delta G_{d_0}^{AB} = {} & 2\sqrt{\gamma_l^+}\left(\sqrt{\gamma_{s1}^-} + \sqrt{\gamma_{s2}^-} - \sqrt{\gamma_l^-}\right) \\ & + 2\sqrt{\gamma_l^-}\left(\sqrt{\gamma_{s1}^+} + \sqrt{\gamma_{s2}^+} - \sqrt{\gamma_l^+}\right) - 2\left(\sqrt{\gamma_{s1}^+\gamma_{s2}^-} + \sqrt{\gamma_{s1}^-\gamma_{s2}^+}\right)\end{aligned} \tag{3.15}$$

$$\Delta G_{d_0}^{EL}(d) = \frac{\varepsilon_0 \varepsilon_r \kappa}{2}(\zeta_{s1}^2 + \zeta_{s2}^2)\left[1 - \coth(\kappa d_0) + \frac{2\zeta_{s1}\zeta_{s2}}{(\zeta_{s1}^2 + \zeta_{s2}^2)}\operatorname{csc} h(\kappa d_0)\right] \tag{3.16}$$

where ε_0 is the absolute dielectric constant, equal to 8.854×10^{-12} $C^2/(J\cdot m)$, ε_r is the permittivity of the liquid (78.5 for water), ζ_{s1} and ζ_{s2} are the surface potentials of solid 1 and solid 2 respectively, d_0 the contact distance between two solids and is usually adopted as 0.158 nm, κ is the inverse Debye screening length (1/m) which is given by (Elimelech et al. 1995):

$$\kappa = \left(\frac{2e^2 N_A \sum_i (c_i z_i^2)}{\varepsilon_0 \varepsilon_r kT}\right)^{1/2} \approx 5.58\times10^{10}\sqrt{\frac{\sum c_i z_i^2}{T}} \tag{3.17}$$

where e is the electron charge (1.6×10^{-19}C), N_A the Avogadro constant (6.022×10^{23}/mol), k the Boltzmann's constant (1.38×10^{-23}J/K), c_i the concentration of positive ion I in the bulk solution (mol/L), z_i the valence of positive ion I, and T is the absolute temperature. In this study, 0.01 M of NaCl solution was used as the background electrolyte. At the average working temperature of 300 K, κ was estimated as 3.22×10^8 which was then used in this study.

3.2.5 Field Emission Scanning Electron Microscope (FE-SEM) Analysis

In order to visualize the TEP formation, 10-20 mL of the MG-, MM- and GG-blocks solutions as used in the filtration experiments were filtered through polycarbonate filters at low pressure. The dried filters with TEP were examined by a FE-SEM (Jeol JSM-7600F, Japan).

3.3 RESULTS AND DISCUSSION

3.3.1 Alginate Composition of Alginate

In this study, alginate was fractionated into MG-, MM- and GG-blocks with a total recovery yield of 79.4±3.5% which was comparable with the recovery efficiency reported in the literature, e.g. about 75% (Leal et al. 2008). Figure 3.4 shows the appearances of the fractionated blocks. The alginate used in this study was composed of 13.8±1.9% of MG-block, 53.5±1.3% of MM-block and 32.7±0.6% for GG-block. Obviously, MM-block was the main component of the alginate sodium studied.

Figure 3.4 Appearances of MG-, MM- and GG-blocks fractionated from alginate sodium.

Figure 3.5 showed the respective FTIR spectra of the three alginate blocks. The broad bands were centered at the wave numbers of 3393 cm^{-1}, 3401 cm^{-1}, 3381 cm^{-1} which could be assigned to the hydrogen bonded O-H stretching vibrations. The weak signals at the wave numbers of 2923 cm^{-1}, 2935 cm^{-1}, 2939 cm^{-1} were likely due to C-H stretching vibrations, while the asymmetric stretching of carboxylate O-C-O vibration would be responsible for the bands observed at 1618 cm^{-1}, 1610 cm^{-1}, 1615 cm^{-1}. It had been reported that the bands at 1420/1412/1419 cm^{-1} could be due to C-OH deformation vibration coupled with O-C-O symmetric stretching vibration of carboxylate group (Steyermark 1976, Leal et al. 2008). The medium absorption observed at 1305 cm^{-1}, 1303 cm^{-1}, 1320 cm^{-1} may be assigned to O-C stretching vibration of carboxylic acid and derivatives (Steyermark, 1976). In addition, the

medium to strong IR absorption bands at 1200-970 cm^{-1} were mainly due to C-C and C-O stretching in pyranoid ring as well as a C-O-C stretching of glycosidic bonds (Gómez-Ordóñez and Rupérez 2011). In fact, an intense absorption in this spectral region is common for all polysaccharides (Synytsya et al. 2010). The fingerprint or anomeric region at 950-750 cm^{-1} showed three typical absorption bands in all alginate polysaccharides. The band at 957/938/949 cm^{-1} was probably due to the C-O stretching vibration of uronic acid residues and the bands at 886/889/904cm^{-1} was assigned to the C1-H deformation vibration of β-mannuronic acid residues. Lastly, the band observed at 814/820/812 cm^{-1} reflected the presence of mannuronic acid residues (Chandía et al. 2004).

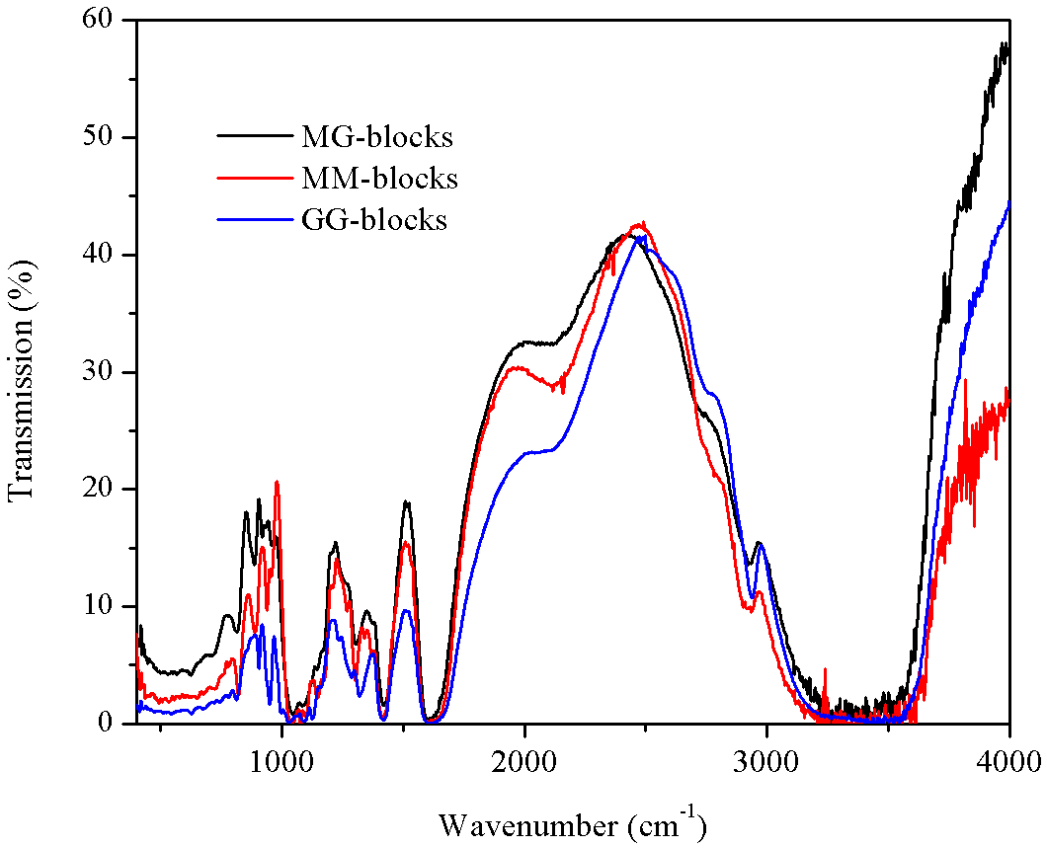

Figure 3.5 FTIR spectra of MG-, MM- and GG-blocks.

3.3.2 Filtration behaviors of MG-, MM- and GG-blocks

Figure 3.6 shows the respective flux profiles observed during the microfiltration of MG-, MM- and GG-blocks. Although these blocks were derived from the same

alginate, their filtration behaviors appeared to be very different. Minimum flux decline was observed during the filtration MM-block, while a much severer flux reduction was recorded in the filtration of GG-block. Meanwhile, the membrane fouling during the MG-block filtration was found to be the severest, especially in the initial period of filtration. Table 3.2 shows the respective filtration resistances of MG-, MM- and GG-blocks, and it can be seen that pore-blocking resistances of three alginate blocks tended to increase in the order of MM-block<GG-block<MG-block, while the resistances due to cake layer appeared to be comparable for the three blocks. In fact, these results were consistent with the flux profiles presented in Figure 3.6. The fraction of the cake resistance in the total filtration resistance varied from 52.9% to 73.6% for different blocks, implying that cake formation was the major contributor of the observed membrane fouling. However, for MG-block and GG-block filtration, pore blocking resistance accounted for 34.4% and 29.2% of the total filtration resistance respectively, suggesting that pore blocking was not negligible though cake resistance was dominant. On the contrary, the pore blocking resistance was only about 4.4% of the total resistance in MM-block filtration, i.e. 16.8-fold lower than cake resistance.

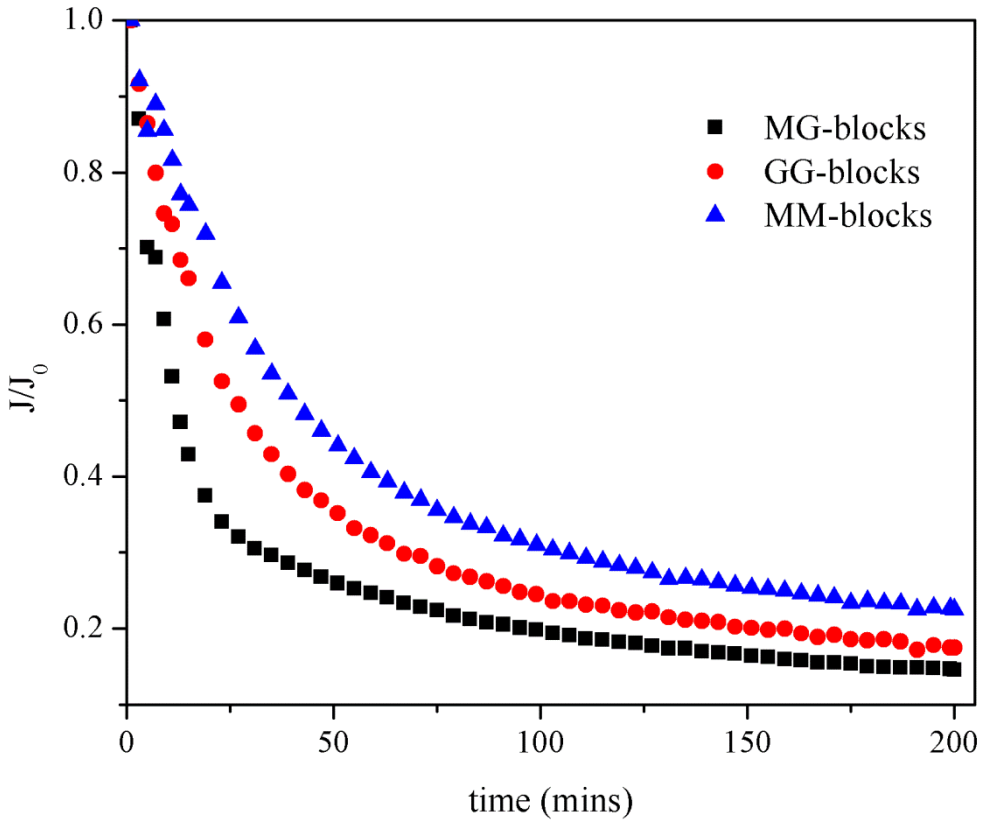

Figure 3.6 Flux profiles of MG-, MM- and GG-block. Experimental conditions: MG-, MM- and GG-blocks concentration = 50 mg/L, background electrolyte (NaCl) concentration = 10 mM.

Table 3.2 Respective resistances of the MG-, MM- and GG-block during filtration.

	R_m ($\times 10^{11}$ m^{-1})	R_m/R_t (%)	R_p ($\times 10^{11}$ m^{-1})	R_p/R_t (%)	R_c ($\times 10^{11}$ m^{-1})	R_c/R_t (%)	R_t ($\times 10^{11}$ m^{-1})
MG	8.49	12.68	23.04	34.43	35.39	52.89	66.92
MM	8.49	22.02	1.69	4.38	28.37	73.6	38.55
GG	8.49	13.76	17.98	29.15	35.21	57.09	61.68

In this study, flux data of MG-, MM- and GG-blocks filtration were fitted to Eqs. (3.4)-(3.7), respectively (Table 3.3). Results were further analyzed at three different time intervals, i.e. initial filtration (0-15 minutes), intermittent to stable filtration (15-200 minutes) and the entire filtration period (0-200 minutes). When the entire filtration period was considered, all flux data could be best fitted to the cake filtration model, suggesting that cake formation was the main cause of fouling in the 200-minutes filtration of three different alginate blocks. Furthermore, it appears from Table 3 that in the initial filtration period (0-15 minutes), complete blocking model can provide best description for flux data obtained from MG-block filtration, whereas flux data of MM-block and GG-block can be best fitted to cake filtration model and intermediate blocking model respectively. These results implied that pore blocking was dominant during the initial filtration period of MG-block filtration, while cake formation became significant in MM-block filtration. As for filtration of GG-blocks, it was governed by a combined fouling mechanism of pore blocking and cake formation. In the intermittent to stable filtration period (15-200 minutes), it was found that cake filtration model can explain all flux data obtained from filtration of MG-, MM- and GG-blocks, implying cake formation was the main causes of membrane fouling during this period. Indeed these analyses were consistent with the experimental results presented above.

Table 3.3 Model analysis of data obtained from microfiltration of MG-, MM- and GG-block.

Filtration time	Feed solutions	f			
		Complete blocking (Eq.(3.4))	Standard blocking (Eq.(3.5))	Intermediate blocking (Eq.(3.6))	Cake filtration (Eq.(3.7))
0-15 minutes	MG	**1.0000**	0.5734	0.2125	0.0592
	MM	0.3512	0.5156	0.7282	**1.0000**
	GG	0.5395	0.7184	**1.0000**	0.9017
15-200 minutes	MG	0.0073	0.0144	0.0355	**1.0000**
	MM	0.0982	0.2405	0.9237	**1.0000**
	GG	0.0296	0.0694	0.2616	**1.0000**
0-200 minutes	MG	0.0187	0.0351	0.0837	**1.0000**
	MM	0.1024	0.2459	0.6926	**1.0000**
	GG	0.0754	0.1742	0.6707	**1.0000**

It appears from the above discussion that the flux data can best fit into cake filtration model for the whole filtration period. According to Eq.(3.7), K_cR_r is an important indicator of the cake formation, which can be calculated from the gradient of the plot of $(J/J_0)^{-2}$ versus filtration time. It can be seen in Figure 3.7 that the filtration MG-block solution possessed had the highest a K_cR_r value among all the three blocks studied. These in turn suggest that more cake layer formed on membrane in the filtration of MG-blocks. Such an observation indeed is consistent with the resistance analysis as discussed above (Table 3.2).

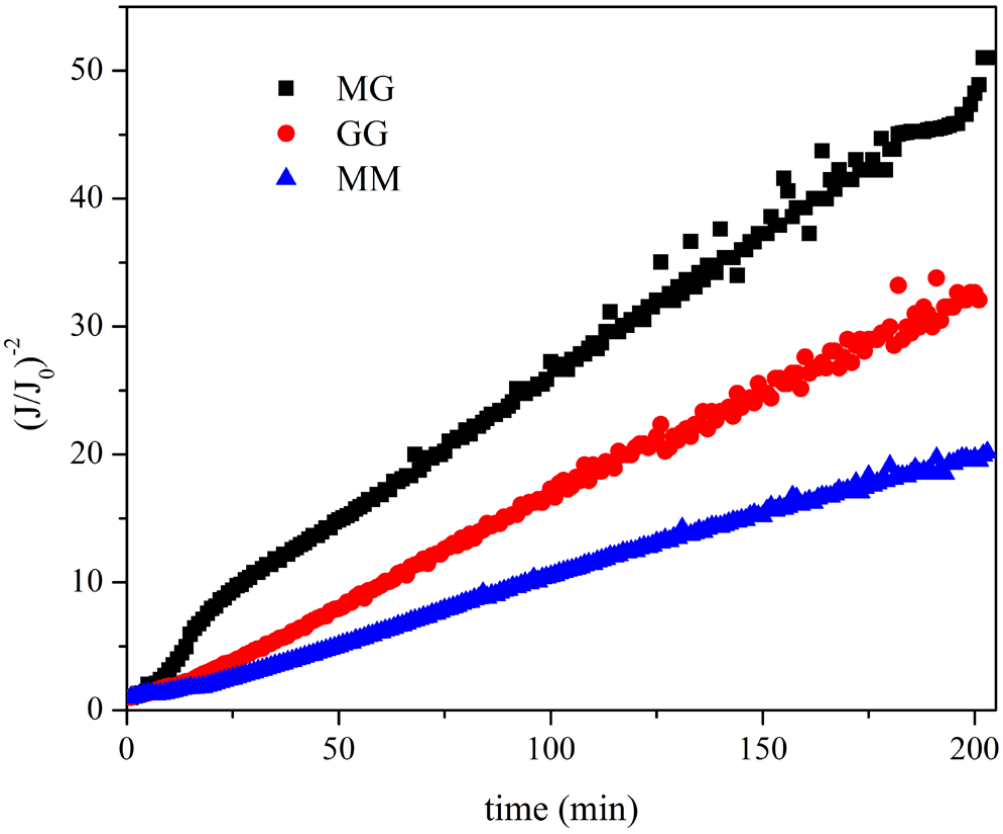

Figure 3.7 Time evolution of $(J/J_0)^{-2}$ for MG-block, MM-block and GG-block.

As MG-, MM- and GG-blocks have distinct chemical and physical properties, it is reasonable to consider that they may have different fouling propensities. The respective flux profiles of these three blocks (Figure 3.6) indeed revealed that MG-blocks caused the most serious fouling, while the least fouling for filtration of MM-blocks. The theoretical analysis by various models further confirmed that pore blocking was the main fouling mechanism in initial filtration period (0-15 min) of

MG-block, and subsequently cake formation became the dominant afterwards. On the contrary, for filtration of MM-blocks, cake formation was responsible for fouling development throughout the whole filtration process (Table 3.3). These suggested that in filtration of MG-blocks, a certain amount of MG-blocks penetrated into the membrane pores, and subsequently were adsorbed onto the internal walls of membrane, leading to reduced radius and number of the effective membrane pores. Different from MG-blocks, some MM-blocks first accumulated onto the membrane surfaces to form a cake layer which acted as a pre-filter to prevent membrane from further pore blocking. This observation was also supported by the results obtained from resistance-in-series model (Table 3.2). The pre-filter effect of cake layer was also observed by Liu and Sun (2012) in study of membrane fouling by different size particles. In this study, pore blocking observed in filtration of MG-blocks accounted for 34.4% of total filtration resistance, whereas only 4.38% of total resistance was due to pore blocking infiltration of MM-blocks. The high R_c value observed in filtration of MG-blocks was possibly due to the subsequent accumulation of MG-blocks on membrane surface after pore blocking. The fouled membranes after 200 minutes filtration were further examined by FE-SEM (Figure 3.8), and cake layer was observed on membrane surface in filtration of all three alginate blocks, leading to blockage of membrane surface.

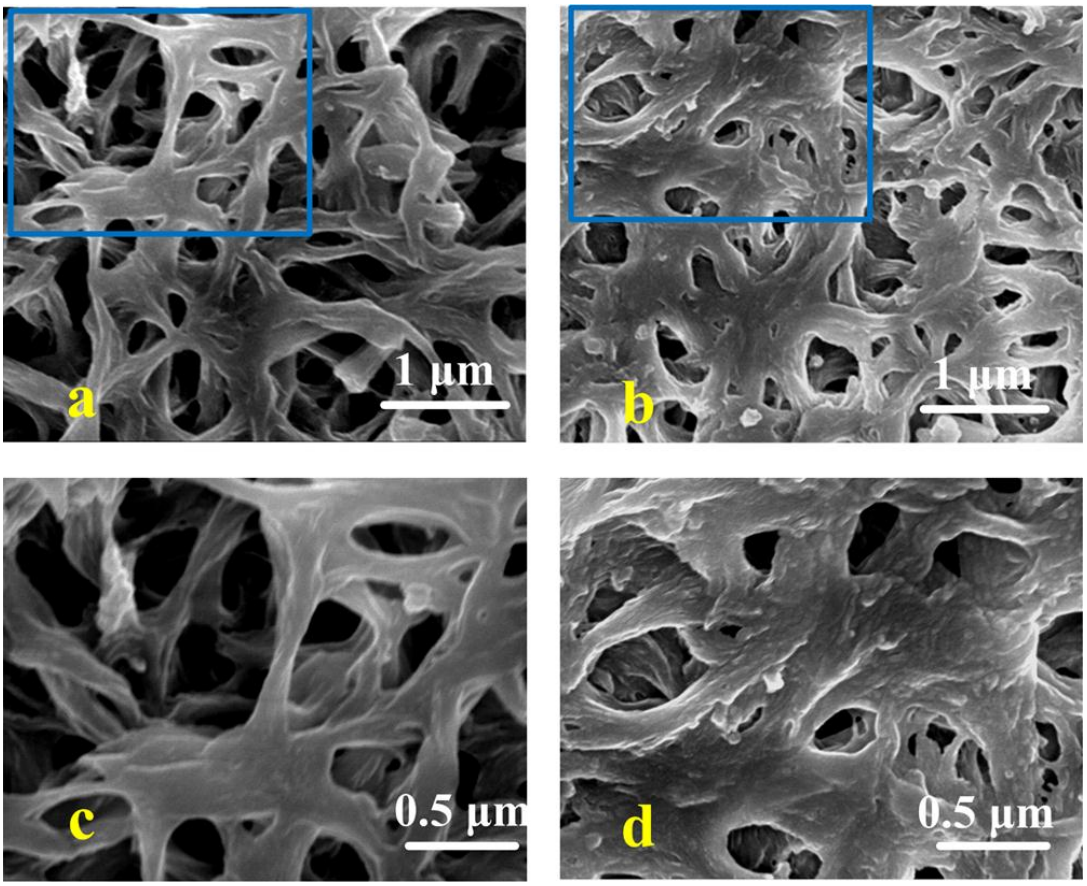

Figure 3.8 Autopsy of fouled membrane surface by an FE-SEM. a: clean membrane surface; b: fouled membrane surface; c: zoom in of the blue area in a; d: zoom in of the blue area in b.

So far, more than 200 kinds of alginates derived from different sources are commercially available (Tønnesen and Karlsen 2002), which would be different in MG-, MM- and GG-blocks contents as well as in the length of each block (Lee and Mooney 2012). As discussed above, it is reasonable to consider that alginates extracted from different sources may behave differently in development of membrane fouling. As alginates have been commonly used as a model polysaccharide in numerous studies of membrane fouling (Lee and Elimelech 2006, Sioutopoulos et al. 2013), these would pose a new challenge on interpretation and reliability of filtration data if alginates used in filtration experiments were not well characterized.

3.3.3 TEP Formation and Interaction Energy of Alginate Blocks

3.3.3.1 TEP Formed from MG-, MM- and GG-blocks

Results showed that TEP with highest concentration was observed in MM-block solution, while the lowest TEP levels were found in MG-block solution (Figure 3.9). Besides, the concentration of TEP formed from GG-blocks was slightly higher than that from MG-blocks, but much lower than those from MM-block (Figure 3.9). In particular, the TEP with sizes bigger than 0.2 μm and in between 0.1-0.2 μm in MG-block solution were 7.02- and 8.73-fold lower than TEP in the MM-block solution. These suggest that MG-blocks had the lowest ability to form TEP, especially TEP bigger than 0.2 μm, while MM-blocks exhibited the highest potential towards TEP formation. In addition, it should be noted that most TEP produced from three alginate blocks fell into a size range of 0.05 to 0.1 μm, and the TEP fraction in this range accounted for 72.0% to 92.7% of total TEP.

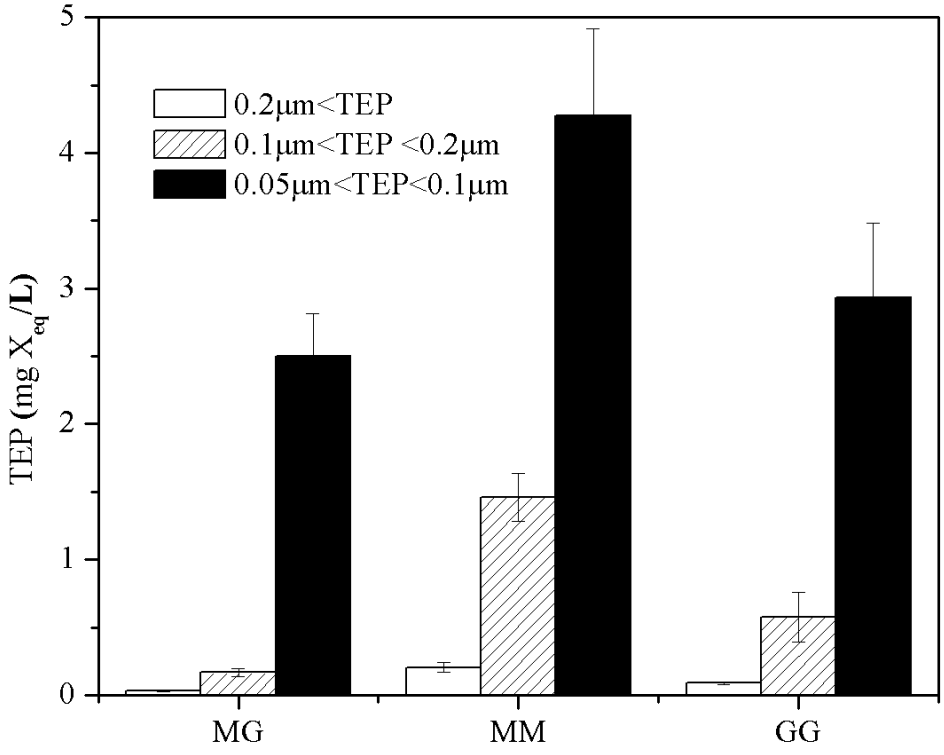

Figure 3.9 TEP levels in MG-, MM- and GG-blocks solutions. Data are shown as the mean±s.d.

Figure 3.10 shows microscopic observation of TEP formed from different alginate blocks which were retained on membrane surfaces. It can be seen that MG-blockstended to form small cluster with a few blocks (Figure 3.10a), while MM-blocks could form bigger clusters through agglomeration of much more MM-blocks (Figure 3.10b). Compared with MG-block and MM-block, GG-block morphologically seemed to be thinner and longer, and produced fibril-like TEP (Figure 3.10c). These indicated that MG-, MM- and GG-blocks would have different self-affinities and abilities in formation of TEP with various morphologies. Consequently, it is reasonable to consider that TEP found in natural water environments (e.g. surface water and seawater) would be developed through self-aggregation of alginates secreted by bacteria and algae.

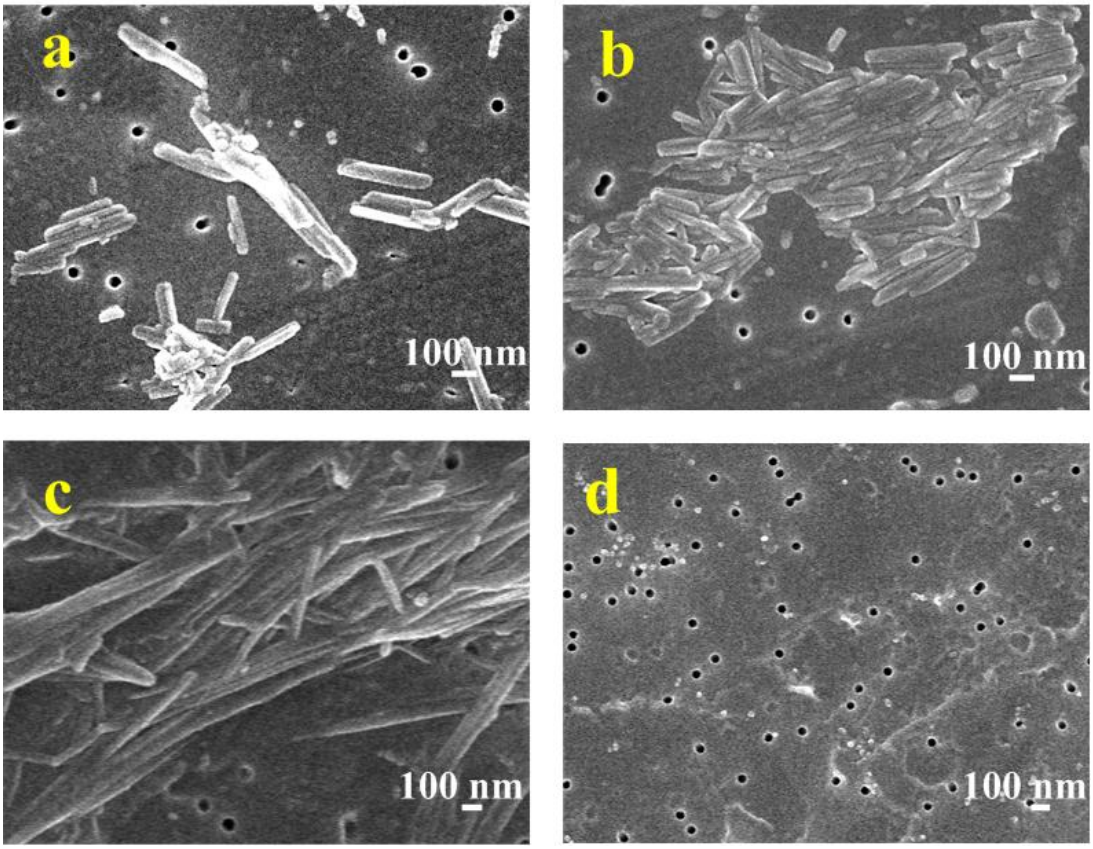

Figure 3.10 FE-SEM images of TEP formed from alginate blocks. a: MG-block; b: MM-block; c: GG-block; d: clean filter.

3.3.3.2 Contact Angles and Zeta Potentials of MG-, MM- and GG-blocks

Table 3.4 shows the contact angles of the three alginate blocks and their respective zeta potentials at pH of about 6.5. It can be seen that MG-, MM- and GG-blocks had almost the same water contact angle, while significant differences in their contact angles were observed when glycerol and diiodomethane were used as probe liquids. As shown in Figure 3.11, all the samples were negatively charged , in the pH range of 3 to 10, while the zeta potentials were in the order of alginate<GG-block<MG-block<MM-block. It appears that alginate was the most stable with the lowest zeta potential in the pH range studied. Among the three blocks, MM-block with the lowest zeta potential of -15.7 mV appears to be most unstable alginate block, and tended to self-aggregate. On the other hand, MG-block and GG-block are more stable in water solutions with respective zeta potential of -28.2 mV and -38.4 mV, indicating that their molecules are more dispersible into solution. In general, these results are consistent with amounts of TEP formed in MG-, MM- and GG-block solutions (Figure 3.9), i.e. MM-block produces most TEP, while MG-block and GG-block solutions generate much less TEP.

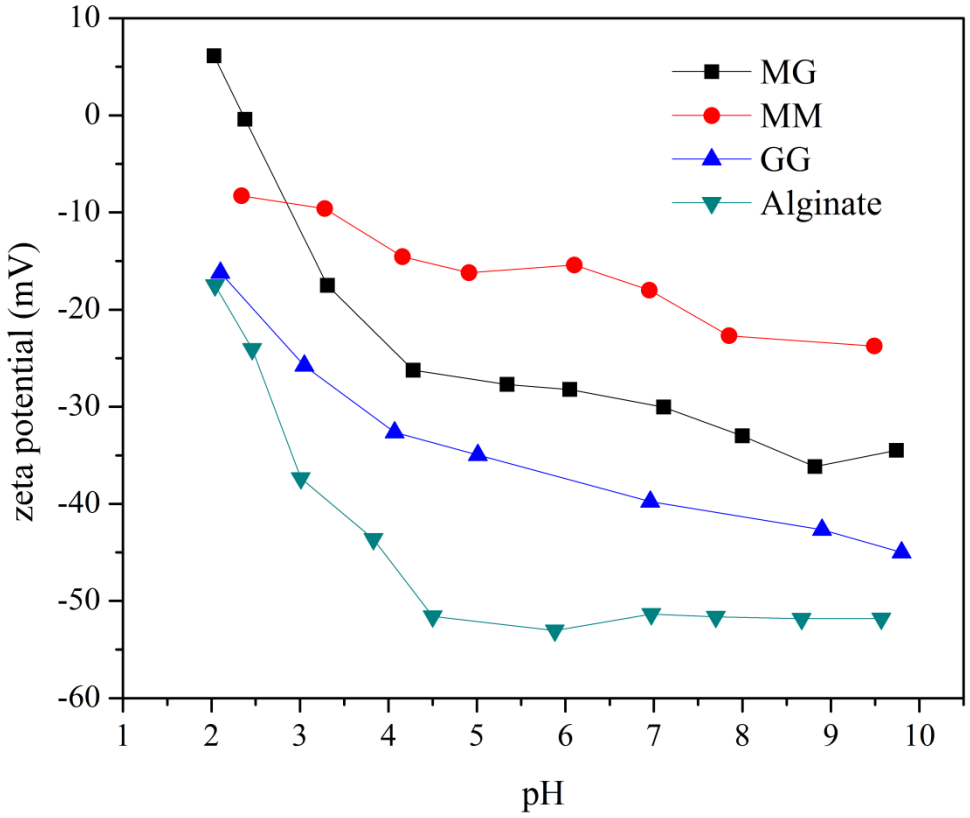

Figure 3.11 Zeta potentials of alginate sodium, MG-, MM- and GG-blocks in 10 mM NaCl as a function of pH.

Table 3.4 Contact angles and zeta potentials (pH 6.5) of MG-, MM- and GG-blocks.

	Contact angles (°)			Zeta potential (mV)
	Ultrapure water	Glycerol	Diiodomethane	
MG	20.6±1.4	64.8±1.3	50.3±0.9	-28.2±1.1
MM	21.3±1.0	25.9±1.2	61.2±2.0	-15.7±1.3
GG	25.7±0.9	62.1±0.8	52.6±1.5	-38.4±1.6

3.3.3.3 Free Energy of Cohesion of MG-, MM- and GG-block

Table 3.5 shows the surface tension parameters of three alginate blocks, which were calculated by Eqs. (3.10) to (3.12). It was found that all alginate blocks had high

electron donor components (γ^-) and relatively lower electron acceptor components (γ^+). The higher γ^- values may be due to the presence of abundant carboxyl (COO-) and hydroxyl (-OH) function groups in alginate. Similar results were also reported by Jin et al. (2009).In particular, MG-blocks and GG-blocks had much higher electron donor parameter (γ^-) compared with MM-blocks, revealing that the former surfaces may carry more electrons. These implied that the repulsive forces due to polar interactions were greater among MG-blocks and GG-blocks, i.e. more difficult for MG-blocks and GG-blocks to aggregate. In fact, such analysis was supported by the TEP data showing less TEP formed in MG- and GG-block solutions than in MM-block solution.

Table 3.5 Surface tension properties (mJ/m^2) of MG-, MM- and GG-block

	γ^{LW}	γ^+	γ^-	γ^{AB}	γ^{TOT}
MG	34.12	0.92	90.51	18.25	52.37
MM	27.94	4.66	47.37	29.70	57.64
GG	33.41	0.34	80.04	10.48	43.89

Table 3.6 shows the respective free energy of cohesion per unit area for MG-, MM- and GG-blocks, determined according to XDLVO theory. Cohesion energy describes the energetic favorability of alginate block interacting through water with itself. For all three alginate blocks, the Lewis acid-base component ΔG^{AB} largely contributed to the total interfacial free energy, whereas the Lifshitz-van der Waals component ΔG^{LW} was found to be negative with a much lower absolute value. Compared with other two terms, the electrostatic double layer component ΔG^{EL} seemed to contribute least to the total interfacial energy, and could be ignored in the calculations of organic compounds cohesive energy (Van Oss 2006). A positive value of cohesion free energy suggested repulsive interfacial surfaces. According to the total interfacial free energy, ΔG^{TOT} (Table 3.6), the highest repulsive force was observed in MG-blocks, i.e. MG-block would have the smallest tendency toward self-aggregate in water solution as compared to other two alginate blocks. On the other hand, with a much lower ΔG^{TOT}, MM-blocks were more likely to aggregate together and further form TEP as compared with MG-blocks. In addition, GG-

blocks had a ΔG^{TOT} value slightly smaller than MG-blocks, thus GG-block had a low ability to form TEP. The relationship between interfacial free energies and TEP derived from alginate blocks is shown in Figure 3.12. These in turn provided a plausible explanation for the formation ability of TEP by GG-, MM- and MG-blocks as presented in Figure 3.9.

Table 3.6 Interfacial free energies (mJ/m^2) of MG-, MM- and GG-block.

	ΔG^{LW}	ΔG^{AB}	ΔG^{EL}	ΔG^{TOT}
MG	-2.75	73.04	0.18	70.47
MM	-0.76	21.20	0.057	20.50
GG	-2.47	69.62	0.34	67.49

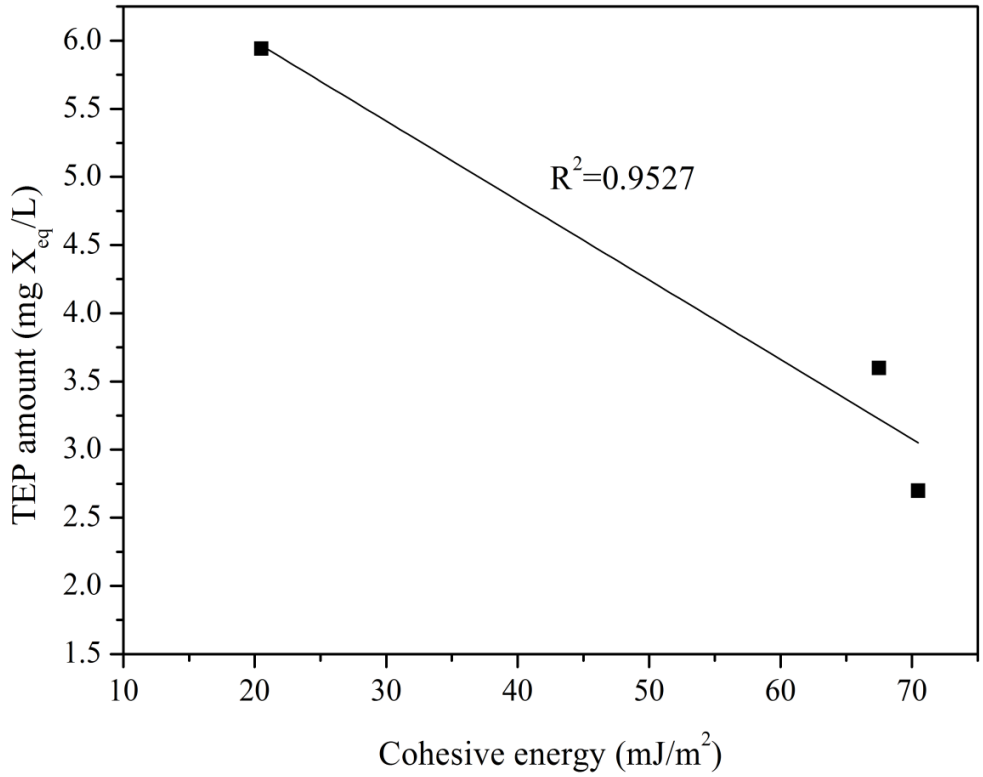

Figure 3.12 Relationship between cohesive energy and TEP levels in the alginate blocks solutions.

3.3.4 Effects of TEP on Membrane Fouling

As shown in Table 3.4, the respective zeta potentials of MG-, MM- and GG-blocks were -28.2±1.1, -15.7±1.3 and -38.4±1.6mV. Figure 3.13 shows the pH-dependent zeta potential profile of the nylon membrane used in this study. Since nylon membrane surface had a zeta potential of 16.6mV at pH 6.5, the attractive electrostatic forces between membrane surfaces and the alginate blocks would be expected. Theoretically, these suggested the highest attraction force between GG-blocks and the membrane surface. However, the severest fouling was not observed in the filtration of GG-blocks, i.e. electrostatic forces might not be the main cause of observed membrane fouling in this study.

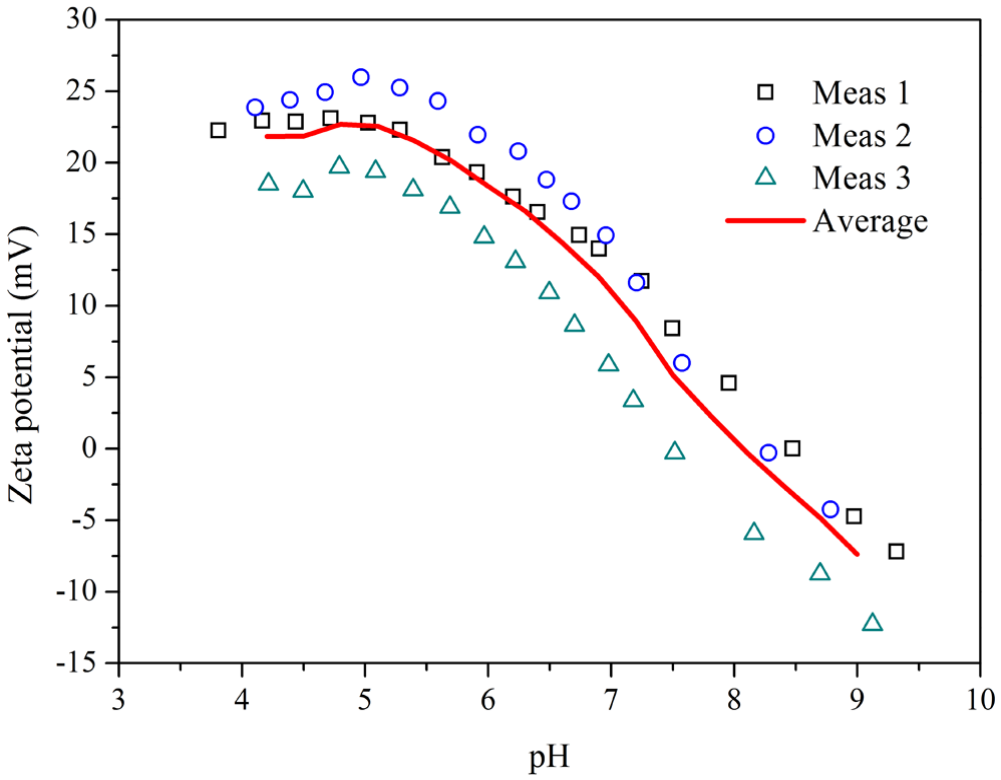

Figure 3.13 Zeta potential of nylon membrane surface as a function of pH.

It can be seen in Figure 3.10 that MG-, MM- and GG-blocks, to some extent, all had tendency to form TEP through self-aggregation, which was in order of MM-block>GG-block>MG-block in terms of quantity (Figure 3.9). These indeed were in good agreement with the predictions by XDLVO theory. For example, the cohesive

interaction energy of MM-blocks was the lowest among all three alginate blocks, suggesting that MM-block had the highest self-aggregation potential in water. As the result, the highest amount of TEP was produced from MM-blocks (Figure 3.9).

As can be seen in Figure 3.6, the smallest flux decline was observed in the filtration of MM-blocks, while the largest flux decrease was found in the filtration of MG-blocks. Such fouling behaviors were likely related to the amount of TEP produced by each kind of alginate blocks (Figure 3.9). Due to their bigger sizes, more TEP than individual blocks would be retained by membrane, leading to the development of cake on membrane surfaces. This is supported by the results in Figure 3.14, showing a positive correlation between of TEP amount in feed water and the ratio of cake resistance to total resistance. In fact, such results were consistent with the theoretical analyses of MG-, MM- and GG-block filtrations (Table 3.3). For example, cake formation was a dominant fouling mechanism in filtration of MM-block solution with high TEP concentration, while pore blocking appeared to be the main cause of membrane fouling for filtration of MG-block solution with the lowest TEP concentration. In fact, Bar-Zeev et al. (2012) reported that TEP tended to attach to solid surfaces. Moreover, Discart et al. (2013) also observed the presence of TEP on microfiltration membrane surfaces. It is a reasonable consideration that TEP should be involved in development of membrane fouling.

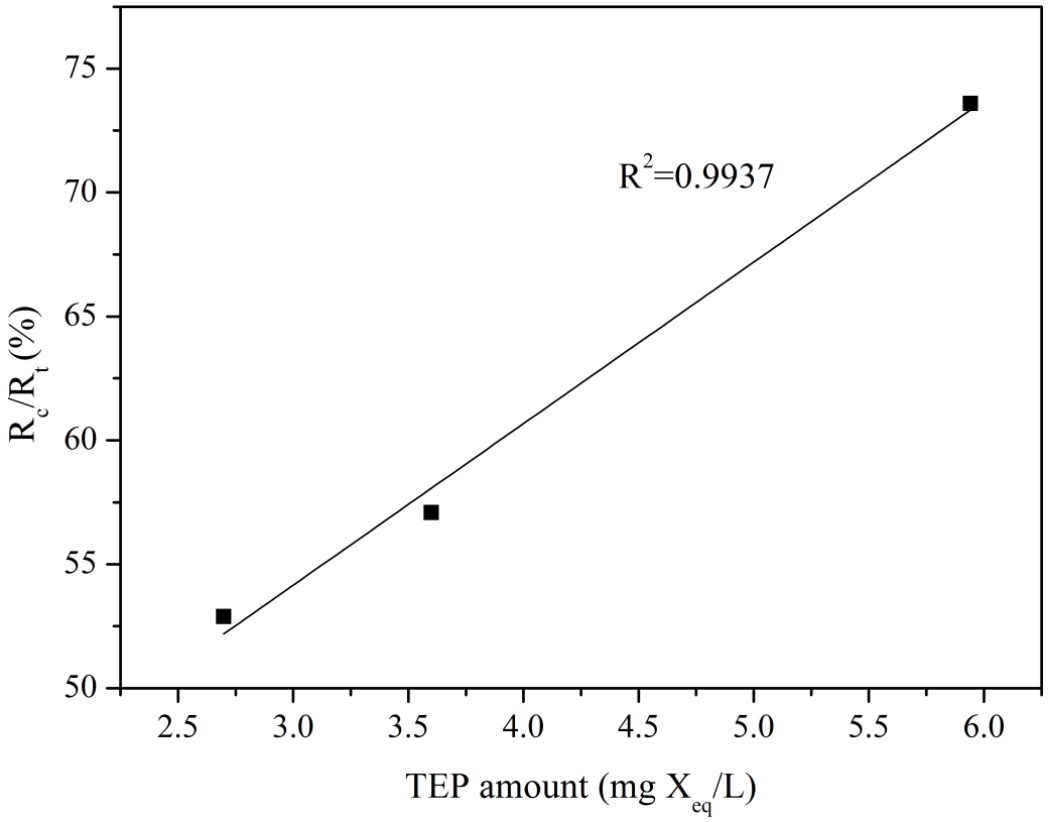

Figure 3.14 Relationship between TEP concentrations and the percent of cake layer resistance in total resistance (R_c/R_t).

3.4 CONCLUDING REMARKS

Alginate was composed of MG-, MM- and GG-blocks, and these three different blocks exhibited distinguished propensities and behaviors of membrane fouling. The severest fouling was observed in the filtration of MG-blocks, while the least flux decline was recorded for MM-blocks. GG-blocks had a fouling tendency in between MG- and MM-blocks. It was also found that the initial pore blocking was responsible for the severe fouling in MG-block filtration, while the cake layer formed on membrane surface during MM-block filtration would serve as a pre-filter that prevented membrane from further pore blocking. The observed fouling behaviors of the alginate blocks, in part, could be explained by their abilities to form TEP. TEP could be developed through self-aggregation or cross-link of alginate blocks. The cake formation was dominant fouling mechanisms at higher TEP concentration (e.g. MM-block solution), while severer membrane pore

blocking was observed at lower TEP concentration (e.g. MG-block solution). This study clearly revealed the effects of TEP on membrane fouling which was related to molecular structure of alginate.

CHAPTER 4 TEP FORMATION FROM ALGINATE BLOCKS AT VARIOUS CALCIUM CONCENTRATIONS AND THEIR EFFECTS ON MEMBRAEN FOULING

4.1 INTRODUCTION

Membrane technology has been intensively employed worldwide for clean water production and wastewater reclamation. However, membrane fouling has been known as a factor leading to increased operation and maintenance costs (Shannon et al. 2008, Elimelech and Phillip 2011, Zhang et al. 2014). Alginate as a typical model foulant has often been used in study of membrane fouling under various conditions (Lee and Elimelech 2006, van den Brink et al. 2009, Katsoufidou et al. 2010, Mi and Elimelech 2010). The combinations and sequences of blocks in alginate may vary widely, and determine the chemical and physical properties of alginate which in turn affect their filtration behaviors (Draget et al. 2005, Lee and Mooney 2012, Meng and Liu 2013). Evidence also showed that the filtration behaviors of alginates were also significantly influenced by the presence of divalent cations, e.g. calcium ion (Katsoufidou et al. 2007, van de Ven et al. 2008, Listiarini et al. 2009). For example, a strong correlation between calcium ion concentration and membrane fouling rate by alginate had been reported by van den Brink et al. (2009). Such an observation can be explained by the classic “egg-box” model according to which calcium ions tend to bind preferentially to the GG-blocks of alginate and form an egg-box-like structure with alginate molecules (Grant et al. 1973, Draget et al. 2005). In turn, the later may lead to the development of alginate cake layer on membrane surfaces (Katsoufidou et al. 2007, van den Brink et al. 2009). It should be realized that no study has explored the effects of calcium ion on membrane fouling development in consideration of alginate molecular composition. As MG-, MM- and GG-blocks of alginate have distinguished chemical and physical

This chapter has been published as: Meng S., Winters H, Liu Y. Ultrafiltration behaviors of alginate blocks at various calcium concentrations. Water Research, 2015, 83: 248-257.

characteristics, it is reasonable to consider that these alginate blocks may possess highly different fouling propensities in the presence of calcium ion.

Increasing evidence suggests that transparent exopolymer particles (TEP) are responsible for the development of membrane fouling (Berman and Holenberg 2005, Meng et al. 2013, Bar-Zeev et al. 2015). TEP originally found in marine environment is a class of transparent particulate acidic polysaccharides that can be stained by alcian blue (Alldredge et al. 1993). Operationally, TEP has been defined as particles retained by 0.4 μm polycarbonate filter that can be stained by alcian blue (Passow and Alldredge 1995). This pore size 0.4 μm was chosen due to the fact that in limnological research, substances passing through 0.2-0.4 μm filters are usually considered as "soluble" (Discart et al. 2015). Concurrently, polysaccharide materials stained by alcian blue and passing through 0.4 μm polycarbonate filters are considered as precursors of TEP, which can further form TEP (Passow 2000). Subsequently, to better understand the role of TEP in the development of membrane fouling, Villacorte et al. (2009a) further fractionated TEP according to their sizes by using in-series filtrations with filters of different pore sizes (i.e. 0.05 to 0.4 μm). So far, the involvement of TEP in the fouling development in various membrane systems including microfiltration (MF), ultrafiltration (UF) and reverse osmosis (RO) had been reported (Villacorte et al. 2009a,b, 2010a,b, 2012). Alginate as a common and widespread polysaccharide has been reported to generate TEP-like particles that can be stained by alcian blue and was used as standard calibration substance for TEP determination (Passow and Alldredge 1995, Thornton et al. 2007). Previous study showed that TEP can form from alginate blocks (e.g. MG-, MM- and GG-blocks) (Meng and Liu 2013). Therefore, it is reasonable to use alginate blocks as a model of TEP and this study mainly aimed to explore the effects of calcium ion on the formation of TEP from MG-, MM- and GG-blocks as well as the specific roles of the formed TEP in the development of membrane fouling.

4.2 MATERIALS AND METHOD

4.2.1 Alginate Fractionation

The alginate was fractionated following the method as described in Chapter 3 to obtain MG-, MM- and GG-blocks. Results show that the alginate sodium used was composed of 13.8±1.9% of MG-block, 53.5±1.3% of MM-block and 32.7±0.6% for GG-block. MM-block was the main component of the alginate studied. All alginate blocks samples should be stored in a copper sulfate dryer to prevent them from being exposed to the damp room condition.

4.2.2 TEP Formation from Alginate Blocks at Different Levels of Calcium Ion

4.2.2.1 Determination of TEP

TEP formed in respective MG-, MM-, and GG-blocks solutions with and without the presence of calcium ion were determined similarly with the method described in Chapter 3. Briefly, 50 mg/L of sample solutions were prepared by dissolving the required amount of MG-, MM- and GG-blocks into ultrapure Milli-Q water with continuous stirring for 2 hours. $CaCl_2 \cdot 2H_2O$ (Sigma, USA) was used to make up solutions with different calcium ion concentration. All sample solutions were freshly prepared just before the determination of TEP. A series of polycarbonate filters (Whatman, United Kingdom) of pore size 0.05, 0.1, 0.2 and 0.4 μm were employed to determine the TEP respectively. Three to five measurements were conducted for each sample and every sample was measured at least three times. The average absorbance was then used to calculate the TEP concentration in each sample. Gum xanthan (Sigma, USA) was used as a standard substance of TEP for calibration and the TEP concentration was finally expressed as mg gum xanthan equivalent per liter of water (mg $X_{eq} \cdot L^{-1}$). It should be noted that the term TEP used in this study was subjective to the definition by Villacorte et al. (2009a), i.e. alcian blue-stainable particles that can be retained by 0.05 μm polycarbonate filter.

4.2.2.2 Microscopic Observation of TEP

The appearance of TEP derived from alginate blocks in the presence or absence of calcium ion was observed by a microscope (Keyence, Japan). The fresh TEP solutions were prepared prior to observation as described in Section 4.2.2.1. In order to visualize TEP with the bright-field microscope, alginate block solutions with or without presence of calcium ion were stained by freshly pre-filtered (0.05 μm polycarbonate filter) alcian blue solution as presented in Chapter 3 (Passow and Alldredge, 1995). Stained samples were then observed under the microscope. For each sample, about 20 images were randomly taken.

4.2.3 Field Emission Scanning Electron Microscope (FE-SEM) Analysis and Zeta Potential Measurements

The changes in the microstructures of alginate blocks due to addition of calcium ion were observed by an FE-SEM (Jeol JSM-7600F, Japan). For FE-SEM observation, MG-, MM- and GG-blocks in the absence and presence of calcium ion were first collected. 10-20 mL of the same sample solutions as used in above section were filtered through 0.1 μm polycarbonate filters (Whatman, United Kingdom) at 0.2 bars and then freeze dried completely in a freeze dryer (Christ, Germany) for further examination. All samples were observed at least three times and each time 5-10 pictures were randomly recorded.

The zeta potentials of alginate blocks in the absence and presence of calcium ion were also measured using a Malvern ZetaSizer Nano ZS. All samples were freshly prepared prior to the measurements and each measurement was repeated at least five times.

4.2.4 Cross-flow Ultrafiltration Experiments

The filtration behaviors of various alginate blocks solutions in the presence or absence of calcium ion were examined in a standard laboratory-scale cross-flow ultrafiltration module (Sterlitech, USA) at a constant pressure of 2 bars and a temperature of 25±2°C. Feed solutions were prepared as described in Section

4.2.2.1. A commercial polyethersulfone (PES) UF membrane (AMFOR INC, Beijing) with molecular weight cut off (MWCO) of 20 kDa was used in this study. The flat sheet PES membrane was soaked in the Milli-Q water for at least 12 hours for membrane wetting prior to use. Feed water was circulated in the close-loop module by a gear pump (Cole-Parmer, USA) at a cross-flow velocity of 10 cm/s. Permeate was collected in a beaker which was placed on an electronic balance. The weight of permeate was recorded at the time interval of 15 s by the data logger system which was connected to a computer. Before each filtration test run, Milli-Q water was first filtered for 24 hours to compact and equilibrate the membrane. Filtration test of each sample was repeated at least three times. Furthermore, in order to determine the rejection rate of MG-, MM- and GG-blocks by the UF membrane, the total organic carbon (TOC) concentrations in the feed and the permeate were analyzed by a TOC analyzer (Shimadzu, Japan). The respective TOC concentrations in the feed water prepared from MG-, MM- and GG-blocks were found to be 18.0±0.2 mg/L, 18.0±0.1 mg/L and 17.9±0.2 mg/L.

4.2.5 Analyses of Fouling Rate and Foulant Mass

The total membrane filtration resistances were calculated according to Darcy's law:

$$J = \frac{\Delta P}{\mu R_t} \tag{4.1}$$

where J is the permeate flux ($m^3m^{-2}s^{-1}$); R_t is the total filtration resistance (m^{-1}); ΔP is the applied pressure (Pa); and μ is the solution viscosity (Pa•s). Fouling rates were determined from the slope of the plot of total resistance versus time, whereas the initial fouling rate was calculated from the initial linear part in the plot of total resistance against filtration time as shown in Figure 4.1. In addition, total foulant mass deposed on the membrane surface was measured as the difference between the initial amount of alginate blocks in the feed and that left in the solution after the filtration.

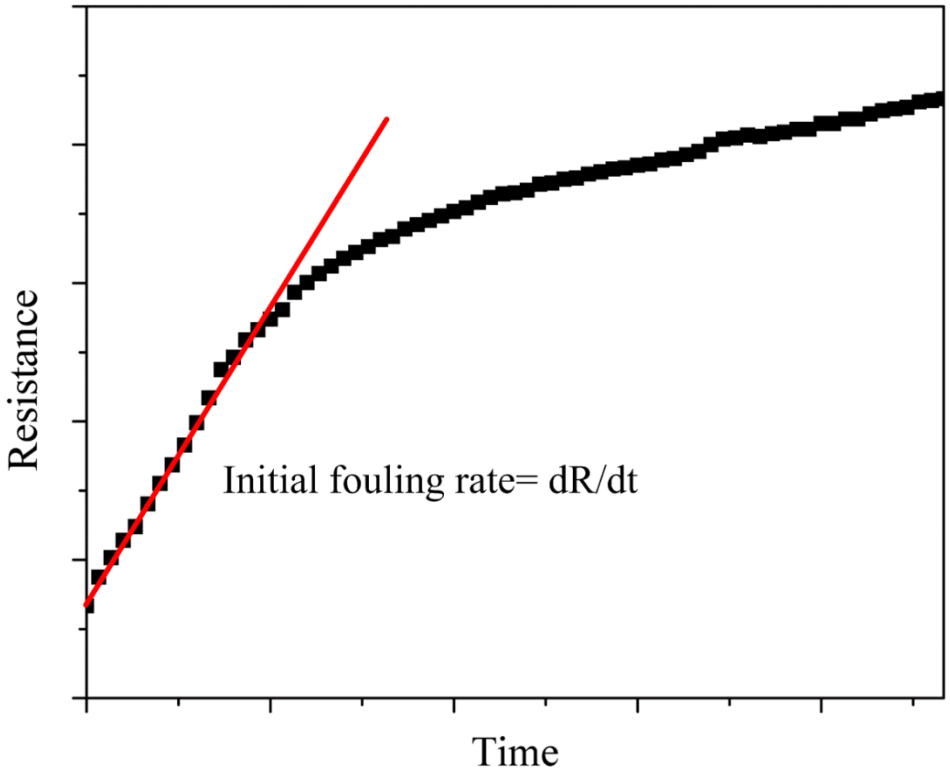

Figure 4.1 Calculation of initial fouling rate (d*R*/d*t*) from the filtration data.

4.2.6 Characterization of Fouled Membrane

Surface morphology and topography of the fouled membranes were examined by the FE-SEM and a XE 100 atomic force microscope (AFM, Park Systems, Korea) respectively. In order to track of the development of cake layer on the membrane surface, membrane samples taken at different filtration times of 10 min, 30 min and 1,500 min were examined. The sampled membranes were completely dried in a freeze dryer (Christ, Germany) prior to observation. For the purpose of comparison, samples used for respective FE-SEM and AFM observations were cut from the same location of fouled membranes. For each observation, at least 16-20 pictures were randomly recorded.

4.3 RESULTS AND DISCUSSION

4.3.1 TEP Derived from Alginate Blocks at Various Calcium Concentrations

4.3.1.1 TEP Concentrations Derived from Alginate Blocks

Figure 4.2 shows the concentrations of TEP derived from the MG-, MM- and GG-blocks in the absence and presence of calcium ion. Without addition of calcium ion, the MM-blocks exhibited greatest tendency of self-aggregation, as the result, the highest concentration of TEP was recorded among three alginate blocks, whereas the lowest-concentration TEP was observed in the solution of MG-blocks. These can be reasonably explained by different cohesive interaction energies between alginate block molecules that can be calculated by extended Derjaguin-Landau-Verwey-Overbeek (XDLVO) theory (Meng and Liu 2013). For example, the cohesive interaction energies of MG-, MM- and GG-blocks are all positive and tend to decrease in the order of MG>GG>MM. A positive cohesion free energy indeed reflects a repulsive force between interfacial surfaces. Therefore, MG-blocks should have the lowest self-aggregation tendency for TEP formation, whereas TEP would likely be easily formed from self-aggregation of MM-blocks as observed.

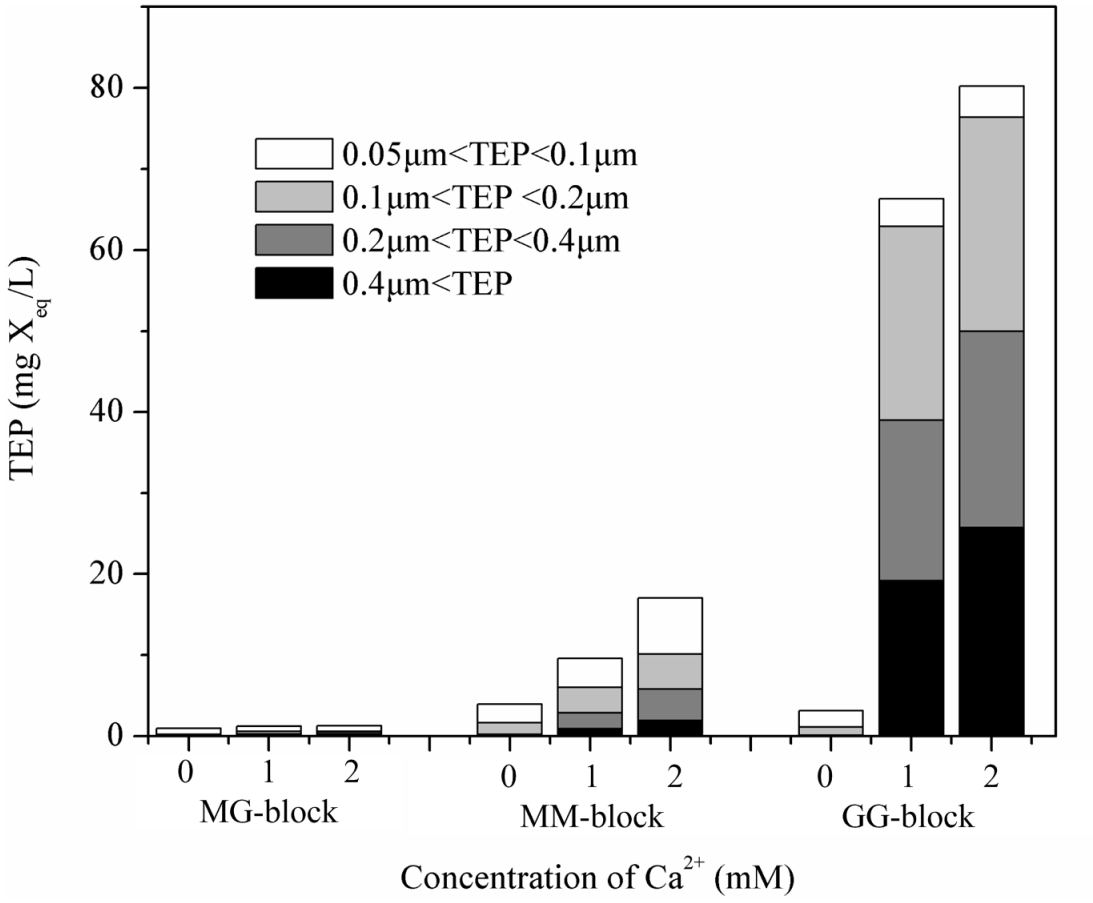

Figure 4.2 TEP concentrations derived from MG-, MM- and GG-blocks at various calcium concentrations.

It should be noted that the formation of TEP in the presence of calcium ion appeared to be different from those observed in the cases without addition of calcium ion. In sense of chemical coagulation, calcium ion can enhance the aggregation of all the alginate blocks, leading to more TEP production as shown in Figure 4.2. It was found that the concentrations of TEP derived from alginate blocks tended to increase in the order MG<MM<GG in the presence of calcium ion. In fact, it was not surprising to observe that GG-blocks generated the highest-concentration TEP. As documented in the literature, there is a strong binding between GG-block and calcium ion, resulting in a three dimensional network of alginate strands held together through ionic interactions, known as "egg-box" structure (Figure 4.3) (Grant et al. 1973, Draget et al. 2005). The biaxially linked G residues in GG-blocks form a cavity that can accommodate divalent calcium ion, i.e. GG-blocks can easily link together through the bridging of calcium ion. As

such, more TEP can develop from GG-blocks in the presence of calcium ion as observed in Figure 4.2.

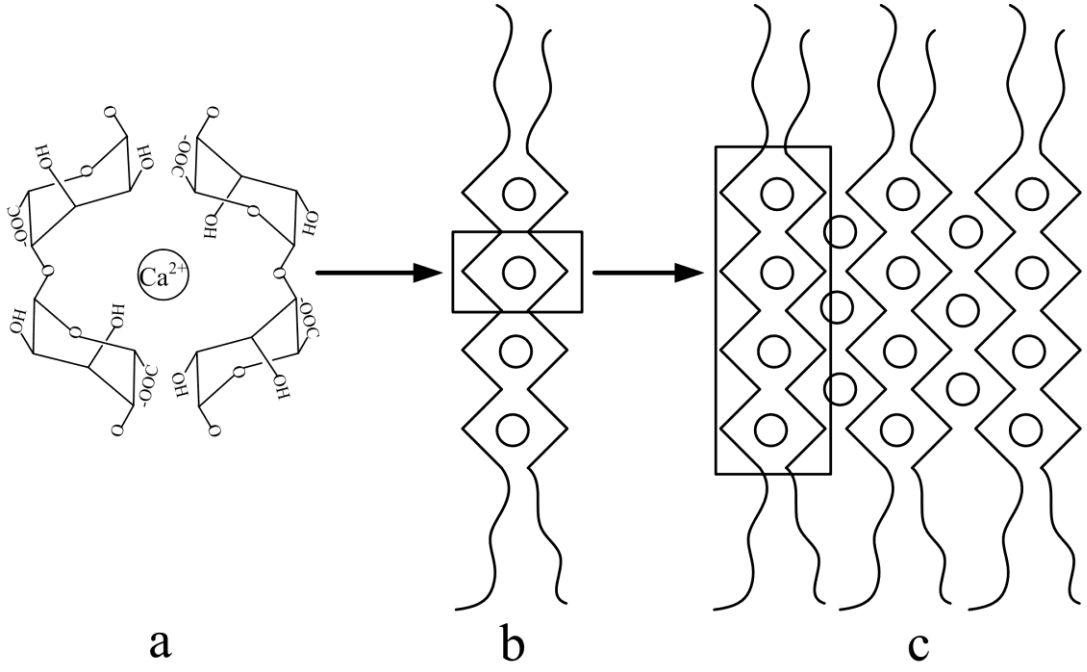

Figure 4.3 The egg-box model of GG-blocks binding with calcium ions (Grant et al. 1973, Draget et al. 2005).

Figure 4.4 further shows TEP formation from GG-blocks at various Ca^{2+} concentrations with a fixed Na^{+} concentration of 10 mM. According to Ca^{2+} concentration, the phases pertaining to TEP development can clearly be derived from Figure 4.4: (i) at low Ca^{2+} concentration (0 to 0.015 mM), TEP formation was not sensitive to Ca^{2+} concentration; (ii) at medium Ca^{2+} concentration of 0.15 to 0.5 mM, the formation of TEP from GG blocks appeared to be proportionally related to Ca^{2+} concentration, and as the result, a sharp increase in TEP concentration was observed in this phase; (iii) at high Ca^{2+} concentration of 0.5 to 2.0 mM, further increase of the Ca^{2+} concentration had insignificant effect on TEP formation from GG-blocks at a given concentration of GG-blocks. These results indeed provide direct evidence showing the dependence of TEP formation on calcium ion, i.e. Ca^{2+} should play a critical role in TEP formation.

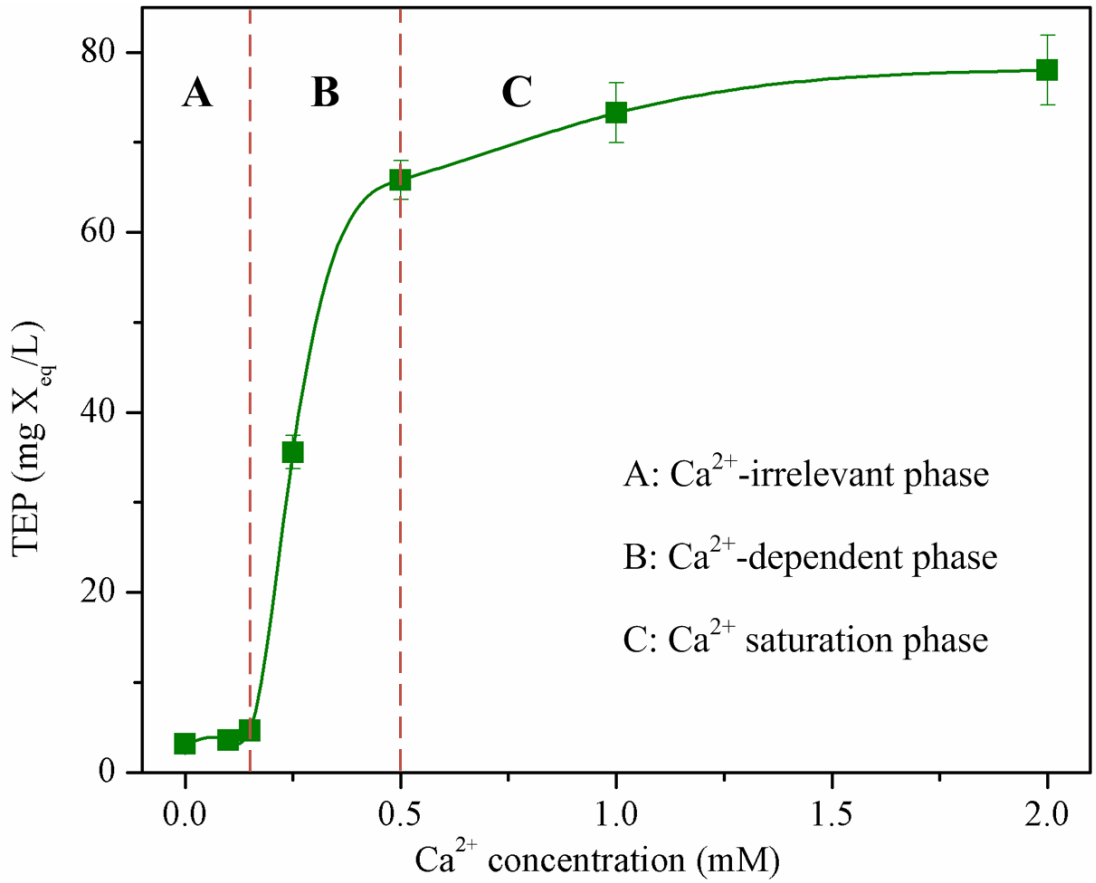

Figure 4.4 The total TEP concentrations (TEP retained by 0.05 μm polycarbonate filters) formed from GG-blocks with increasing Ca^{2+} concentration.

Although the TEP produced from MG- and MM-blocks was also enhanced by addition of calcium ion, it was much lower than that from GG-blocks. The binding mechanisms of MG- and MM-blocks with calcium are currently unclear. It had been reported that hydrogels formed by alginates rich in M residues were softer, less porous and unstable towards disintegration with time as compared with those developed from alginates rich in G residues (De Vos et al. 1996, Simpson et al. 2004). These imply that MG- and MM-blocks can't firmly bind to calcium ion, evidenced by differences in the stiffness of alginate blocks which are in the order MG<MM<GG (Smidsrød 1974, Vold et al. 2006). The differentiation lying in the molecule conformations of MG-, MM- and GG-blocks is shown in Figure 4.5. The highly flexible MG-blocks preferably tend to bind to water molecules instead of forming complexes with calcium ion (Smidsrød, 1974). Therefore, such behavior of MG-blocks indeed unfavors the formation of TEP even in the presence of calcium

ion. This is further supported by the observation of that the TEP concentration was increased insignificantly with increasing the calcium concentration from 1 mM to 2 mM (Figure 4.2). As the rigidity of MM-blocks was higher than that of MG-blocks, MM-blocks should preferably react with calcium ion, as a result, more TEP was produced (Figure 4.2).

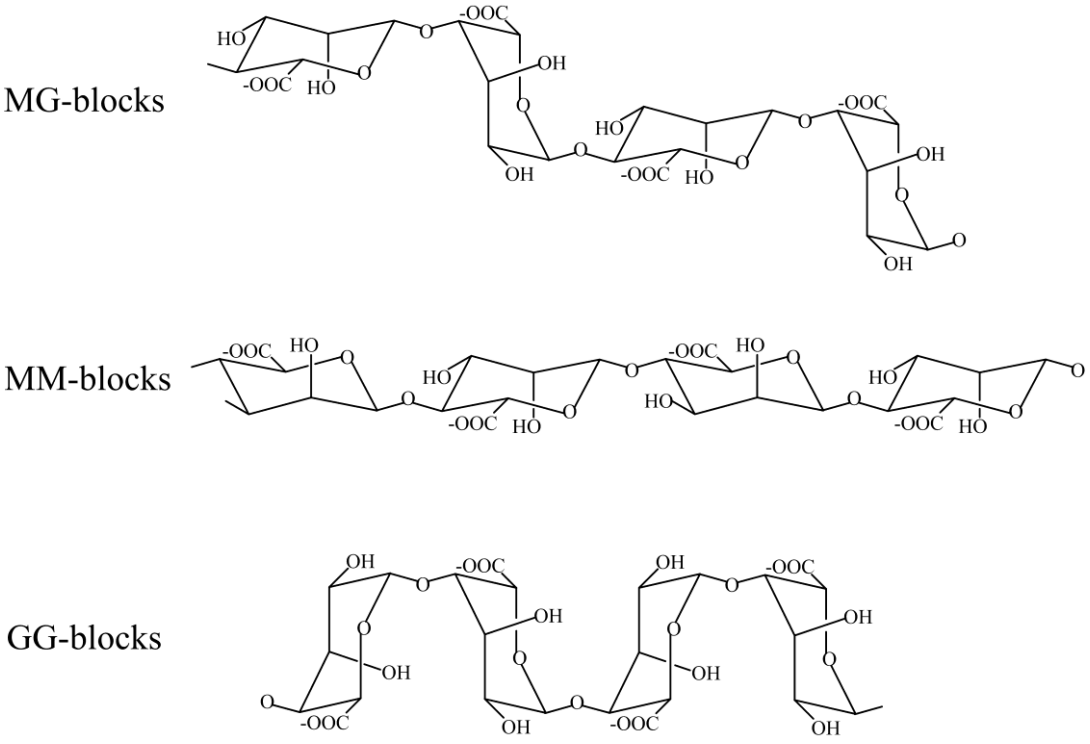

Figure 4.5 The differentiation lying in the molecule conformations of MG-, MM- and GG-blocks.

In addition, the positive correlation between TEP in different size ranges and calcium concentrations in solutions of MM-blocks are observed in Figure 4.6, suggesting the dependence of the TEP formation on the level of calcium ion in the solution MM-blocks.

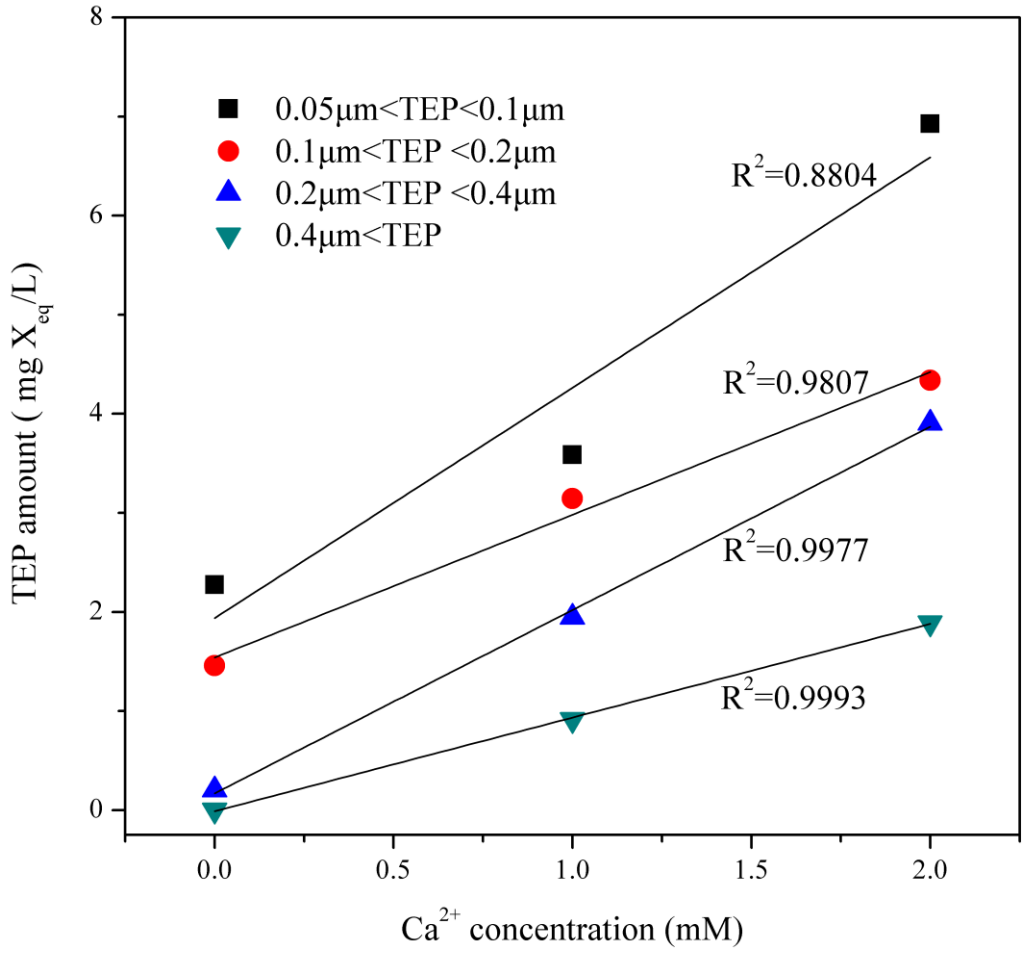

Figure 4.6 Relationship between calcium ion concentrations and TEP levels in MM-block solutions.

4.3.1.2 Effect of Calcium Ion on the Morphology of TEP

TEP formed from MG-, MM- and GG-blocks in the presence or absence of calcium ion were visualized by a light-field microscope. Figure 4.7 provides direct observation of the morphology and structure of TEP derived from alginate blocks. In the absence of calcium ion (Figure 4.7 a-c), only few small TEP were observed. However, much more and large TEP with complex structures were captured in the vision field of the microscope in the presence of calcium ion, as indicated by strong blue color (Figure 4.7 d-f). For example, both the concentration and the size of TEP derived from GG-blocks were significantly increased in the presence of calcium ion. These indeed are in good agreement with the TEP results presented in Figure 4.2. As discussed above, GG-blocks can generate more TEP through the formation

of the complex “egg-box” structure among GG-blocks and calcium ion.

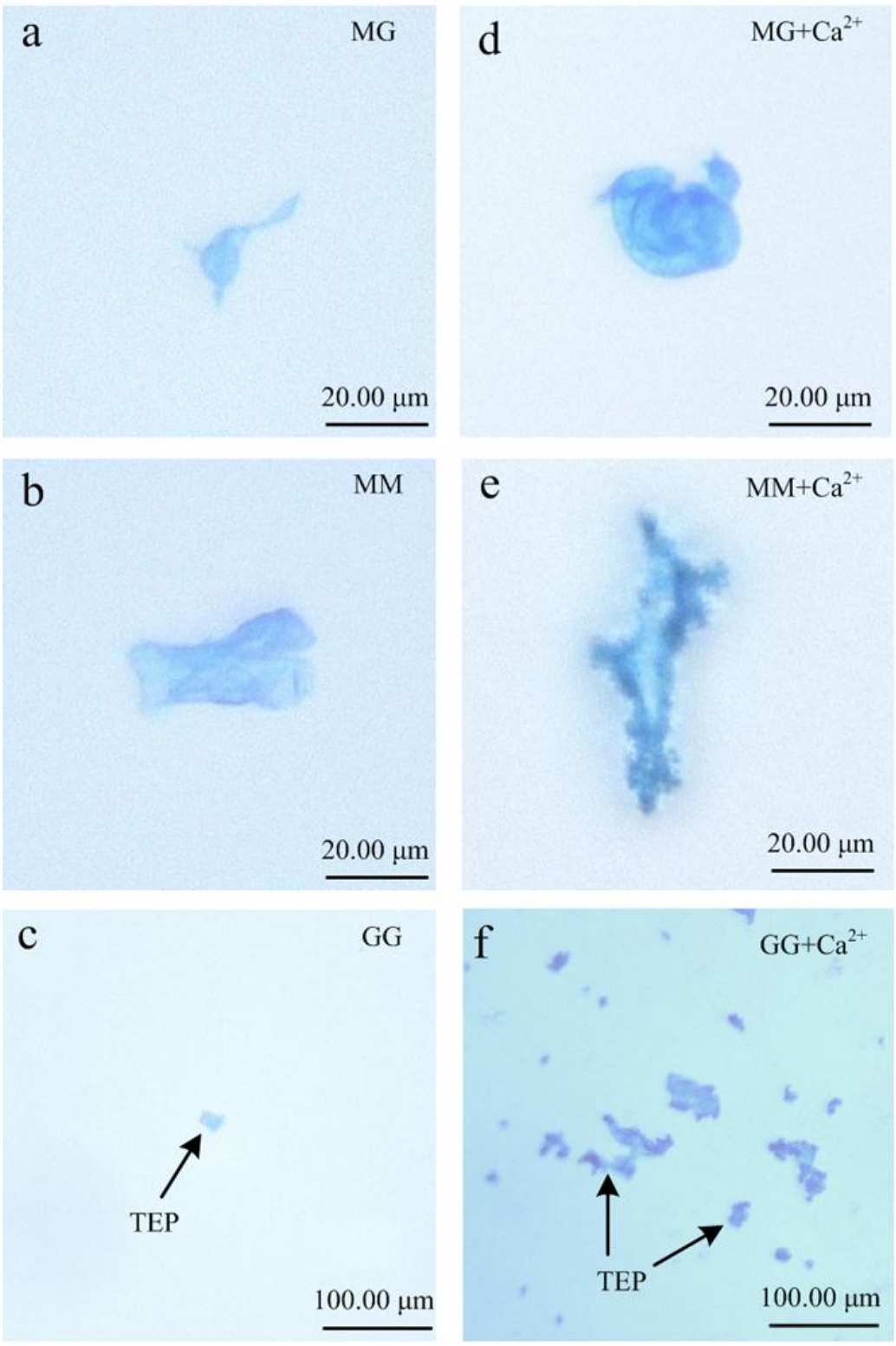

Figure 4.7 Microscopic images of TEP derived from MG-, MM- and GG-blocks without (a, b, c) and with calcium ion (d, e, f). TEP were stained with alcian blue.

4.3.2 Structural Changes of Alginate Blocks with Addition of Calcium Ions

FE-SEM images revealed the changes in microstructure of alginate blocks induced by calcium ion. The filament-type alginate blocks were observed in the absence of calcium ion (Figure 4.8a-c), whereas much bigger and more compact structure was developed for all the three alginate blocks after addition of calcium ion (Figure 4.8 d-f). Moreover, the microscopic morphologies of MG-, MM- and GG-blocks were completely altered by calcium ion. Such changes in the microstructure of alginate blocks are likely due to the binding with calcium ion as discussed above.

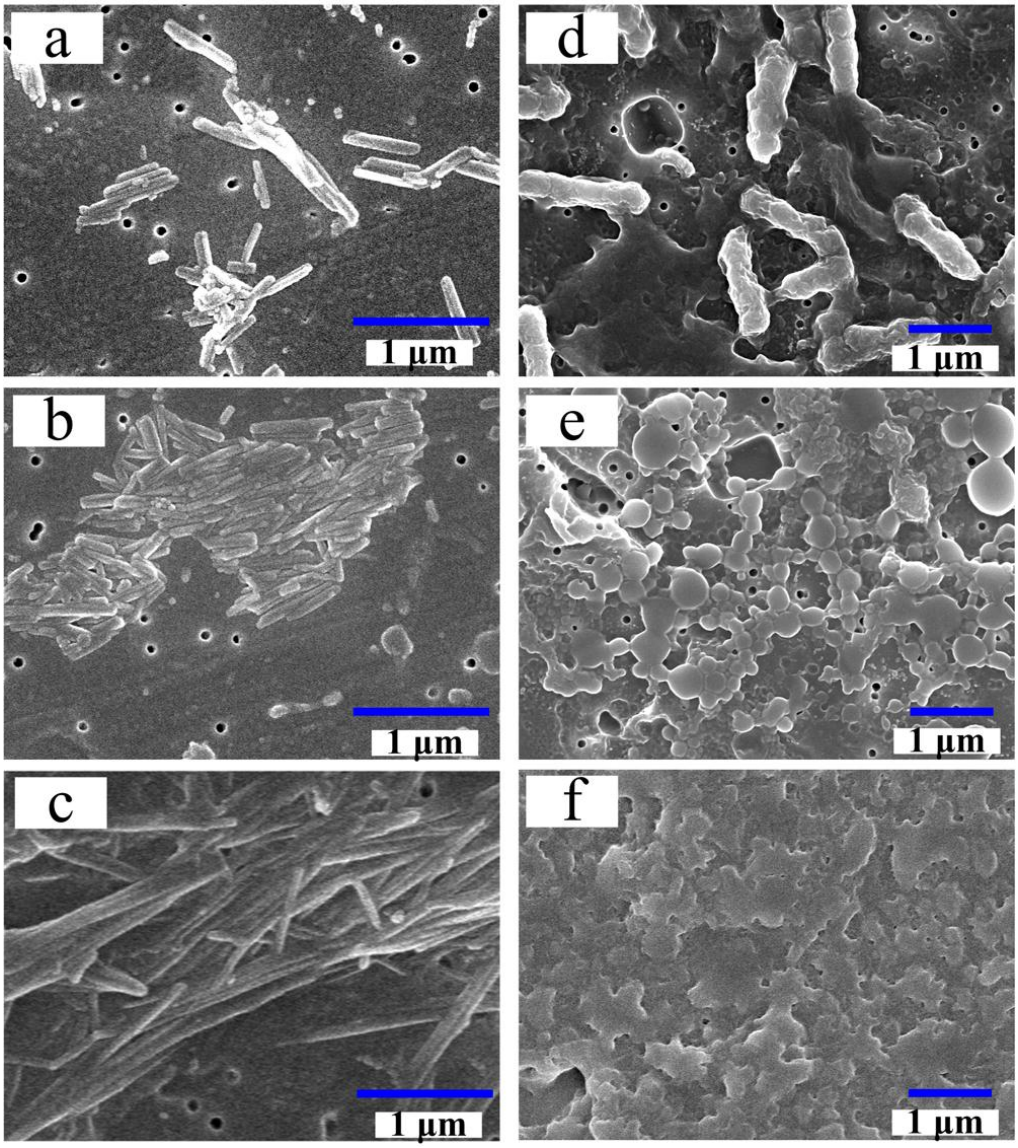

Figure 4.8 Microstructure observation of MG-, MM- and GG-blocks without (a, b, c) and with calcium ion (d, e, f).

Table 4.1 summarizes the zeta potentials of MG-, MM- and GG-blocks solutions at various concentrations of calcium ion. With the addition of calcium ion, the zeta potentials of alginate blocks all tended to decrease, indicating that alginate blocks became less stable and had greater tendency of aggregation among themselves. Consequently, this may affect their fouling propensity during membrane filtration.

Table 4.1 Zeta potentials (mV) of alginate blocks at various calcium ion levels

	0 mM	1 mM	2 mM
MG-blocks	-21.2±1.1	-15.9±1.6	-9.7±1.3
MM-blocks	-13.4±1.7	-11.7±0.9	-9.8±1.2
GG-blocks	-29.9±1.4	-23.7±1.3	-16.7±1.0

4.3.3 Filtration Behaviors of Alginate Blocks at Various Calcium Concentrations

4.3.3.1 Flux Profiles of MG-, MM- and GG-blocks

As presented above, it is obvious that calcium ion has significant effects on the physic-chemical properties and microstructures of MG-, MM- and GG-blocks, subsequently their potentials to form TEP. Figure 4.9 shows the permeate flux profiles observed during the ultrafiltration of MG-blocks at various concentrations of calcium ion. The higher of the calcium concentration, the severer membrane fouling is observed. In the absence of calcium ion, the initial flux declines slowly. However, in the presence of 1 mM and 2 mM calcium ion, a rapid decline was observed at the initial phase. The TOC concentration of the permeate further revealed that the rejection rate of MG-blocks (Table 4.2) by the membrane was only about 28.8% without calcium ion, however it increased to 56.9% and 57.2% with the addition of 1 mM and 2 mM Ca^{2+}, respectively. These results indicate that most of MG-blocks were smaller than the pores of membrane, thus could pass through the membrane. On the contrary, with the addition of calcium ion, calcium ion promoted the self-aggregation of MG-blocks (Figure 4.2), leading to the formation of large MG-blocks complexes that can be effectively retained by the ultrafiltration

membrane used in this study.

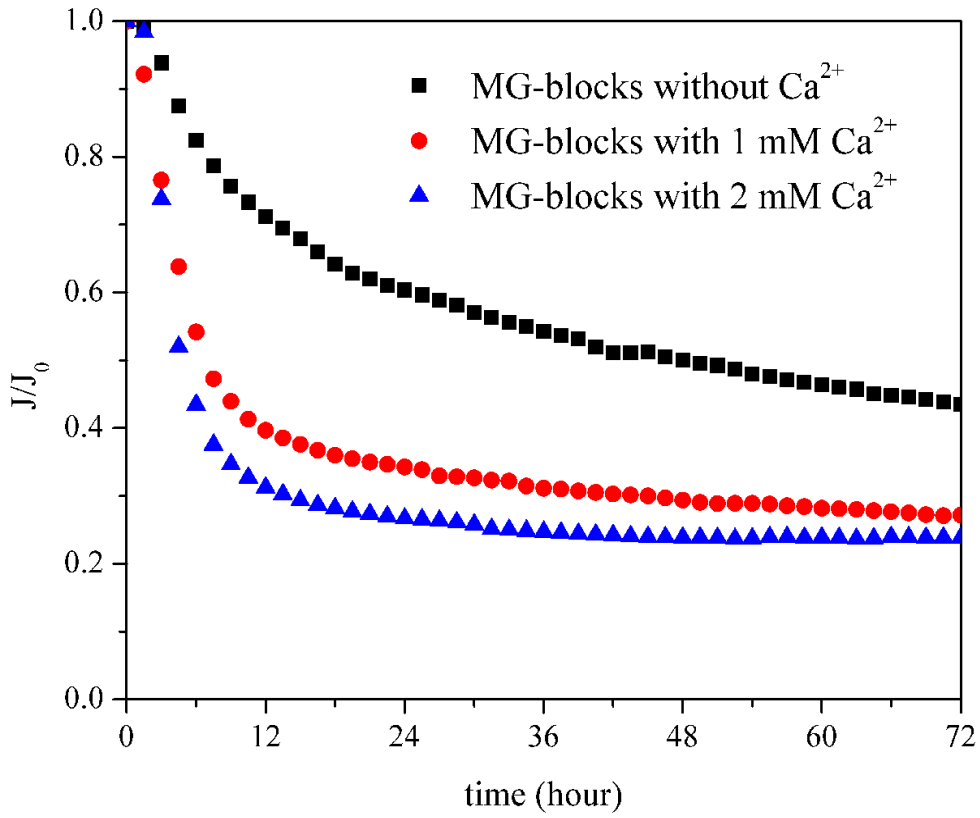

Figure 4.9 Flux profiles of MG-blocks at various calcium ion concentrations

Table 4.2 Membrane rejection rates of MG-, MM- and GG-blocks filtrations at various calcium ion levels

	0 mM	1 mM	2 mM
MG-blocks	28.8±1.3	56.9±1.4	57.2±2.0
MM-blocks	88.7±1.1	96.0±1.5	97.2±1.3
GG-blocks	85.6±1.8	93.7±0.9	95.3±1.6

Figure 4.10 shows the filtration profiles of MM-blocks in the absence and presence of calcium ion. Without addition of calcium ion, the flux decline during the ultrafiltration of MM-blocks was much less than that observed for MG-block. The TOC concentration of the permeate shows that 88.7% of MM-blocks was retained by the ultrafiltration membrane used in this study. According to the filtration data of

MM- and MG-blocks, it is reasonable to consider that most of MM-blocks had a size bigger than MG-blocks. This indeed is supported by the prediction by the XDLVO theory, i.e. MM-blocks possess the highest self-aggregation potential to form bigger TEP in water (Meng and Liu 2013). Furthermore, the addition of calcium ion significantly promotes the self-aggregation of MM-blocks and the formation of TEP. As the result, much severer decline in the permeate flux was observed. As can be seen in Figure 4.10, the severity of the flux decline is proportionally related to the concentration of calcium ion added to the MM-block solutions. For example, the filtration flux of MM-block solution in the absence of calcium ion only decreased to 82.7% of its initial flux after 48-hour ultrafiltration. However, with the addition of 1 mM and 2 mM calcium ion to the MM-block solutions, the respective fluxes significantly dropped to 23.9% and 14.7% of the initial flux. In addition, the measured TOC concentrations in the permeates further indicate that 96.0% and 97.2% of MM-blocks were rejected in the presence of 1 mM and 2 mM of calcium ion, respectively. Previous study also showed that the formation of cake layer on the membrane surface was the main cause of membrane fouling in the filtration of MM-blocks with a 0.2-μm microfiltration membrane (Meng and Liu 2013). Similarly, it is reasonable to consider that the formation of cake layer by MM-blocks was mainly responsible for the observed fouling during the ultrafiltration with a membrane of 20,000 Daltons. As shown in Figure 4.2, the addition of 1 mM and 2 mM of calcium ion greatly promoted the formation of TEP (>0.05 μm) in the MM-blocks solutions from 4.0 mg Xeq/L without calcium ion to 9.6 and 17.1 mg Xeq/L) respectively. On the other hand, Figure 4.7 also reveals that TEP formed in the presence of calcium had more complex structure than TEP developed in the absence of calcium. Obviously, these calcium-induced physical changes to TEP inevitably expedite the formation of cake layer on the UF membrane.

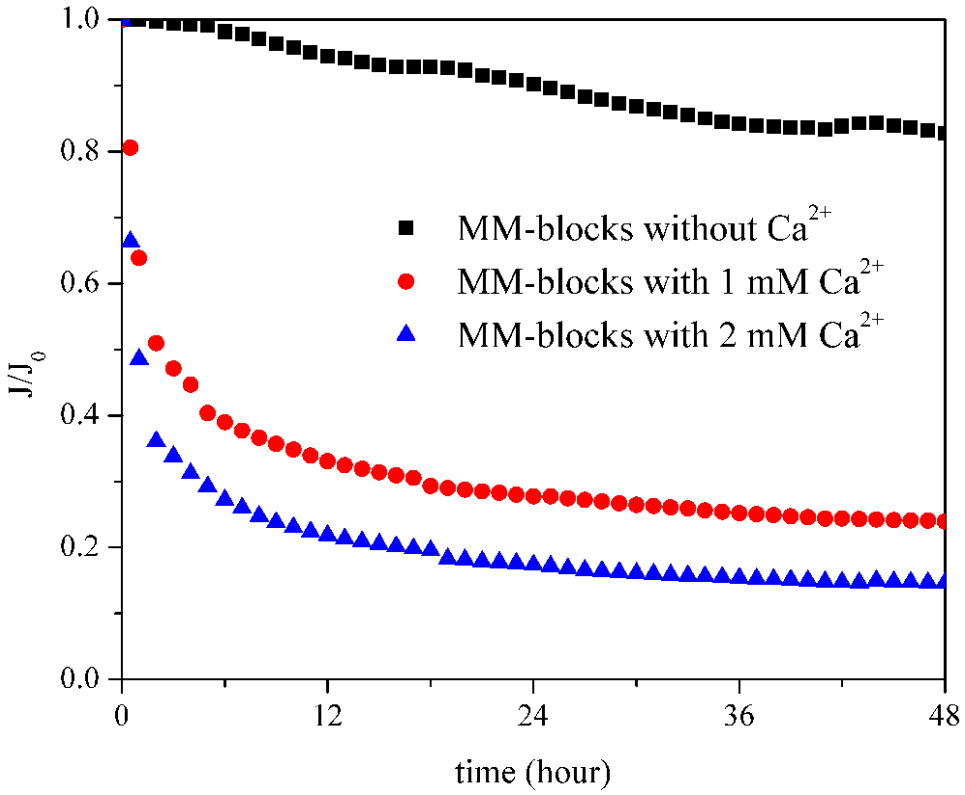

Figure 4.10 Flux profiles of MM-blocks at various calcium ion concentrations

Figure 4.11 shows the effects of calcium ion on the ultrafiltration behaviors of GG-blocks. Compared to the MG- and MM-blocks, calcium ion had a much greater effect on the ultrafiltration of GG-blocks. The permeate flux of GG-blocks in the absence of without calcium, only declined 89.7% of its initial value after 24-hour filtration. However, in the presence of 1 mM and 2 mM of calcium, an extremely quick drop in the respective filtration fluxes of GG-blocks was observed in the initial phase, and only 6.8% and 5.6% of the initial flux remained after 24-hour ultrafiltration. Such severe membrane fouling can be explained by the highest concentration of TEP obtained in the GG-blocks solutions after the addition of calcium (Figure 4.2), as compared to MM- and MG-blocks. For example, only about 3.6 mg Xeq/L TEP > 0.05 μm was determined in the GG-block solution without addition of calcium, whereas 71.1 and 72.2 mg Xeq/L were obtained at the calcium concentrations of 1 mM and 2 mM respectively. Meanwhile, Figure 4.7 showed the structure of TEP derived from GG-blocks in the presence of calcium also became larger and more complex. Furthermore, the TOC concentration in the

permeate showed 93.7% and 95.3% of GG-blocks were rejected after the addition of 1 mM and 2 mM calcium. Therefore, the increases in concentration and size of TEP derived from the GG-blocks solutions in the presence of calcium are definitely responsible for the observed quick and severe membrane fouling (Figure 4.11).

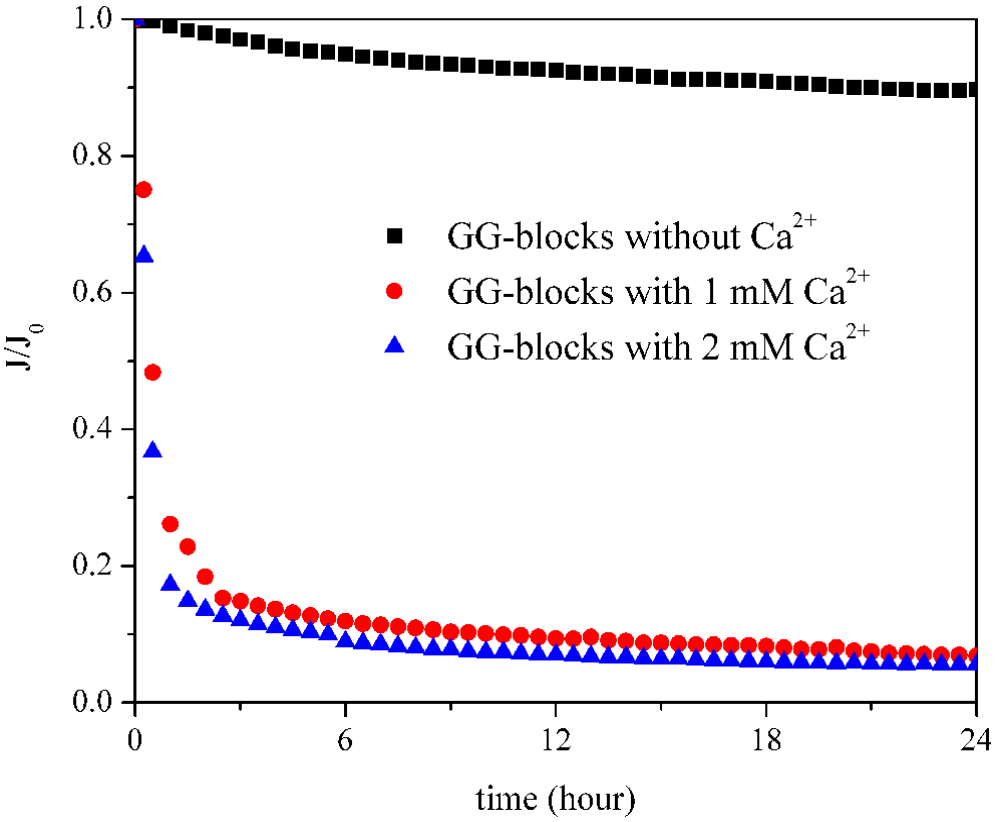

Figure 4.11 Flux profiles of GG-blocks at various calcium ion concentrations.

4.3.3.2 Analysis of Initial Fouling Rate and Foulant Mass Deposited on Membrane Surface

The initial fouling rate and total foulant mass on the membrane surface deposition were calculated in order to establish the relationship between TEP concentration and the fouling development. The ultrafiltration membrane used in this study has a MWCO of 20 kDa, thus TEP measured with a size >0.05 μm should not result in the pore blocking of membrane. Figure 4.12 shows a positive correlation between the TEP concentration (>0.05 μm) and the initial fouling rate. It appears that TEP plays a critical role in the initial development of membrane fouling. These results also

suggest that TEP can adhere onto the membrane surface very quickly to form a gel-like layer as also reported by Bar-Zeev et al. (2012).

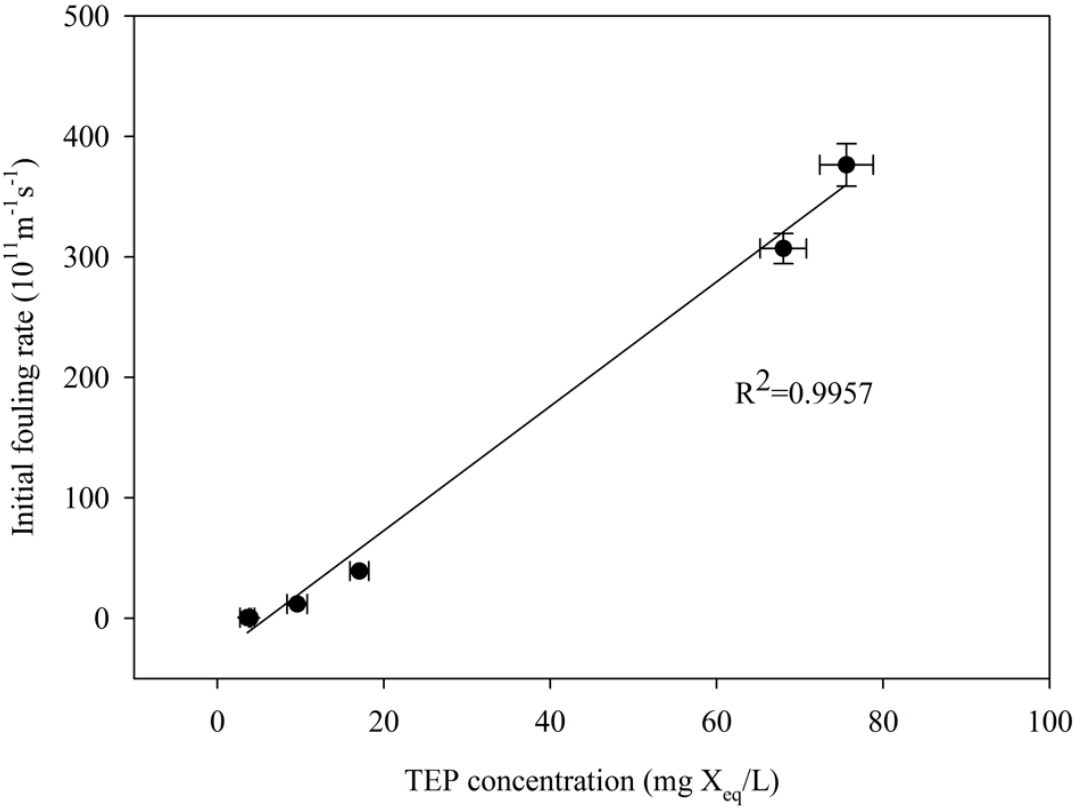

Figure 4.12 Correlation between the TEP concentrations in feed water and the initial fouling rate.

The foulant mass deposed on the membrane surface offers direct insights into the cake layer formed by TEP (TEP>0.05 μm). It can be seen in Figure 4.13 that the amount of foulants is proportionally correlated to the TEP concentration in the feed water. Figure 4.12 and Figure 4.13 offer a much clearer understanding of the role of TEP in the development of membrane fouling. In fact, such an observation is supported by the study of Bar-Zeev et al. (2012) showing that TEP preferably tend to attach to solid surfaces.

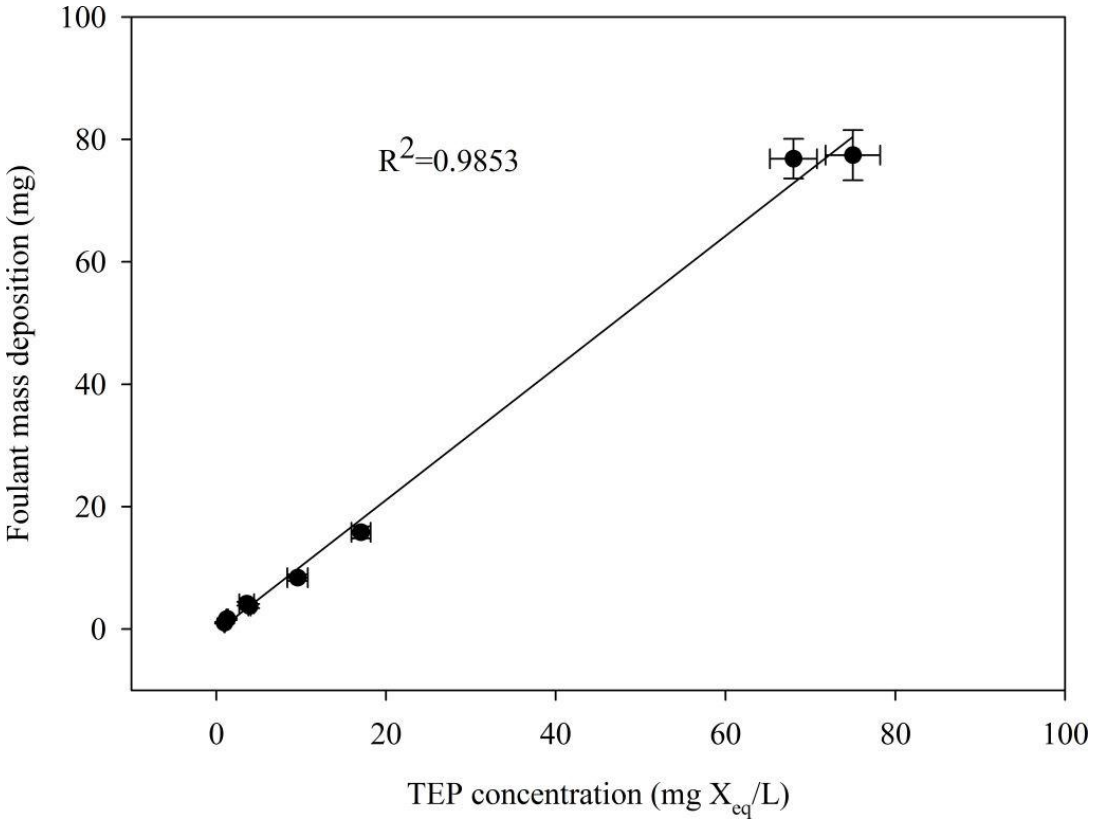

Figure 4.13 Correlation between the TEP levels in feed water and the foulant mass deposition on membrane surface.

4.3.3.3 Development of Cake Layer at Different TEP Concentrations

As discussed above, the formation of cake layer on the membrane surfaces was of critical importance in the ultrafiltration of MM- and GG-blocks. In the present study, FE-SEM and AFM techniques were employed to visualize the membrane surfaces fouled at two different TEP concentrations. Although TEP were freeze-dried prior to microscopic observation, these visualization techniques could still provide direct evidence of the TEP attachment on the membrane surfaces.

As can be seen in Figure 4.14a, only few and small TEP were deposited on the membrane surface after 10-minute filtration at the low TEP concentration, while remarkable accumulation of TEP on the membrane surface was observed at the high concentration (Figure 4.14b). After 30-minute filtration, some membrane still remained blank in the ultrafiltration of low-concentration TEP solution, but the entire membrane surface was eventually completely covered by TEP in the filtration

of the high-concentration TEP solution (Figure 4.14c and Figure 4.14d). These observations indeed are in good agreement with the results in Figure 4.12 showing high-concentration TEP resulted in high initial fouling rate. Figure 4.14e and Figure 4.14f further show the fouled membrane surface after 1500-minute filtration. It should be noted that crafts in these two figures were created by the freeze dry process in the preparation of the samples for FE-SEM. Fortunately, these crafts revealed that the thicker cake layer was developed at the higher TEP concentration.

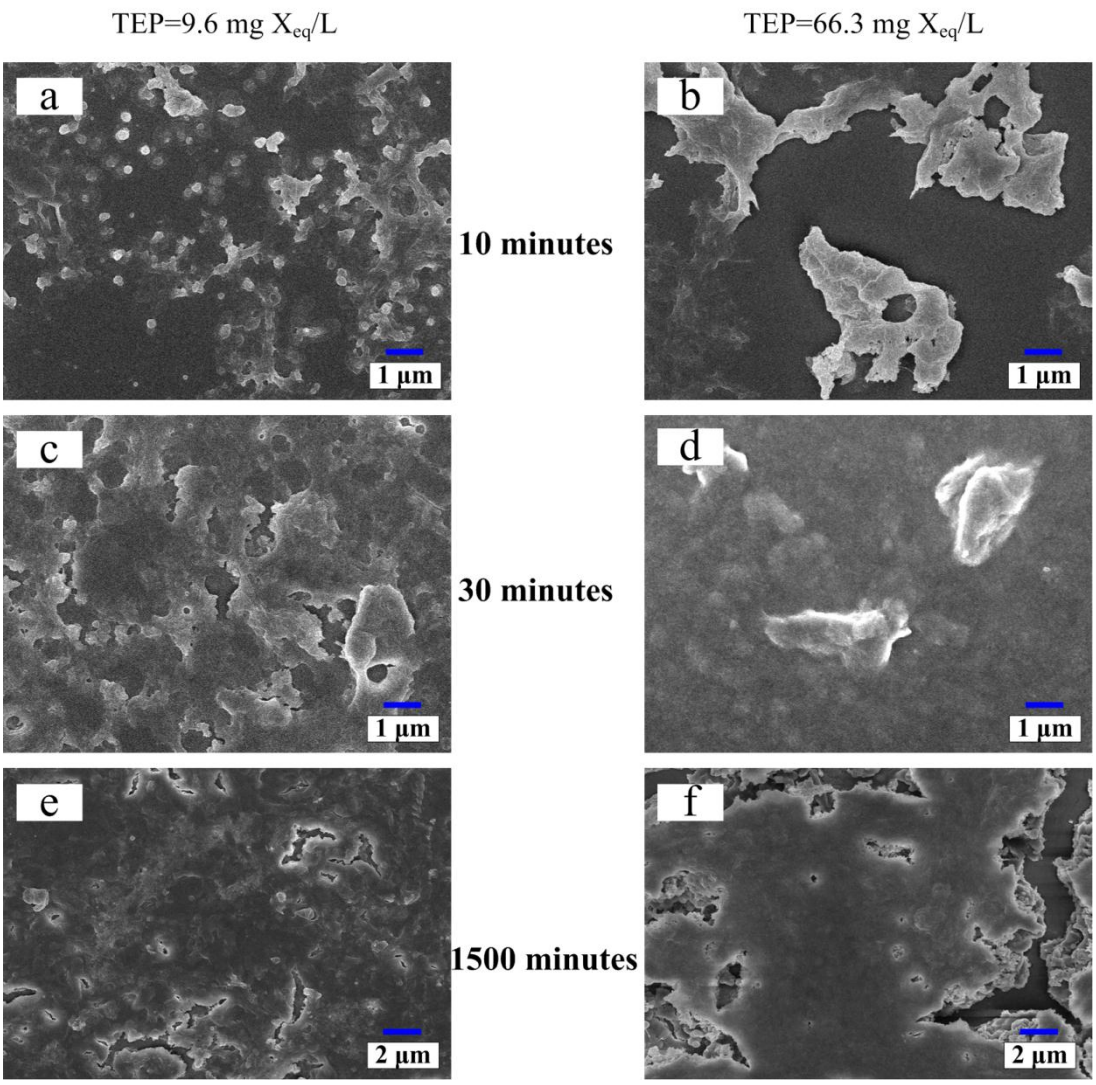

Figure 4.14 FE-SEM images of the membrane fouling processes with different TEP levels.

In addition, three dimensional AFM images (Figure 4.15) also revealed the phenomena similar to those by FE-SEM. The roughness was evaluated from AFM

images on different locations of the same fouled membrane and the average values were reported in Figure 4.15. It appears that the roughness of the fouled membrane surfaces tended to increase with the successive accumulation of TEP, and the changes in the surface roughness was also related to the TEP concentration, e.g. the surface roughness was found to increase rapidly during the filtration of high-concentration TEP solution.

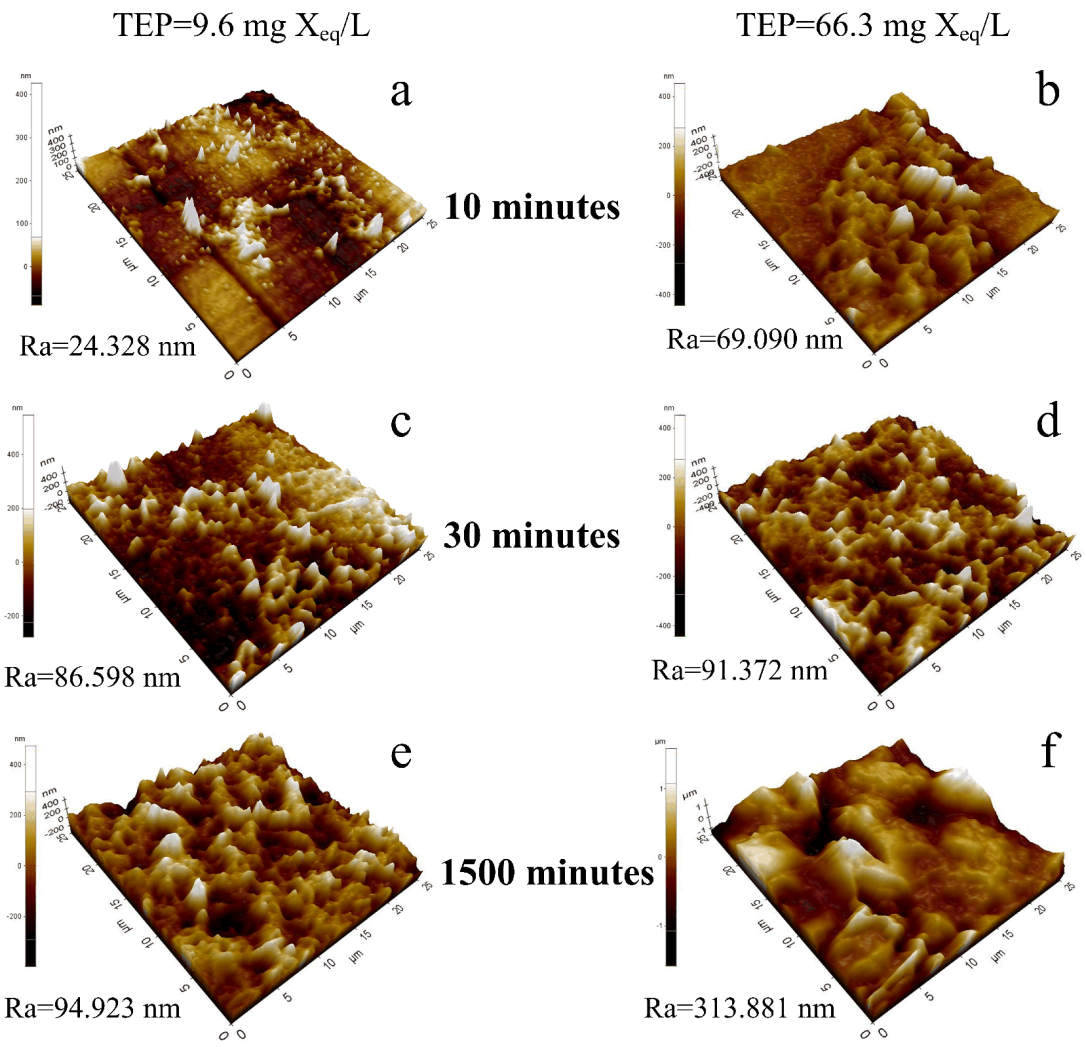

Figure 4.15 The three dimensional AFM images of the membrane fouling processes with different TEP levels. a, c, e and b, d, f are the cake layer formed in the filtration of low and high TEP concentration respectively.

4.3.4 Effects of Calcium Ion on The Cross-linking of MG-, MM And GG-blocks

It is demonstrated above that despite derived from the same source of alginate, MG-, MM- and GG-blocks behaved totally differently in the reactions with calcium ion. Figure 4.16 schematically illustrates possible interactions between various alginate blocks and calcium ion. As discussed above, most of MG-blocks are small enough to pass through the membrane used in present study. After the addition of calcium ion, only few TEP were form from MG-blocks, i.e. the interaction or reaction between MG-blocks and calcium ion is insignificant. Unlike MG-blocks, the binding between MM-blocks and calcium ion appeared to be much stronger and seemingly Ca^{2+}-dependent. As a result, the TEP concentration in the MM-block solution was much higher than that observed in the MG-block solution. The most notable reaction was found between GG-blocks and calcium ion, and the addition of calcium ion to the GG-block solution significantly enhanced the production of TEP, resulting in a quick formation of cake later on the membrane surface.

So far, more than 200 kinds of commercial alginates derived from different sources are available in the market and the MG-, MM and GG-blocks contents in alginates vary largely (Tønnesen and Karlsen 2002, Lee and Mooney 2012). In the literature, alginate from various suppliers has been commonly employed as a model foulant, but with no consideration of possible differences in their molecular compositions and structures. As shown in Figure 4.16, MG-, MM- and GG-blocks indeed exhibit different cross-linking structures with calcium ion which exists extensively in various water and wastewater environments. Therefore, it appears to be necessary to characterize the molecular compositions and structures of alginates from various sources which would be useful for better interpretation of filtration results from different types of membranes.

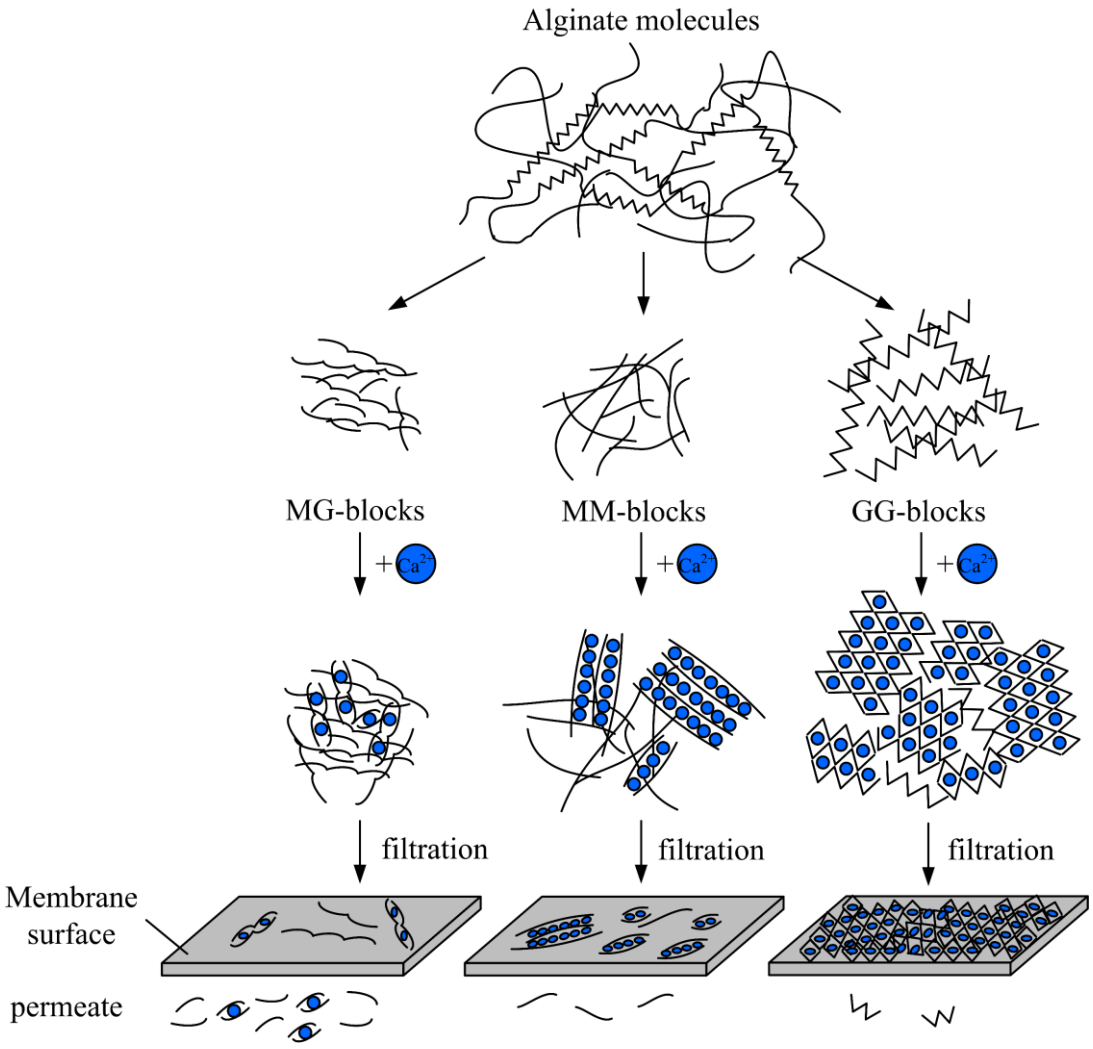

Figure 4.16 Schematic representation of the effects of calcium ion on the MG-, MM and GG-blocks

4.4 CONCLUDING REMARKS

Although derived from the same source alginate, MG-, MM and GG-blocks exhibited distinguished properties, and such differences were further intensified by the presence of calcium ion. The reaction between calcium ion and GG-blocks was found to be strongest, and more TEP was thus produced. As the result, ultrafiltration membrane was quickly fouled by accumulated TEP on its surface. Although the formation of TEP from MM-blocks was enhanced by the addition of calcium ion, it was not as intensive as that observed for GG-blocks. As such, the development of membrane fouling during the ultrafiltration of MM-block solution was slowed

down. The effect of calcium ion on MG-blocks was slightest, and only very limited amount of TEP was produced. Thus, the membrane fouling by MG-blocks was not as serious as those observed during the ultrafiltration of MM- and GG-blocks. More importantly, this study provided experimental evidence showing the critical role of TEP in the development of membrane fouling.

CHAPTER 5 TEP-ASSOCIATED MEMBRANE FOULING AT VARIOUS SODIUM CONCENTRATIONS

5.1 INTRODUCTION

TEP are ubiquitous and abundant in many aquatic environments including freshwater and seawater. As a highly surface-active material, TEP are very sticky in nature and highly foldable in physical structure. Because of their high abundance and unique properties, TEP are essentially involved in many aquatic systems. For example, as gel-like, free swimming particles, TEP can enhance the aggregation of solid non-sticky particles in water systems (Passow 2002) and they also provide surfaces for microbial colonization (Passow and Alldredge 1994, Passow 2002, Azam and Malfatti 2007, Berman and Parparova 2010). It has been shown that about 0.5-25% of all bacteria present in seawater and freshwater were attached onto TEP (Passow 2002). This suggest that free swimming TEP as a carrier can transport bacteria from water phase to another solid surface by adhesion, and evidence shows that TEP can play an active role in the development of aquatic biofilms (Berman and Holenberg 2005, Bar-Zeev et al. 2012, Bar-Zeev et al. 2015). Therefore, the effect of TEP in the development of reverse osmosis (RO) membrane fouling in seawater desalination has attracted more and more concern (Villacorte et al. 2009, Villacorte et al. 2009, Villacorte et al. 2010).

Two pathways have been proposed to illustrate the formation of TEP from dissolved organic matter (DOM) in aquatic environments, i.e. abiotic and biotic (Chin et al. 1998, Passow 2002, Verdugo et al. 2004, Verdugo and Santschi 2010, Meng et al. 2013). In the biotic pathway, microorganism uptakes DOM and produce TEP via mucus/cell coating detachment, particulate material release or TEP can directly form from detritus of the microorganism during their growth or senescence (Berman and Viner-Mozzini 2001, Passow 2002, Berman-Frank et al. 2007, Meng et al.

Part of this chapter has been published: Meng, S. and Liu, Y. (2016). New insights into transparent exopolymer particles (TEP) formation from precursor materials at various Na^{+}/Ca^{2+} ratios. Scientific Reports 6, 19747.

2013). In the abiotic pathway, TEP form from precursor substances under specific environmental conditions. These precursors include dissolved fibrillar polysaccharides released from various planktonic organisms as well as intracellular substances released during lysis or breakage of cells (Passow 2002, Meng et al. 2013, Bar-Zeev et al. 2015). By coagulation, gelation or annealing, such fibrillar polymers form submicron gels which further coagulate to form TEP (Passow 2002). It has been believed that abiotic pathway is predominant in TEP formation in various aquatic environments (Passow 2002, Bar-Zeev et al. 2015). Of particular, the abiotic TEP formation significantly depends on the types of precursors and environmental conditions (Passow 2002).

It had been observed that the formation of TEP can be promoted by divalent cations (e.g. calcium ion) through bridging with neighboring TEP molecular chains (Bar-Zeev et al. 2015). It should be realized that TEP have been detected in many different ecosystems, including freshwater (rivers, lakes even groundwater), wastewater (including brackish water) and seawater (Passow 2002, Bar-Zeev et al. 2015), where TEP concentrations were found to be highly variable, ranging from μg to mg gum xanthan equivalent per liter (Bar-Zeev et al. 2015). Obviously, these water bodies consist of different salts components (e.g. commonly sodium and calcium ions by quantity) which likely play a critical role in TEP development. For example, sodium concentration is much higher in seawater than in freshwater. However, little has been known about the effect of sodium ion on TEP formation in the presence of calcium ion. Therefore, this study aimed to offer new insights into TEP formation from alginate blocks at various Na^+ concentrations at a given Ca^{2+} level and its effect on the development of membrane fouling. This study should be very useful for better understanding TEP formation and abundance in natural aquatic environments and their potential implications in various kinds of membrane-based water and wastewater technologies.

5.2 MATERIALS AND METHOD

5.2.1 Preparation of Alginate Blocks Solutions

To obtain MG-, MM- and GG-blocks, sodium alginate (Wako, Japan) was partially hydrolyzed with HCl according to the method employed by Leal et al. (2008). As described in Chapter 3, the fraction soluble in 0.3 M HCl is MG-blocks, accounting for 13.8±1.9% in the alginate molecule. The fractions soluble and insoluble at pH 2.85 are MM-blocks and GG-blocks respectively, composing 53.5±1.3% and 32.7±0.6% of the alginate. Sample solutions were prepared by dissolving MG-, MM- and GG-blocks respectively into ultrapure Milli-Q water with continuous stirring for 2 hours to make a final concentration of 50 mg/L. $CaCl_2 \cdot 2H_2O$ (Sigma, USA) and NaCl (Wako, Japan) were used to set calcium ion and sodium ion concentrations. All sample solutions were freshly prepared just before use. Although pH was not adjusted, it remained approximately 6.7±0.3 in all alginate blocks solutions.

5.2.2 Determination of TEP in Solutions of Alginate Blocks

TEP levels formed from alginate blocks at various sodium ion concentrations were determined similarly with the method described in Chapter 3. Briefly, prepared sample solutions were filtered through a series of polycarbonate filters (Whatman, United Kingdom) of pore size 0.05, 0.1, 0.2 and 0.4 μm by applying a constant vacuum of 0.2 bars. Subsequently, 1 mL of Milli-Q water was then filtered through the filter to wash out the remaining salinity as shown in Figure 5.1 (Villacorte et al. 2015). TEP accumulated on the filters were stained by pre-filtered alcian blue solution and excess dye was then removed by vacuum filtration and another 1 mL of Milli-Q water rinse. Washed filters with TEP were immersed in 80% H_2SO_4 solution for about 2 hours. A light green color developed in the beakers. Finally, the absorbance of the sulfuric acid solution with eluted alcian blue was measured. Absorbance corrections due to stain adsorption on filter and interference because of high salinity were also performed (Villacorte et al. 2009, Villacorte et al. 2015). Three replicates were conducted for each sample and every sample was measured at

least three times. Average result of TEP concentration was reported. Calibration was conducted with Gum xanthan (Sigma, USA) and the TEP concentration was finally expressed as mg gum xanthan equivalent per liter of water (mg $X_{eq} \cdot L^{-1}$). In following discussion, TEP refer to all alcian blue-stainable particles that can be retained by 0.05 µm polycarbonate filters, unless mentioned otherwise.

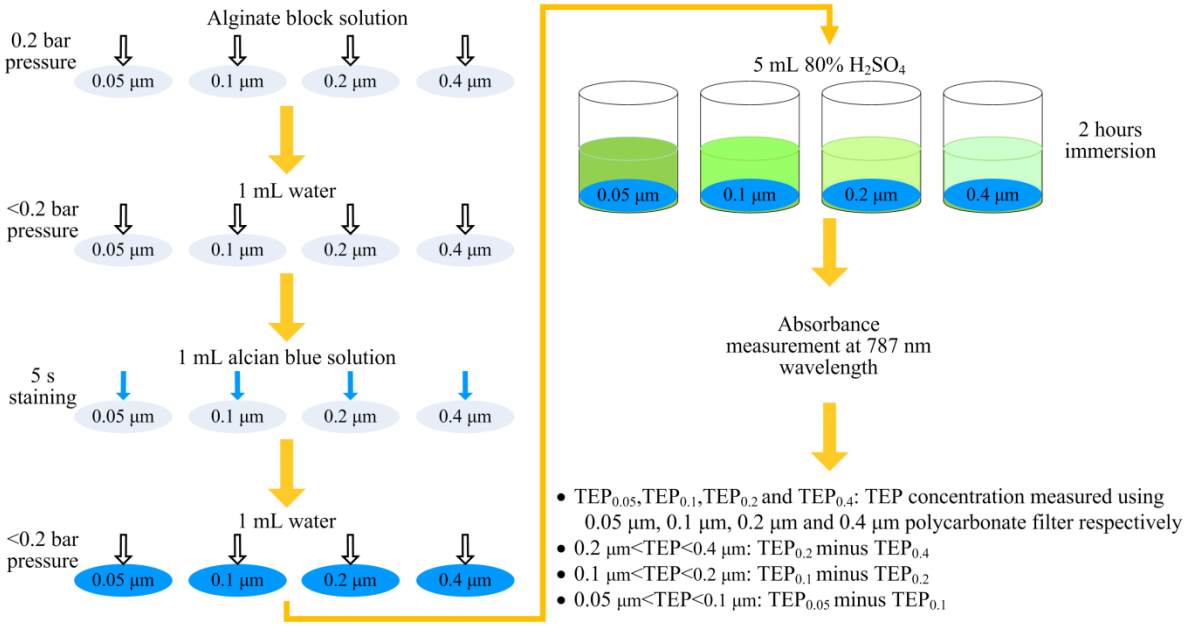

Figure 5.1 The procedure of TEP determination in water samples with high salinity. To prevent the interference of high salinity to alcian blue staining, samples need to be washed before staining.

5.2.3 Microscopic Observation of TEP

The effect of increasing Na^+ concentrations on the morphology of TEP derived from alginate blocks was observed by a microscope (Keyence, Japan. The fresh sample solutions were prepared prior to observation as described in Section 5.2.1. In order to visualize TEP with the bright-field microscope, MG-, MM- and GG-blocks solutions were stained by freshly pre-filtered (0.05 µm polycarbonate filter) alcian blue solution as presented before (Passow and Alldredge 1995, Berman and Parparova 2010). Stained samples were then observed under the microscope. For each sample, about 20 images were randomly taken.

The micro-structures of TEP derived from MG-, MM- and GG-blocks at different Na^+ concentrations were observed by a field emission scanning electron microscopy (FE-SEM) (Jeol JSM-7600F, Japan). Although TEP were freeze dried prior to microscopic observation, this microscopic technique could still provide direct visualizations of evidence of TEP micro-structures. 10-50 mL of sample solutions prepared as described above were filtered through 0.1 μm polycarbonate filters (Whatman, United Kingdom) at a constant pressure of 0.2 bars and was then rinsed by 1 mL of Milli-Q water. Filters with retained alginate blocks were completely freeze-dried completely in a freeze dryer (Christ, Germany) for further examination. All samples were observed at least three times and 8-10 images were randomly recorded each time.

5.2.4 Viscoelasticity Properties of TEP Measured by AFM

A XE-100 AFM (Park Systems, Korea) was employed to determine the stickiness and micromechanical characteristics of TEP developed from GG-blocks at different Na^+ concentrations. For force measurements on TEP, TEP films were prepared by filtering 1 mg X_{eq} TEP onto 0.1-μm polycarbonate filters at a constant pressure of 0.2 bars. Subsequently, the filter with retained TEP was carefully glued onto a holder using double-sided sticky tape with TEP film upwards. All TEP samples were prepared right before the force measurements. To prevent TEP film dehydration, the TEP samples were analyzed in a liquid cell filled completely with the test solution of interest. The chemistry composition of the test solution was the same as that used in the corresponding TEP samples, while a clean 0.1-μm polycarbonate filter was used as a reference surface. The clean filter was first soaked in Milli-Q water for 24 hours and 50 mL Milli-Q water was then filtered through it just before the measurement. Force measurements on the clean filters were conducted with all test solutions.

The force measurements were conducted at room temperature of 22±2°C. Surface architecture was first imaged using non-contact mode to minimize the contact of the tip with the TEP film and subsequently a suitable position on the surface was located for force measurements. For the force measurements, the scan rate was set

at 1 Hz with image resolution at 512 data number per trace. The force measurements were approached for an area of 5×5 μm^2 at a respective forward and backward speed of 0.3 μm/s. A minimum of four different places on the TEP film was measured and 16 force measurements were conducted at each location. XEI 1.8.0.Build32 software was used to flatten image as well as to calculate the maximum retract force (adhesion) and total adhesion energy.

5.2.5 Filtration Tests

Similar with the method described in Chapter 4, filtration behaviors of alginate blocks solutions with various Na^+ concentrations were examined in a standard laboratory-scale cross-flow ultrafiltration module (Sterlitech, USA). Feed water was prepared as described in above Section 5.2.1 and the cross-flow velocity is set to be 10 cm/s. The same commercial polyethersulfone (PES) UF membrane (AMFOR INC, Beijing) with molecular weight cut off (MWCO) of 20 kDa was used in this study. Before each filtration test run, the cross-flow system was carefully cleaned and then Milli-Q water was first filtered for 24 hours to compact and equilibrate the membrane after which feed water was added. Permeate was collected in a beaker which was located on an electronic balance. The weight change of permeate was recorded to calculate the flux change of permeate. Filtration test of each sample was repeated at least three times.

In order to determine the fouling rate, total membrane filtration resistances were first calculated according to Darcy's law:

$$J = \frac{\Delta P}{\mu R_t} \tag{5.1}$$

where J is the permeate flux ($m^3m^{-2}s^{-1}$); R_t is the total filtration resistance (m^{-1}); ΔP is the applied pressure (Pa); and μ is the solution viscosity (Pa·s). Fouling rate was then determined from the slope of the plot of total resistance versus time, whereas the initial fouling rate was calculated from the initial linear region of the plot as described in Chapter 4 (Figure 4.1). The linear filtration resistance increase with respect to filtration time represents a constant rise of the TEP attached on the

membrane.

5.2.6 Fouling Layer Formed on Membrane Surface

AFM technique was also employed to assess the influence of TEP on the cake layer development on membrane surface, operated in non-contact and contact mode, respectively. Membrane samples fouled by GG-blocks with the addition of 10 and 100 mM Na^+ at a fixed Ca^{2+} concentration of 1 mM taken at 30 min filtration time were examined. For the purpose of comparison, samples used were cut from the same location of fouled membranes. Before measurements, freshly prepared membrane samples were carefully rinsed with the test solution. Subsequently, the membrane sample was carefully glued onto a holder using double sides adhesive tape with fouled membrane surface upwards. All the membrane samples were prepared just before the force measurements. To prevent cake layer dehydration, the membrane samples were analyzed in a liquid cell filled completely with the test solution of interest. The chemistry of the test solution was the same as that used in the corresponding filtration tests.

All force measurements were performed at room temperature (22±2°C). Surface architecture was first imaged using non-contact mode to minimize the contact of the tip with the membrane surface and subsequently a suitable position on the surface was located for force measurements. For the force measurements, the scan rate was set at 1 Hz with image resolution at 512 data number per trace. The force measurements were approached for an area of 20×20 μm^2, with a forward and backward speed of 0.3 μm/s. The force measurements were performed at a minimum of four different places on the sampled membrane surface, and 16 force measurements were conducted at each location to ensure representative sampling. XEI 1.8.0.Build32 software was used to flatten image and calculate the retract force (adhesion). Averaged AFM raw force-distance data were used to produce a force versus separation distance curve. In addition, the thickness of cake layer was also measured using Line View function of the software.

5.3 RESULTS AND DISCUSSION

5.3.1 TEP Formation from Alginate Blocks

5.3.1.1 TEP Derived from MG-, MM- and GG-blocks at Various Sodium Concentrations

Figure 5.2-5.4 show that increasing Na^+ concentration at a fixed Ca^{2+} concentration of 1 mM leads to a remarkable reduction in TEP formation from all alginate blocks, i.e. MM-, MG-, and GG-blocks. Such a trend is completely different from that observed at various Ca^{2+} concentrations as shown in Chapter 4 (Figure 4.2). In the case of MG-blocks (Figure 5.2), the concentration of TEP developed at 10 mM Na^+ was about 47-, 14-, 12- and 9-times higher than those at a Na^+ concentration of 100 mM for TEP in the size range of 0.05-0.1 μm, 0.1-0.2 μm, 0.2-0.4 μm and >0.4 μm. The more significant impact of Na^+ on the formation of TEP from MM-blocks was observed in Figure 5.3. At a Na^+ concentration of 100 mM, extremely low-level TEP was developed with both MG- and MM-blocks. Similar to MG- and MM-blocks, total concentration of TEP developed from GG-blocks tended to decrease with increasing Na^+ concentration from 10 mM to 100 mM at a given Ca^{2+} concentration of 1 mM (Figure 5.4). In contrast to Ca^{2+}, it appears from Figure 5.2-5.4 that Na^+ exerts a significant adverse effect on TEP development from all alginate blocks.

Ca^{2+} can act as "bridges" to connect alginate block molecules in a complex structure. However, increased Na^+ concentration can out-compete Ca^{2+}, thus prevents the Ca^{2+} bridging and decreases the TEP formation. As discussed in Chapter 4, in the solutions of MG- and MM-blocks, the bindings between calcium ions and these alginate blocks are weaker than that between GG-blocks and calcium ions. Therefore, the bridging effect by calcium ion in MG-and MM-blocks is weakened or even disappeared at elevated Na^+ concentration, and this in turn explains significantly reduced TEP formation as shown in Figure 5.2-5.3b. Unlike MG- and MM-blocks, GG-blocks can bind with calcium ion more strongly, thus the adverse effect of Na^+ on TEP formation from GG-blocks is less significant (Figure

5.4b).

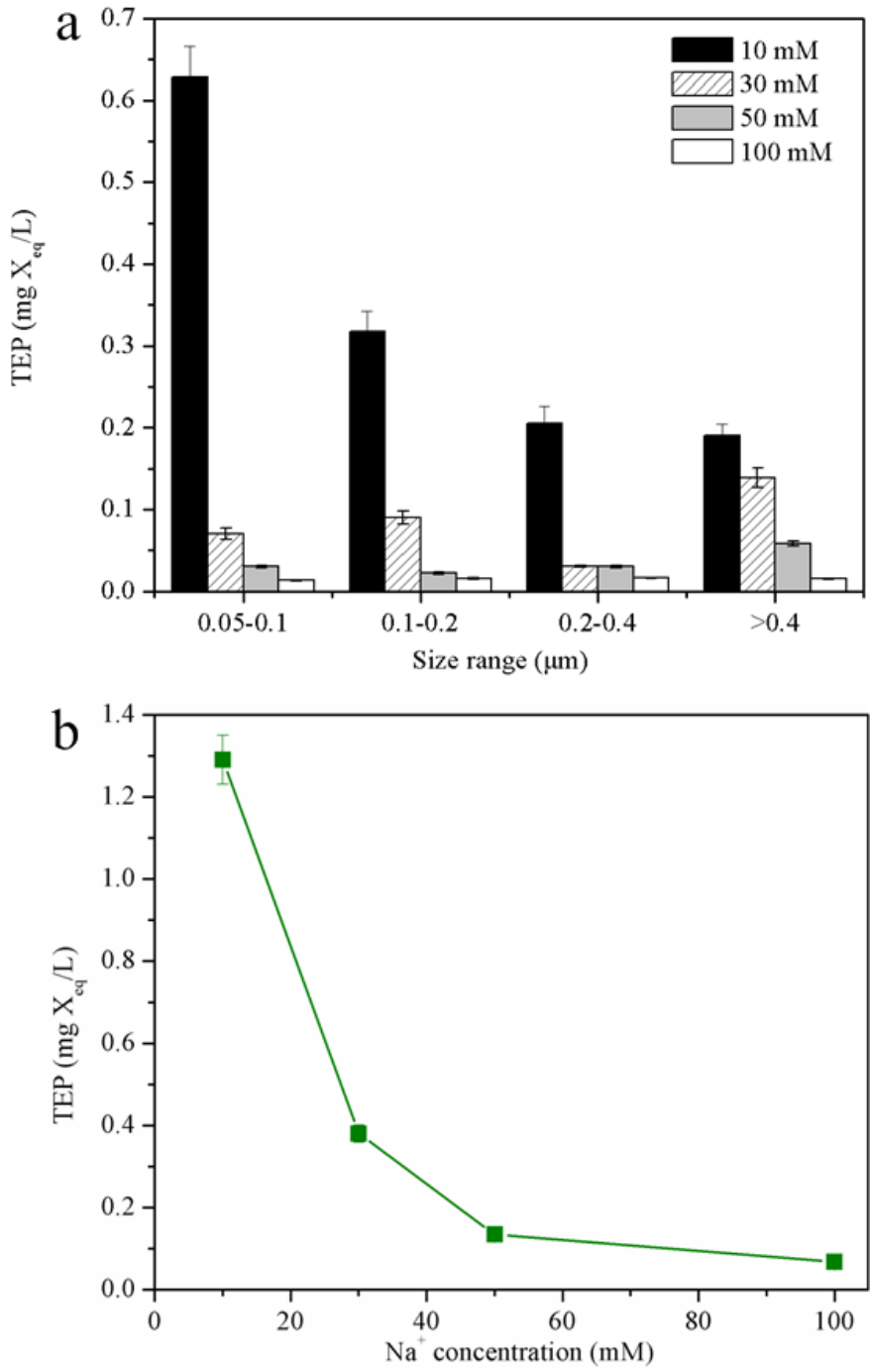

Figure 5.2 TEP concentrations derived from MG-blocks with increasing Na^+ concentration. TEP levels in each size range (a) and the effect of increasing Na^+ concentration on the total TEP concentration (TEP retained by 0.05 µm polycarbonate filters) (b). Experimental conditions: MG-blocks concentration = 50

mg/L, Ca^{2+} concentration = 1 mM, Na^{+} concentrations are 10 mM, 30 mM, 50mM and 100 mM respectively.

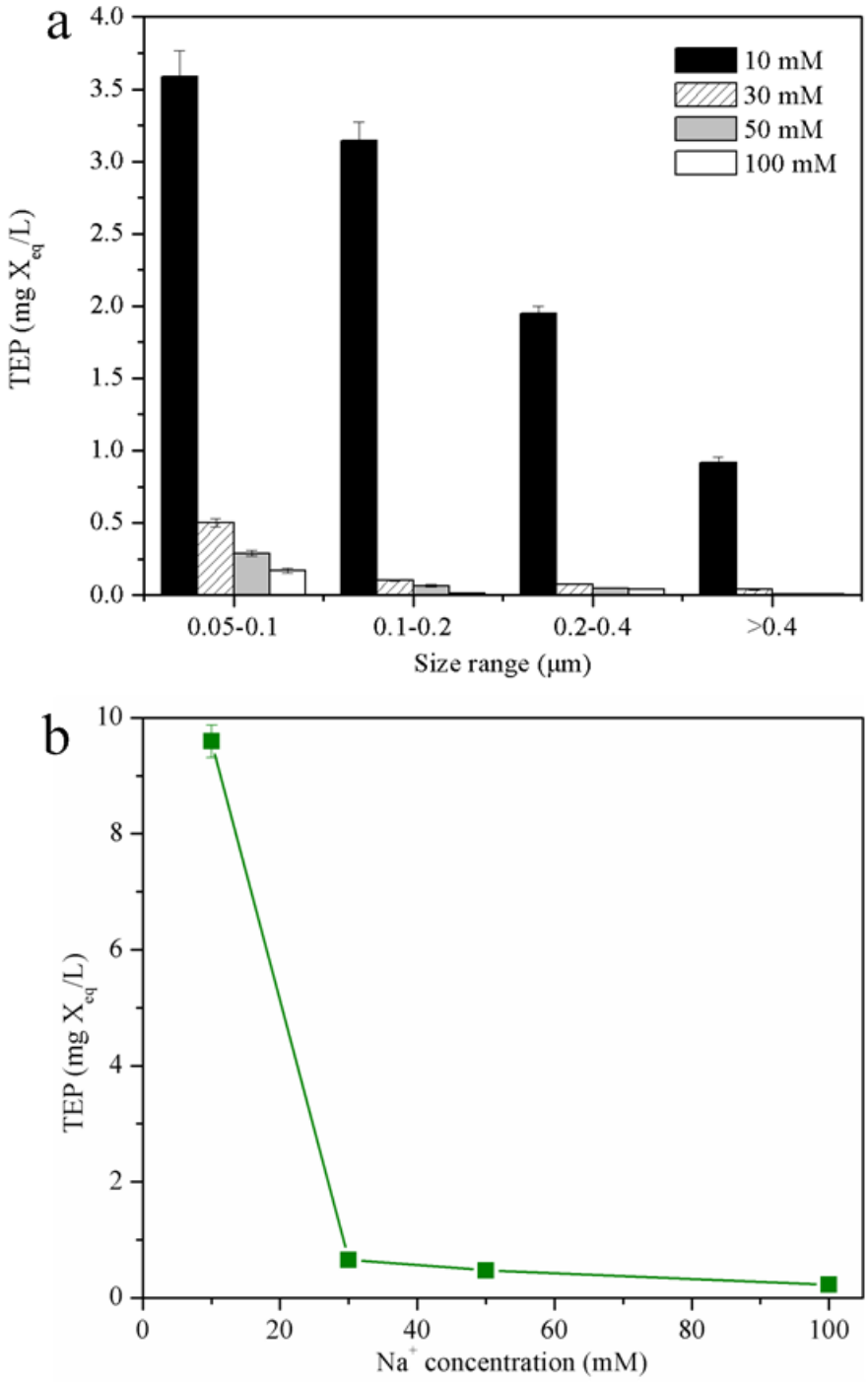

Figure 5.3 TEP concentrations derived from MM-blocks with increasing Na^{+} concentration. TEP levels in each size range (a) and the effect of increasing Na^{+} concentration on the total TEP concentration (TEP retained by 0.05 µm

polycarbonate filters) (b). Experimental conditions: MM-blocks concentration = 50 mg/L, Ca^{2+} concentration = 1 mM, Na^{+} concentrations are 10 mM, 30 mM, 50mM and 100 mM respectively.

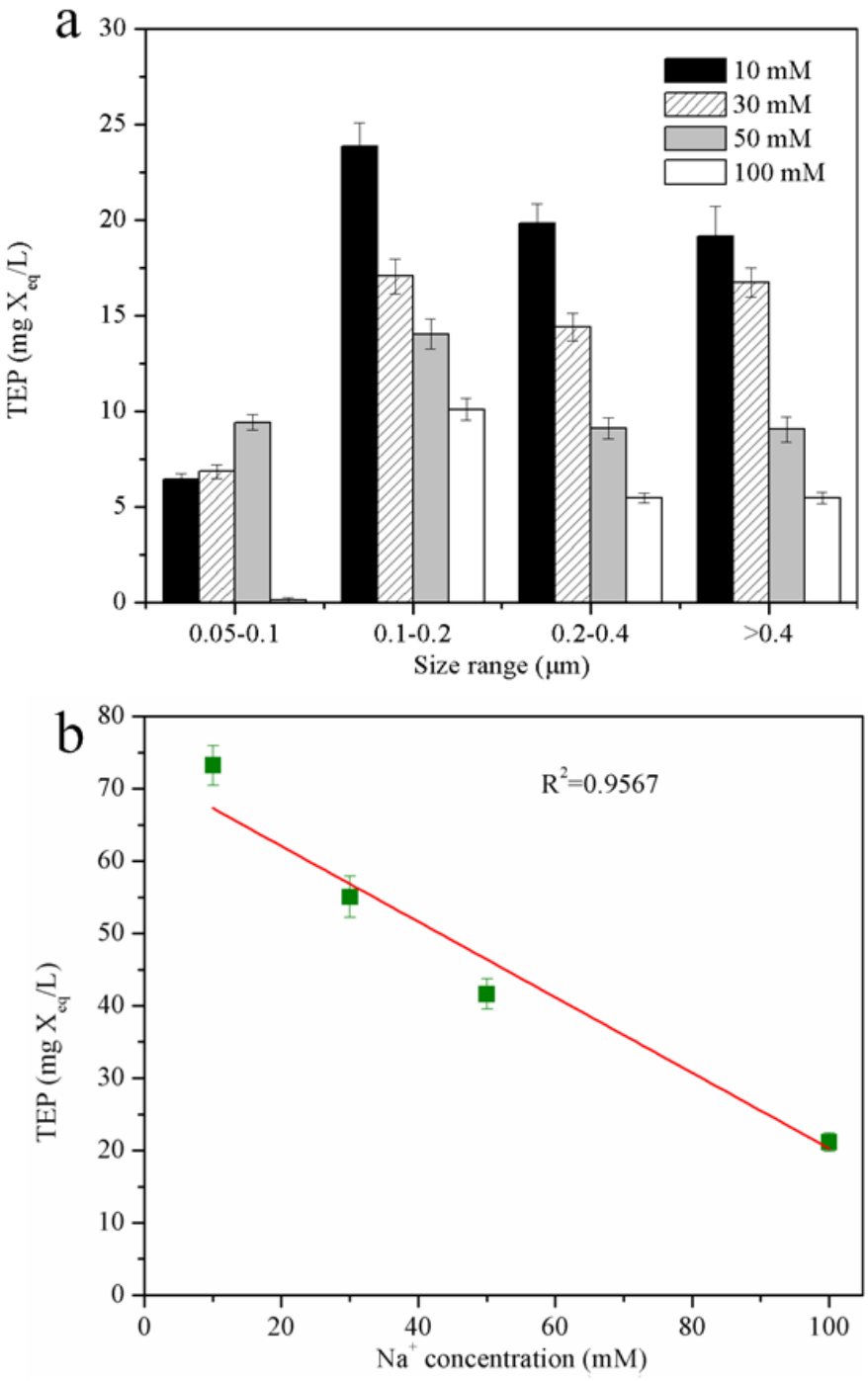

Figure 5.4 TEP concentrations derived from GG-blocks with increasing Na^{+} concentration. TEP levels in each size range (a) and the effect of increasing Na^{+}

concentration on the total TEP concentration (TEP retained by 0.05 μm polycarbonate filters) (b). Experimental conditions: GG-blocks concentration = 50 mg/L, Ca^{2+} concentration = 1 mM, Na^{+} concentrations are 10 mM, 30 mM, 50mM and 100 mM respectively.

In general, freshwater (e.g. lake, river and reservoir) often contains less Na^{+} than seawater. As revealed in this study, presumably more TEP could form in fresh water than in seawater at the same level of precursor materials. This is supported by previous studies showing that the highest TEP concentration reported in seawater was about 20% and 1.8% of those in freshwater and wastewater, respectively (Ramaiah and Furuya 2002, de la Torre et al. 2008, De Vicente et al. 2010, Bar-Zeev et al. 2015). It should be realized that the occurrence of TEP-associated biofilm development would be more frequent in freshwater and wastewater than in seawater. These may imply that TEP-associated fouling would pose a more serious challenge in wastewater reclamation by membrane than in seawater desalination.

5.3.1.2 Microscopic Observation of TEP formed under Different Sodium Concentrations

TEP developed from MG-, MM- and GG-blocks at various Na^{+} concentrations with a fixed Ca^{2+} concentration of 1 mM were directly visualized by means of a light-field microscope. As can be seen in Figure 5.5, at the Na^{+} concentration of 10 mM, the largest TEP in size and the highest concentration (Figure 5.5) were found in the situation of GG-blocks, with markedly complex and compact structure indicated by the strong blue color (Figure 5.5c). On the contrary, TEP derived from MG- and MM-blocks were much smaller in size and less in concentration (Figure 5.5a-b) than that derived from GG-blocks. Similar to the trends observed Figure 5.2-5.4, the microscopic images provide visual evidence that less TEP was generated with increasing Na^{+} concentration for all the three alginate blocks studied due to the competition between sodium and calcium ions for the binding sites on the alginate blocks. At 100 mM Na^{+} concentration, it was difficult to capture TEP in the solutions of MG- and MM-blocks (Figure 5.5d-e) and the TEP derived from GG-blocks are much smaller with simpler structure than that formed at 10 mM Na^{+}

concentration as shown in Figure 5.5f.

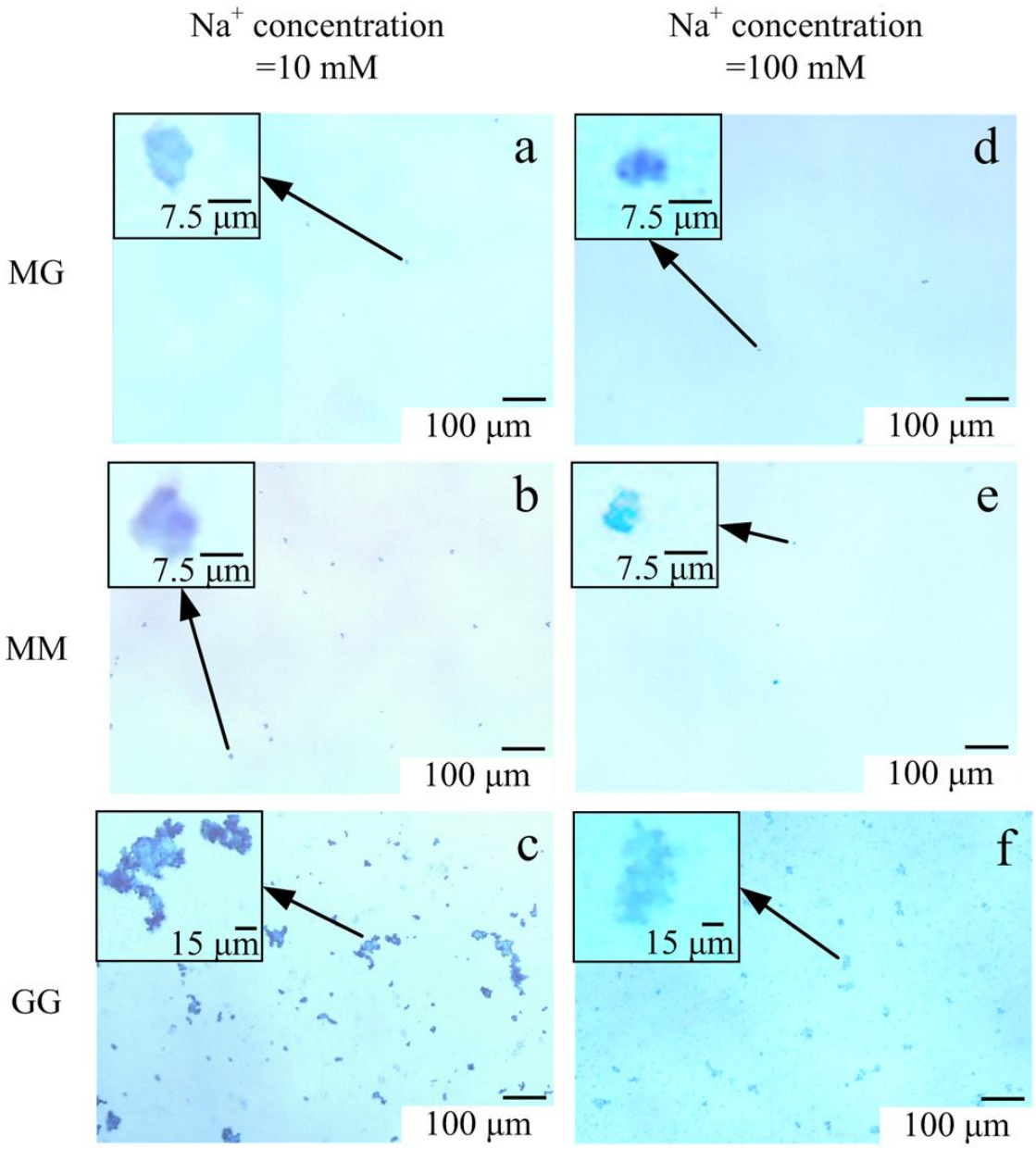

Figure 5.5 Microscopic observation of the effect of increasing Na^+ concentration on TEP derived from alginate blocks. TEP formed from MG-, MM- ang GG-blocks at 10 mM (a,b,c) and 100 mM (d,e,f) Na^+ concentration. Experimental conditions: MG-, MM- and GG-blocks concentration = 50 mg/L, Ca^{2+} concentration = 1 mM. TEP were stained with alcian blue.

FE-SEM images (Figure 5.6) further reveal the micro-structures of the TEP developed at various Na^+ concentrations, which provide insights into the crosslink

of alginate blocks via calcium bonding. For example, at the Na^+ concentration of 10 mM, some kind of concrete structure was observed for all the alginate blocks studied, which probably resulted from the bridging or cross-linking effect of calcium ion among precursors. However, when the Na^+ concentration was increased from 10 mM to 100 mM, nearly no TEP was developed from MG- and MM-blocks (Figure 5.6b and 5.6d), whereas a significantly reduced amount of TEP-like aggregate was observed (Figure 5.6f). Together with the results presented in Figure 5.2-5.4, these microscopic observations offer strong and direct evidence in supporting the argument of that sodium ion at its elevated concentration can outcompete with calcium ion for the bonding sites in the alginate blocks' molecules, and such competition in turn suppresses the cross-linking among alginate blocks. In study of gelation of alginate solution, it had been reported that the formation of alginate gel beads was impossible at molar ratio of Na^+ to Ca^{2+} of 97 (Ouwerx et al. 1998), which is nearly the same ratio as used in this study at the Na^+ concentration of 100 mM.

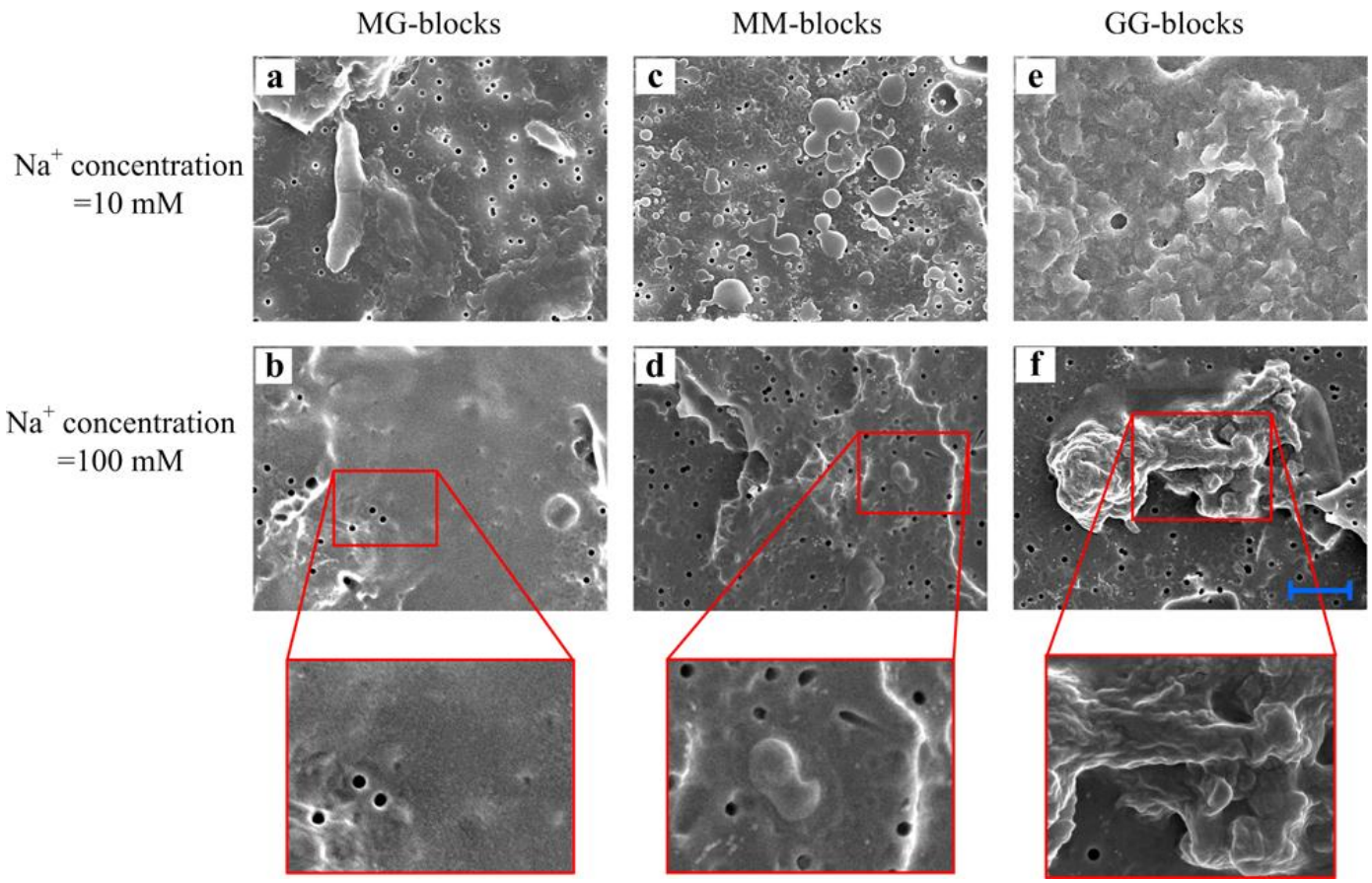

Figure 5.6 Micro-structure change of TEP derived from alginate blocks caused by increasing Na^+ concentration. FE-SEM images of the micro-structure of TEP formed from MG-, MM- and GG-blocks at 10 mM (a,c,e) and 100 mM (b,d,f) Na^+ concentration. Experimental conditions: MG-, MM- and GG-blocks concentration = 50 mg/L, Ca^{2+} concentration = 1 mM. Scale bar = 1 μm.

5.3.1.3 Viscoelasticity of TEP Developed at Different Sodium Ion Concentrations

It has been known that TEP are highly sticky and deformable (Passow 2002, Berman and Holenberg 2005, Villacorte et al. 2009). In this study, AFM was employed to measure adhesion force of the TEP layer, which provides quantitative information about the viscoelasticity and stickiness of TEP derived from GG-blocks at various Na^+ concentrations with a fixed Ca^{2+} concentration. The force measurements were performed on the clean filter surface (Figure 5.7a) and the filter surface covered by TEP (Figure 5.7b), respectively. For force measurements on the clean filter surfaces, the 10 mM and 100 mM Na^+ solutions were used and no notable difference lying in the force curves was found. The elastic properties of a sample could be corroborated from the slope of the force curve. For a stiff surface, when the tip of cantilever touching the surface, the deflection of the tip is proportional to the distance between the tip and sample surface (Domke and Radmacher 1998, Radmacher 2002), which is the case presented in Figure 5.7a for the filter surface. However, as for soft surface, like the filter covered by TEP (Figure 5.7b), the tip of the cantilever tends to indent the sample, resulting in a force curve with a smaller slope (Domke and Radmacher 1998, Radmacher 2002). Therefore, it can be reasonably considered that the TEP derived from GG-blocks at the Na^+ concentration of 100 mM should be much softer than the TEP generated from GG-blocks at the lower Na^+ concentration of 10 mM (Figure 5.8). Increasing Na^+ concentration at a fixed Ca^{2+} concentration led to a decreased stiffness of TEP. In addition, the adhesion force and energy were concurrently measured based on the retract force curve. As can be seen in Figure 5.9, higher adhesion force and energy are required to pull off the cantilever tip from the surface of TEP developed from GG-blocks at the higher Na^+ concentration of 100 mM, indicating that the TEP formed at higher Na^+ concentration appeared to be softer and stickier than that formed at the lower Na^+ concentration of 10 mM. These are likely due to the outcompeting of Na^+ against Ca^{2+}, leading to lesser crosslinking degree among the GG-blocks molecules. In the presence of calcium ion, a highly organized “egg-box” like structure of GG blocks can be developed (Grant et al. 1973). However, increased Na^+ concentration at a fixed Ca^{2+} concentration may outcompete with

Ca^{2+} in forming this "egg-box" like structure of GG-blocks. Therefore, less TEP was developed via the bonding between GG-blocks and Ca^{2+}. Moreover, such TEP should possess a weaker crosslink and network structure that in turn may explain increased softness and stickiness of TEP developed at high Na^{+} concentration as shown in Figure 5.8 and Figure 5.9. According to the Young's modulus value, Ca-alginate beads develop at high Na^{+}/Ca^{2+} ratio are much softer than those form at low Na^{+}/Ca^{2+} condition (Ouwerx et al. 1998). Consequently, it appears that the quantity and quality of TEP produced from precursors studied are largely determined by the concentration of Na^{+} present in aquatic environment.

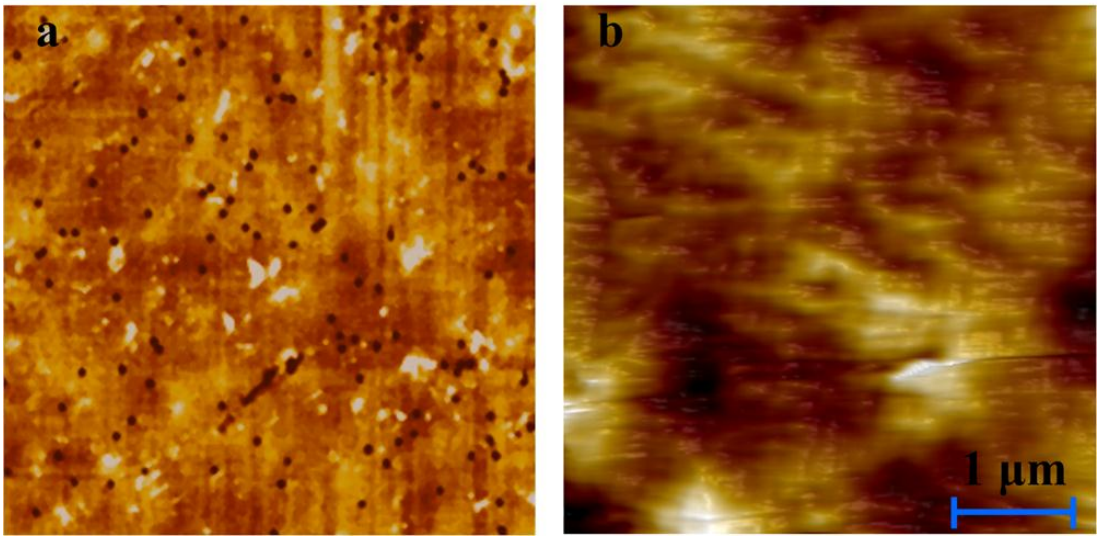

Figure 5.7 AFM images of (a) clean filter surface and (b) TEP film retained on the filter.

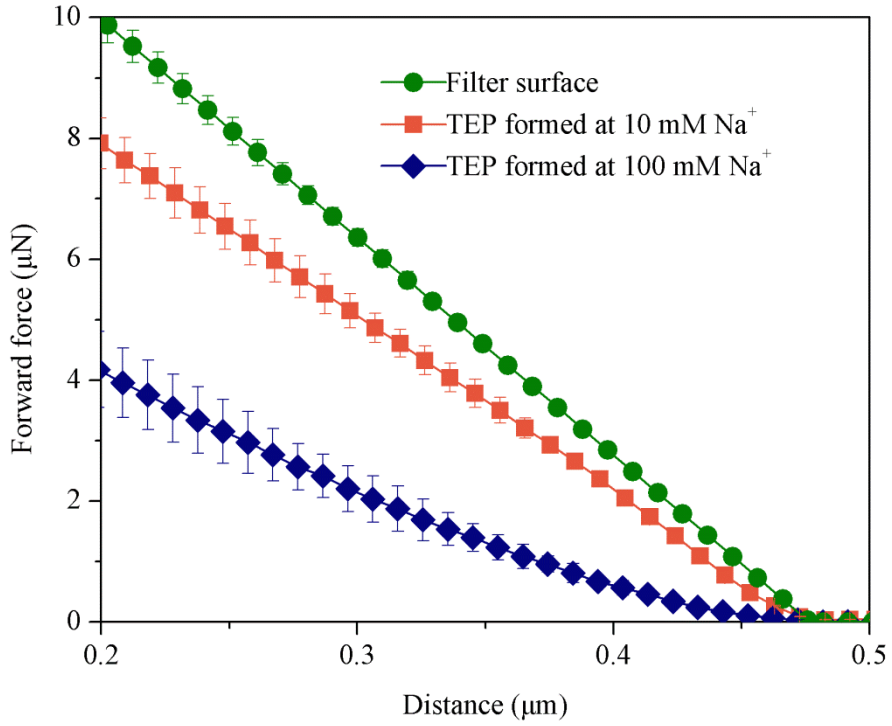

Figure 5.8 The forward force curves measured at the filter surface and TEP film developed at different sodium ion concentrations.

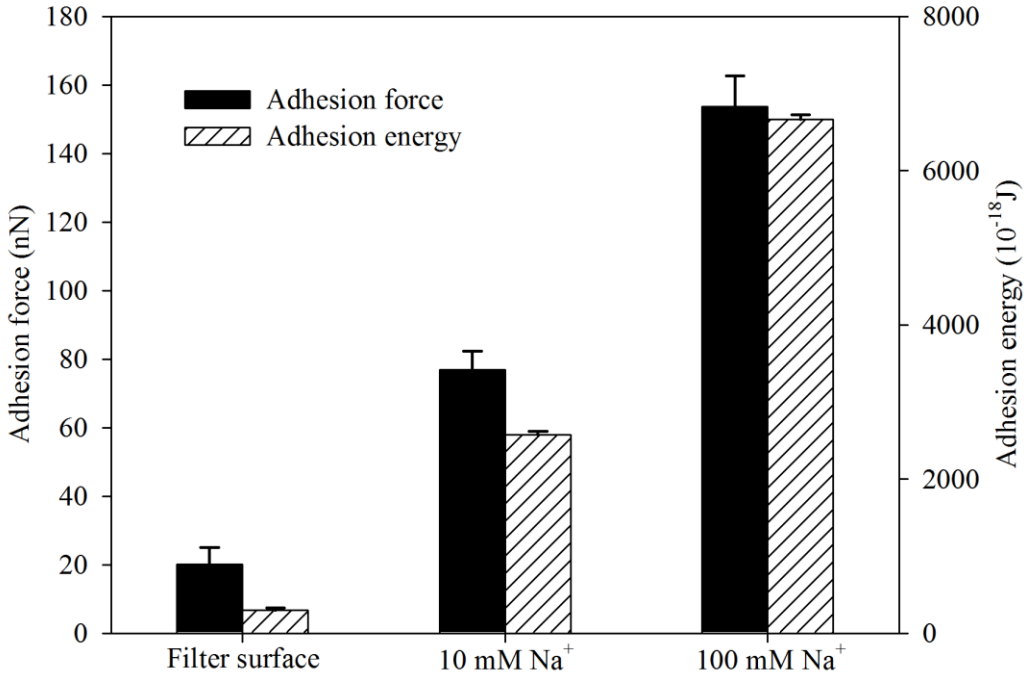

Figure 5.9 Maximum adhesion forces and total energies needed to completely pull off cantilever from the sample surfaces.

5.3.2 Filtration Behaviors of Alginate Blocks at Various Na^+ Concentrations.

5.3.2.1 Permeate Fluxes of MG-, MM- and GG-blocks

As presented above, it is obvious that sodium ion has significant effects on the TEP formation, physic-chemical properties and microstructures of MG-, MM- and GG-blocks. These suggest that the filtration behaviours of these alginate blocks are presumably affected by the presence of sodium ion. In this study, filtration behaviours of the alginate blocks at four different Na^+ concentrations were examined in a laboratory-scale cross-flow filtration module.

Figure 5.10a shows the permeate fluxes observed during the ultrafiltration of MG-blocks at various Na^+ concentrations. At the Na^+ concentration of 10 mM, the permeate flux of MG-blocks dropped quickly at the beginning of the test and 69.9% of a flux decline was recorded at the end of 20-h filtration. In contrast, the permeate fluxes of the MG-blocks decreased much slowly with increasing the Na^+ concentration (Figure 5.10b). As discussed above, increasing Na^+ concentration significantly reduced the TEP formation from MG-blocks (Figure 5.2). This indicates that the aggregation of MG-blocks was greatly prohibited at elevated Na^+ concentration. As the result, most MG-blocks existed in the form of single molecules which could easily pass through the membrane pores, leading to less cake formation on the membrane surface.

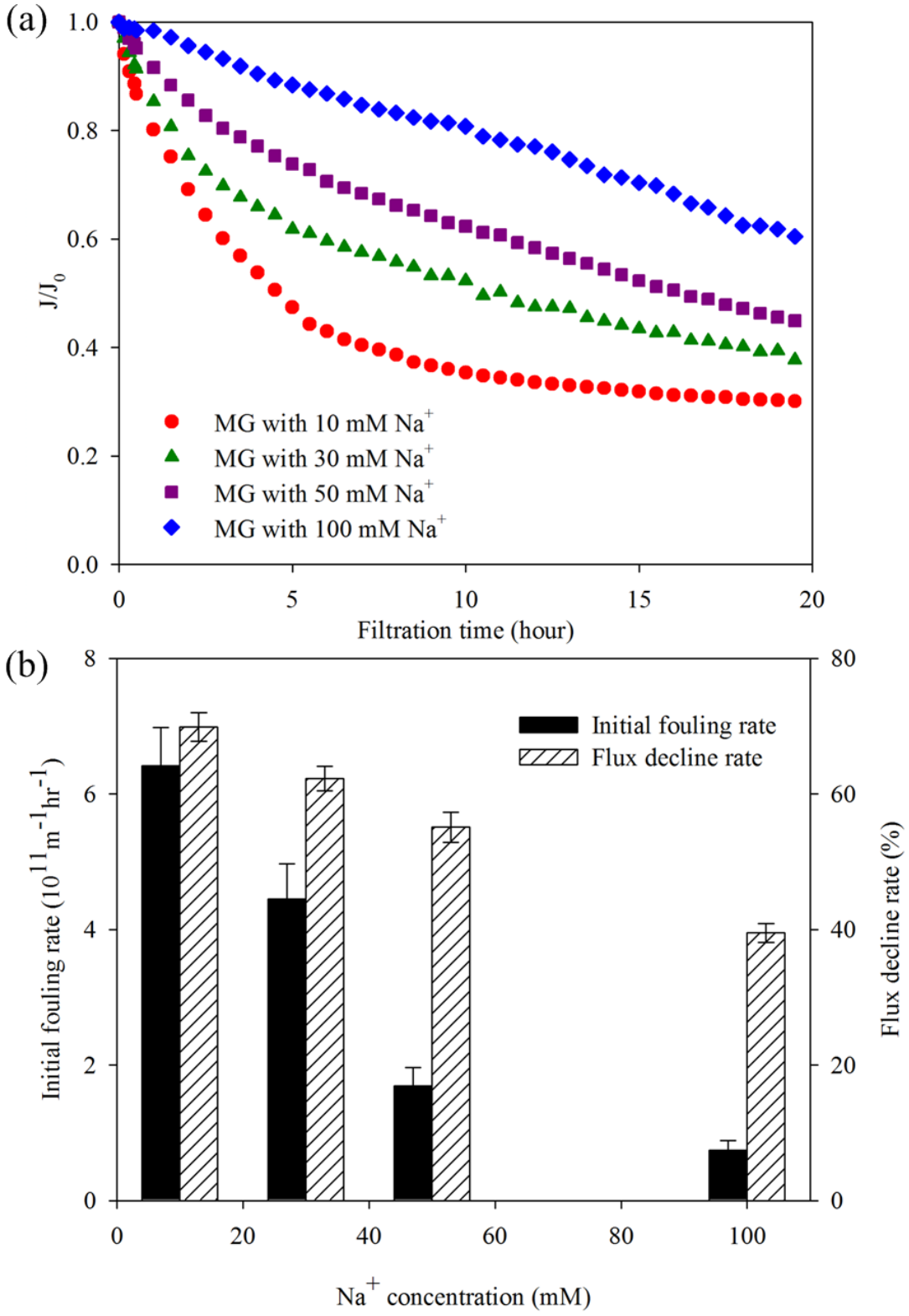

Figure 5.10 Filtration behaviours of MG-blocks. a: Permeate fluxes; b: Initial fouling rates as well as final flux decline rates (b). MG-blocks concentration = 50 mg/L.

The similar effect of Na^+ on the filtration behaviours of MM- and GG-blocks were also observed in Figure 5.11 and 5.12, i.e. the initial fouling rates and the final permeate flux decline rates were reduced at elevated Na^+ concentrations (Figure 5.11b and Figure 5.12b). It appears that the membrane fouling developed during the filtration of MM- and GG-blocks was mainly due to the formation of the cake layer. In this study, the membrane used has a molecular weight cut-off of 20 kDa, thus TEP with a size greater than 0.05 μm can be effectively retained, and accumulated on the membrane surface, contributing to the formation of cake layer. Furthermore, the reduced TEP formation at elevated Na^+ concentrations in the feed water would mitigate the cake layer development during the filtration of alginate blocks (Figure 5.3 and 5.4). These may explain less serious fouling observed in the filtration of MM- and GG-blocks at high Na^+ concentrations. Since the Na^+ concentration in seawater is much higher than in freshwater, a severer TEP-associated fouling could be expected during the membrane filtration of freshwater instead of seawater.

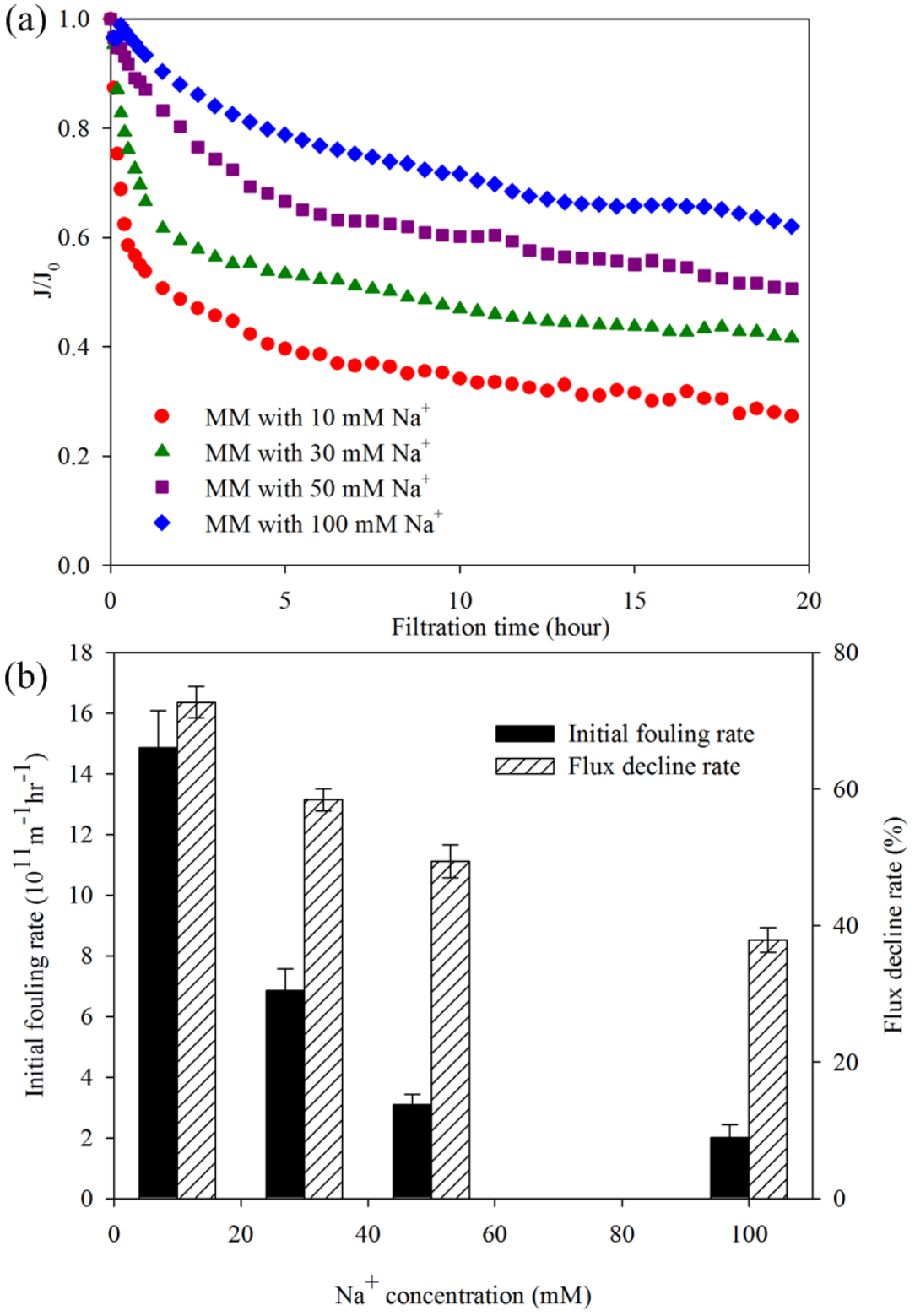

Figure 5.11 Filtration behaviours of MM-blocks. a: Permeate fluxes; b: Initial fouling rates as well as final flux decline rates. MM-blocks concentration = 50 mg/L.

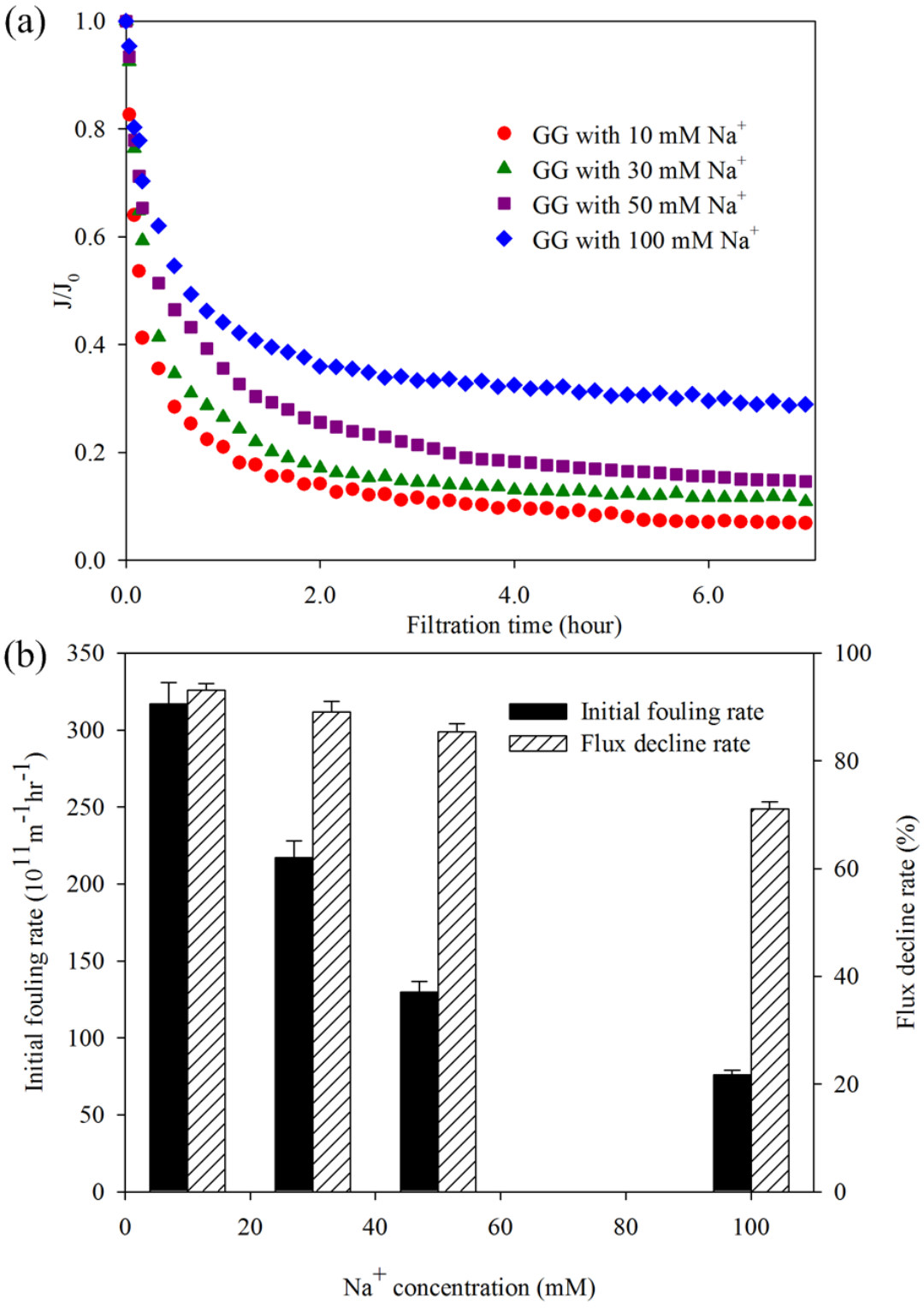

Figure 5.12 Filtration behaviours of GG-blocks. a: Permeate fluxes; b: Initial fouling rates as well as final flux decline rates. GG-blocks concentration = 50 mg/L.

It can be seen in Figure 5.13 that the initial fouling rate was positively related to the TEP concentration in feed water, while low TEP concentration was observed at high Na^+ concentration. Thus, low fouling propensity was found at high Na^+ concentration. The results presented above clearly indicate that the TEP level in feed water determines membrane fouling propensity. In fact, it is reasonable to consider that the ionic condition of feed water may greatly influence the TEP formation that ultimately determines the development of membrane fouling.

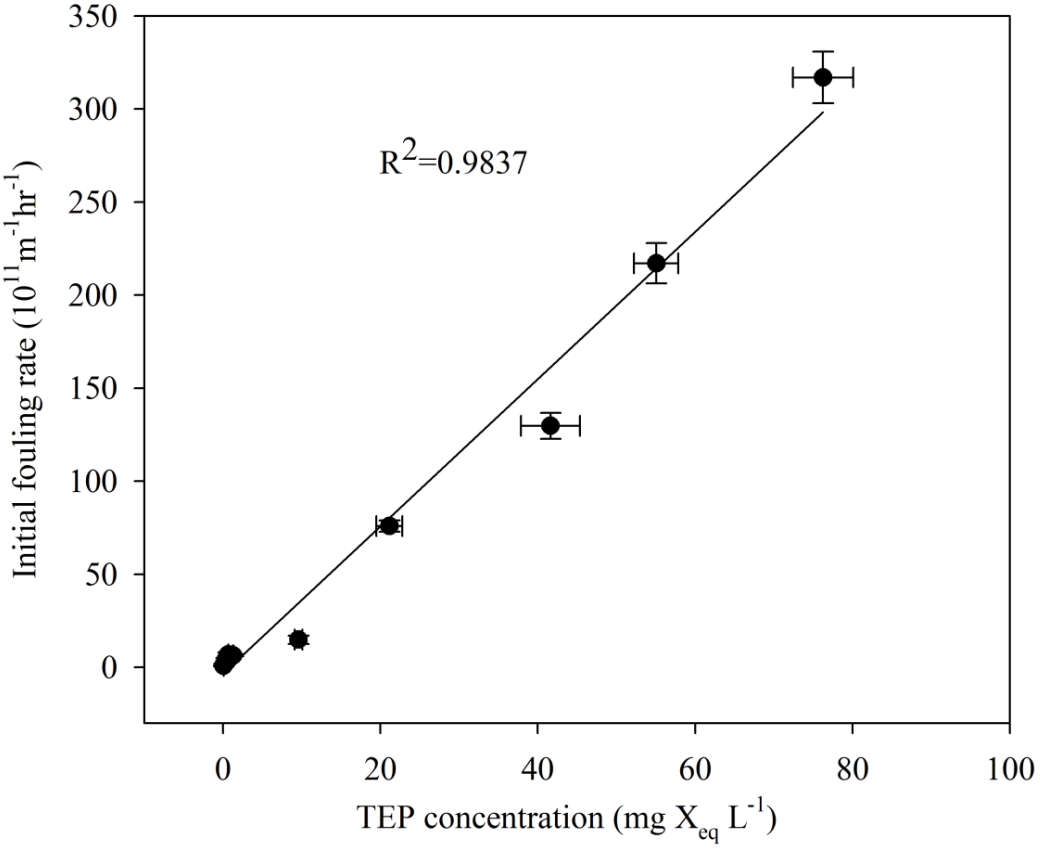

Figure 5.13 Correlation between the TEP concentrations in feed water (TEP retained by 0.05 μm polycarbonate filters) and the initial fouling rates of the alginate blocks in filtration tests.

5.3.3 Cake layer formed on membrane surface

The cake layers developed at the end of 30-min filtration of GG-blocks solution with the respective Na^+ concentrations of 10 mM and 100 mM were characterized

by AFM. AFM deflection images (Figure 5.14a and b) show the surface topography of corresponding areas that were further subjected to the measurements of adhesion forces as presented in Figure 5.15 and Figure 5.16. It is impossible to measure the adhesion forces on every points of the cake layer, so that four places were randomly sampled and the average data of two points is reported. At the Na^+ concentration of 100 mM, only a small portion of the membrane surface was covered by scattered pin cakes with a mean thickness of 20-120 nm (Figure 5.14a), whereas the adhesion forces of these pin cake layers were measured to be in the range of 1.6-3.6 nN (Figure 5.15). On contrast, at the Na^+ concentration of 10 mM, the membrane surface was entirely covered by the larger and thicker cake layers (~100-300 nm) (Figure 5.14b) with adhesion forces in the range of 10.5 and 21.5 nN (Figure 5.16). It is obvious that more TEP attach on the membrane surface at low Na^+ concentration, leading to a thicker and stickier cake layer formed on membrane surface. These observations are in good agreement with the permeate flux decline trends observed in Figure 5.12, where much severer fouling is recorded at low Na^+ concentration than at high Na^+ concentration. Concurrently, TEP quantification (Figure 5.4) results are also consistent with the AFM measurements. These once again provide direct visual evidence showing that more TEP was formed and further deposited on the membrane surface at low Na^+ concentration, leading to the formation of a thicker and stickier cake layer on membrane surface. As such, the TEP-associated membrane fouling would be more serious in freshwater than in seawater at the given concentrations of precursor and calcium ion.

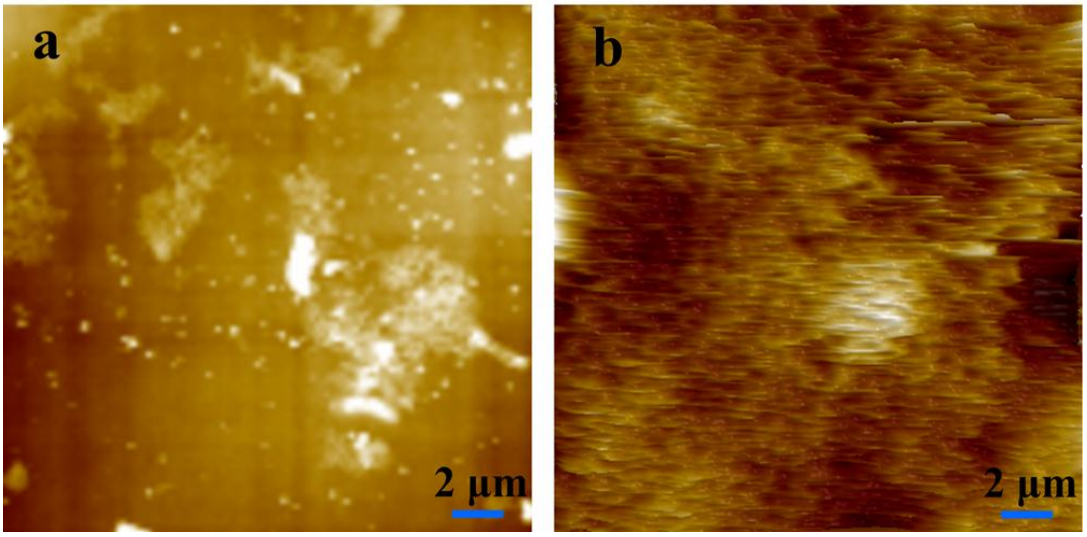

Figure 5.14 AFM images of cake layer in the filtrations of GG-blocks at the Na^+ concentrations of 100 mM (a) and 10 mM (b), taken at the end of 30min filtration.

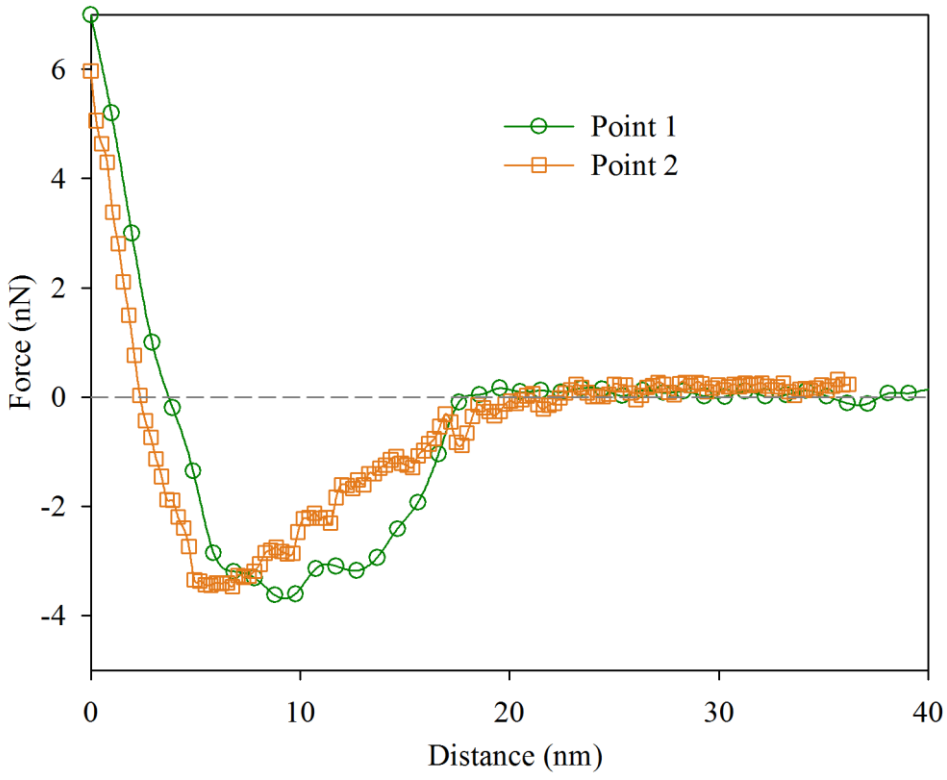

Figure 5.15 AFM force measurements of the cake layer developed on membrane surface at the end of 30-min filtration of GG-blocks. Na^+ concentration = 100 mM.

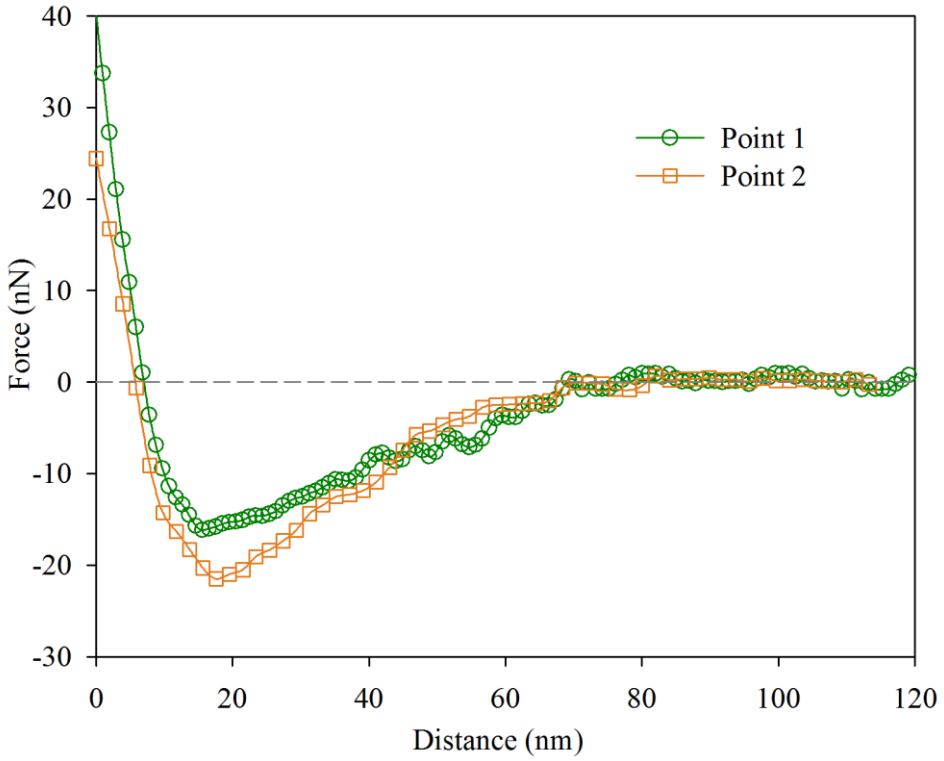

Figure 5.16 AFM force measurements of cake layer developed on membrane surface at the end of 30-min filtration of GG-blocks. Na^+ concentration =10 mM.

5.3.4 Mechanistic Interpretation of TEP Formation at Various Na^+ Concentrations

As shown above, TEP formation from alginate blocks is significantly affected by calcium and sodium ions. Using GG-blocks as an example, Figure 5.17 illustrates possible competition of Na^+ against Ca^{2+} in bonding with alginate blocks. As discussed above, at the Na^+ concentration of 10 mM, a fair amount of GG-blocks are cross-linked together through bridging by calcium ions, producing TEP with large size and complex structure. With the increase in the Na^+ concentration from 10 mM to 100 mM, the bonding opportunity of GG-blocks to calcium ions is out-competed by sodium ions. As the result of such completion between Na^+ and Ca^{2+}, TEP formation was remarkably reduced as observed in Figure 5.4. Moreover, a substantial amount of alginate blocks still remained as single molecules without inter-aggregation. This in turn may explain that TEP developed at the Na^+ concentration of 100 mM were much smaller in size than those formed at 10 mM of

Na^+. It should also be pointed out that similar competition between Na^+ and Ca^{2+} was also observed during the formation of alginate gel beads (Draget et al. 1998, Qin 2004). Chemically, similar mechanisms are applicable for TEP formation with MG- and MM-blocks.

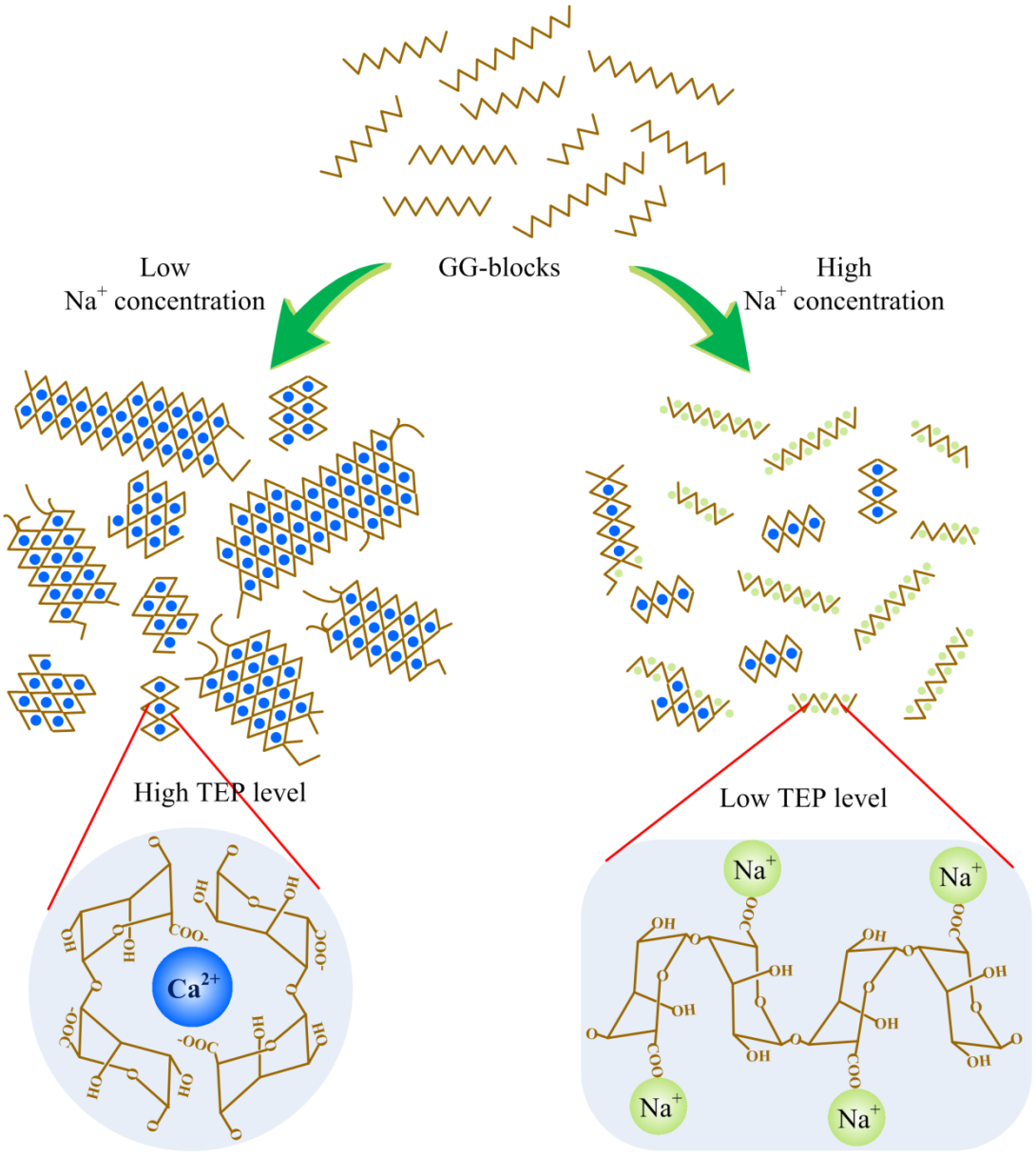

Figure 5.17 Mechanistic interpretation of structural changes occurring in GG-blocks bonding with calcium ions in competition with sodium ions. The blue, green dots and brown lines represent the calcium, sodium ions and GG-blocks respectively.

5.4 CONCLUDING REMARKS

The current study investigated the effect of Na^+ concentration on the TEP formation from three types of alginate blocks as well as the role of TEP in membrane fouling. The results from this study demonstrated that the formation of TEP was highly Na^+ concentration-dependent under defined conditions. Increasing Na^+ concentration could markedly reduce the TEP formation from alginate blocks studied due to out-competition of Na^+ ion to Ca^{2+} ion, especially for MG- and MM-blocks. As the result, membrane fouling by TEP was found to be much less, and kinetically slower at higher Na^+ concentrations. Applying AFM measurements provided direct observation and quantitative information about the cake layer formed on membrane surface, revealing that at low concentration of Na^+ the cake layer developed was thicker and stickier than that at high Na^+ concentration The present study offers experimental evidence showing that a more abundant TEP can be expected in freshwater than in seawater. This in turn implies that TEP-associated biofilm development and membrane fouling would be more significant in membrane filtration of freshwater than seawater.

CHAPTER 6 CONCLUSIONS AND RECOMMENDATIONS

6.1 CONCLUSIONS

This study investigated the TEP formation from alginate blocks and their effects on membrane fouling. The following conclusions have been reached.

(1) MG-, MM- and GG-blocks which were fractionated from the alginate exhibited distinguished propensities in membrane fouling. The fouling propensities of these alginate blocks increased in the order MM<GG<MG. Initial pore blocking was responsible for the severe fouling in MG-block filtration, while the cake layer formed on membrane surface during MM-block filtration would serve as a pre-filter that prevented membrane from further pore blocking. The observed fouling behaviors of these alginate blocks could be explained by their abilities to form TEP.

(2) The analysis by XDLVO theory further revealed that MM-blocks had the lowest cohesive interaction energy among all three alginate blocks, which favoured aggregation of MM-blocks, and ultimately led to more substantial formation of TEP. Since TEP had larger dimension than single molecule of alginate blocks, they can effectively promote the formation of cake layer through attachment onto membrane surface.

(3) The cohesive interaction energy between MG-blocks was much higher than other alginate blocks, which prevented the formation of TEP in MG-blocks solution. This made the penetration of MG-blocks through membrane pores possible.

(4) Although derived from the same alginate source, MG-, MM and GG-blocks exhibited highly different fouling behaviors during membrane filtration and

their fouling propensities were found to be related to their abilities to form TEP.

(5) The reaction between calcium ion and GG-blocks was found to be the strongest, thus the highest TEP concentration was produced. Although the formation of TEP from MM-blocks was also enhanced by the addition of calcium ion, it was not as intensive as that observed for GG-blocks. As to the MG-blocks, the effect of calcium ion was the lightest and only very limited amount of TEP was produced.

(6) Ultrafiltration membrane was quickly fouled by feed water containing high-concentration TEP due to the deposition and accumulation of TEP on the membrane surface. Correlation between the TEP level in feed water and the initial fouling rate as well as the foulant mass deposited on the membrane further suggested that the extent of membrane fouling was largely determined by the amount of TEP.

(7) In contrast to Ca^{2+}, Na^{+} exerted a significant adverse effect on TEP formation from various alginate blocks. It was found that increasing Na^{+} concentration may markedly reduce the TEP formation from the alginate blocks due to out-competition between Na^{+} and Ca^{2+} ions, especially for MG- and MM-blocks. As the result, membrane fouling by TEP was much less, and kinetically slower at higher Na^{+} concentrations.

(8) Lastly, the present study offers experimental evidence showing that a more abundant TEP can be expected in freshwater than in seawater. This in turn implies that TEP-associated biofilm development and membrane fouling would be more significant in membrane filtration of freshwater than seawater.

6.2 RECOMMENDATIONS

This study sheds the lights into TEP formation under various water chemistry conditions and the TEP-associated membrane fouling.

Due to their high stickiness, TEP usually can absorb other compounds, such as

protein, lipid. The interaction between polysaccharides and these substances should be investigated to observe the TEP formation as well as the membrane fouling development under defined conditions.

In natural water environments, TEP are extensively colonized by diverse bacteria. The term “protobiofilm” refers to TEP with extensive microbial outgrowth and colonization. TEP are considered to play a critical role in the biofilm development. The future study should investigate “protobiofilm” with isolated TEP and selected bacteria and examine the attachment of “protobiofilm” on membrane surface. Besides, the presence of bacteria on TEP maybe changes the structure of TEP as well as their effect on membrane fouling. Furthermore, the membrane fouling by “protobioflim”, TEP and bacteria should be studied and compared quantitatively in order to clarify their respective roles in initiating membrane fouling.

REFERENCES

Al-Juboori, R. A. and T. Yusaf (2012). "Biofouling in RO system: Mechanisms, monitoring and controlling." Desalination **302**(0): 1-23.

Alhadidi, A., A. J. B. Kemperman, B. Blankert, J. C. Schippers, M. Wessling and W. G. J. van der Meer (2011). "Silt Density Index and Modified Fouling Index relation, and effect of pressure, temperature and membrane resistance." Desalination **273**(1): 48-56.

Alldredge, A. L., U. Passow and B. E. Logan (1993). "The abundance and significance of a class of large, transparent organic particles in the ocean." Deep Sea Research Part I: Oceanographic Research Papers **40**(6): 1131-1140.

Amin, I. N. H. M., A. W. Mohammad, M. Markom and L. C. Peng (2010). "Effects of palm oil-based fatty acids on fouling of ultrafiltration membranes during the clarification of glycerin-rich solution." Journal of Food Engineering **101**(3): 264-272.

Ang, W. S. and M. Elimelech (2008). "Fatty acid fouling of reverse osmosis membranes: Implications for wastewater reclamation." Water Research **42**(16): 4393-4403.

Armbrust, E. V. (2009). "The life of diatoms in the world's oceans." Nature **459**(7244): 185-192.

Arruda Fatibello, S. H. S., A. A. Henriques Vieira and O. Fatibello-Filho (2004). "A rapid spectrophotometric method for the determination of transparent exopolymer particles (TEP) in freshwater." Talanta **62**(1): 81-85.

Azam, F. and F. Malfatti (2007). "Microbial structuring of marine ecosystems." Nature Reviews Microbiology **5**(10): 782-791.

Baker, R. (2004). Membrane Technology and Applications, Hoboken : John Wiley

& Sons, Ltd., 2004. 2nd ed.

Bar-Zeev, E., I. Berman-Frank, O. Girshevitz and T. Berman (2012). "Revised paradigm of aquatic biofilm formation facilitated by microgel transparent exopolymer particles." Proceedings of the National Academy of Sciences **109**(23): 9119-9124.

Bar-Zeev, E., I. Berman-Frank, B. Liberman, E. Rahav, U. Passow and T. Berman (2009). "Transparent exopolymer particles: Potential agents for organic fouling and biofilm formation in desalination and water treatment plants." Desalination and Water Treatment **3**(1-3): 136-142.

Bar-Zeev, E., U. Passow, S. Romero-Vargas Castrillón and M. Elimelech (2015). "Transparent Exopolymer Particles: From Aquatic Environments and Engineered Systems to Membrane Biofouling." Environmental Science & Technology **49**(2): 691-707.

Bartels, C. R., M. Wilf, K. Andes and J. Iong (2005). "Design considerations for wastewater treatment by reverse osmosis." Water Sci Technol **51**(6-7): 473-482.

Berger, B., B. Hoch, G. Kavka and G. Herndl (1996). "Bacterial colonization of suspended solids in the River Danube." Aquatic Microbial Ecology **10**(1): 37-44.

Berman-Frank, I., G. Rosenberg, O. Levitan, L. Haramaty and X. Mari (2007). "Coupling between autocatalytic cell death and transparent exopolymeric particle production in the marine cyanobacterium Trichodesmium." Environmental microbiology **9**(6): 1415-1422.

Berman, T. (2010). "Biofouling: TEP – a major challenge for water filtration." Filtration & Separation **47**(2): 20-22.

Berman, T. (2012). "Transparent exopolymer particles as critical agents in aquatic biofilm formation: implications for desalination and water treatment." Desalination and Water Treatment: 1-7.

Berman, T. and M. Holenberg (2005). "Don't fall foul of biofilm through high TEP levels." Filtration & Separation **42**(4): 30-32.

Berman, T., R. Mizrahi and C. G. Dosoretz (2011). "Transparent exopolymer particles (TEP): A critical factor in aquatic biofilm initiation and fouling on filtration membranes." Desalination **276**(1–3): 184-190.

Berman, T. and R. Parparova (2010). "Visualization of transparent exopolymer particles (TEP) in various source waters." Desalination and Water Treatment **21**(1-3): 382-389.

Berman, T. and U. Passow (2007). "Transparent Exopolymer Particles (TEP): an overlooked factor in the process of biofilm formation in aquatic environments." Nature Precedings.

Berman, T. and Y. Viner-Mozzini (2001). "Abundance and characteristics of polysaccharide and proteinaceous particles in Lake Kinneret." Aquatic Microbial Ecology **24**(3): 255-264.

Boributh, S., A. Chanachai and R. Jiraratananon (2009). "Modification of PVDF membrane by chitosan solution for reducing protein fouling." Journal of Membrane Science **342**(1–2): 97-104.

Bowen, W. R., J. I. Calvo and A. Hernández (1995). "Steps of membrane blocking in flux decline during protein microfiltration." Journal of Membrane Science **101**(1–2): 153-165.

Boyd, P. W., R. Strzepek, S. Takeda, G. Jackson, C. Wong, R. M. McKay, C. Law, H. Kiyosawa, H. Saito and N. Sherry (2005). "The evolution and termination of an iron-induced mesoscale bloom in the northeast subarctic Pacific." Limnology and Oceanography **50**(6): 1872-1886.

Brant, J. A. and A. E. Childress (2002). "Assessing short-range membrane–colloid interactions using surface energetics." Journal of Membrane Science **203**(1–2): 257-273.

Bremere, I., M. Kennedy, P. Michel, R. van Emmerik, G.-J. Witkamp and J. Schippers (1999). "Controlling scaling in membrane filtration systems using a desupersaturation unit." Desalination **124**(1–3): 51-62.

Bremere, I., M. D. Kennedy, A. Johnson, R. van Emmerik, G.-J. Witkamp and J. C. Schippers (1998). "Increasing conversion in membrane filtration systems using a desupersaturation unit to prevent scaling." Desalination **119**(1–3): 199-204.

Brinck, J., A. S. Jönsson, B. Jönsson and J. Lindau (2000). "Influence of pH on the adsorptive fouling of ultrafiltration membranes by fatty acid." Journal of Membrane Science **164**(1–2): 187-194.

Broeckmann, A., T. Wintgens and A. I. Schäfer (2005). "Removal and fouling mechanisms in nanofiltration of polysaccharide solutions." Desalination **178**(1–3): 149-159.

Chan, R. and V. Chen (2004). "Characterization of protein fouling on membranes: opportunities and challenges." Journal of Membrane Science **242**(1–2): 169-188.

Chandía, N. P., B. Matsuhiro, E. Mejías and A. Moenne (2004). "Alginic acids in Lessonia vadosa: partial hydrolysis and elicitor properties of the polymannuronic acid fraction." Journal of applied phycology **16**(2): 127-133.

Cheryan, M. (1998). Ultrafiltration and microfiltration handbook Lancaster, Pa. : Technomic Pub. Co., c1998.

Childress, A. E. and M. Elimelech (2000). "Relating Nanofiltration Membrane Performance to Membrane Charge (Electrokinetic) Characteristics." Environmental Science & Technology **34**(17): 3710-3716.

Chin, W.-C., M. V. Orellana and P. Verdugo (1998). "Spontaneous assembly of marine dissolved organic matter into polymer gels." Nature **391**(6667): 568-572.

Cogan, N. G. and S. Chellam (2009). "Incorporating pore blocking, cake filtration, and EPS production in a model for constant pressure bacterial fouling during dead-end microfiltration." Journal of Membrane Science **345**(1–2): 81-89.

Cohen, R. D. and R. F. Probstein (1986). "Colloidal fouling of reverse osmosis membranes." Journal of Colloid and Interface Science **114**(1): 194-207.

Condon, R. H., D. K. Steinberg, P. A. del Giorgio, T. C. Bouvier, D. A. Bronk, W. M. Graham and H. W. Ducklow (2011). "Jellyfish blooms result in a major microbial respiratory sink of carbon in marine systems." Proceedings of the National Academy of Sciences **108**(25): 10225-10230.

Daigger, G. T., J. C. Lozier and G. V. Crawford (2006). "Water Reuse Applications Using Membrane Technology." Proceedings of the Water Environment Federation **2006**(10): 2625-2633.

Dam, H. G. and D. T. Drapeau (1995). "Coagulation efficiency, organic-matter glues and the dynamics of particles during a phytoplankton bloom in a mesocosm study." Deep Sea Research Part II: Topical Studies in Oceanography **42**(1): 111-123.

de la Torre, T., M. Kraume, B. Lesjean, A. Drews, J. Stüber, F. Meng and V. Iversen (2010). "Searching for a universal fouling indicator for membrane bioreactors." Desalination and Water Treatment: 264-269.

de la Torre, T., B. Lesjean, A. Drews and M. Kraume (2008). "Monitoring of transparent exopolymer particles (TEP) in a membrane bioreactor (MBR) and correlation with other fouling indicators." Water Sci Technol **58**(10): 1903-1909.

De Vicente, I., E. Ortega-Retuerta, I. P. Mazuecos, M. L. Pace, J. J. Cole and I. Reche (2010). "Variation in transparent exopolymer particles in relation to biological and chemical factors in two contrasting lake districts." Aquatic sciences **72**(4): 443-453.

De Vos, P., B. De Haan, G. H. Wolters and R. Van Schilfgaarde (1996). "Factors

influencing the adequacy of microencapsulation of rat pancreatic islets1." Transplantation **62**(7): 888-893.

Discart, V., M. R. Bilad, D. Vandamme, I. Foubert, K. Muylaert and I. F. Vankelecom (2013). "Role of transparent exopolymeric particles in membrane fouling: Chlorella vulgaris broth filtration." Bioresour Technol **129**: 18-25.

Discart, V., M. R. Bilad and I. F. J. Vankelecom (2015). "Critical Evaluation of the Determination Methods for Transparent Exopolymer Particles, Agents of Membrane Fouling." Critical Reviews in Environmental Science and Technology **45**(2): 167-192.

Domke, J. and M. Radmacher (1998). "Measuring the Elastic Properties of Thin Polymer Films with the Atomic Force Microscope." Langmuir **14**(12): 3320-3325.

Donati, I. and S. Paoletti (2009). Material Properties of Alginates. Alginates: Biology and Applications. B. H. A. Rehm, Springer Berlin Heidelberg. **13:** 1-53.

Draget, K. I., O. Smidsrød and G. Skjåk-Bræk (2005). Alginates from Algae. Biopolymers Online, Wiley-VCH Verlag GmbH & Co. KGaA.

Draget, K. I., K. Steinsvåg, E. Onsøyen and O. Smidsrød (1998). "Na- and K-alginate; effect on Ca2+-gelation." Carbohydrate Polymers **35**(1–2): 1-6.

Elimelech, M., J. Gregory, X. Jia and W. R.A (1995). Particle Deposition and Aggregation - Measurement, Modelling and Simulation, Elsevier.

Elimelech, M. and W. A. Phillip (2011). "The Future of Seawater Desalination: Energy, Technology, and the Environment." Science **333**(6043): 712-717.

Engel, A. (2000). "The role of transparent exopolymer particles (TEP) in the increase in apparent particle stickiness (α) during the decline of a diatom bloom." Journal of Plankton Research **22**(3): 485-497.

Engel, A. (2004). "Distribution of transparent exopolymer particles (TEP) in the northeast Atlantic Ocean and their potential significance for aggregation processes." Deep Sea Research Part I: Oceanographic Research Papers **51**(1): 83-92.

Engel, A. and U. Passow (2001). "Carbon and nitrogen content of transparent exopolymer particles (TEP) in relation to their Alcian Blue adsorption." Marine Ecology Progress Series **219**: 1-10.

Fane, A. G., C. Y. Tang and R. Wang (2011). 4.11 - Membrane Technology for Water: Microfiltration, Ultrafiltration, Nanofiltration, and Reverse Osmosis. Treatise on Water Science. P. Wilderer. Oxford, Elsevier**:** 301-335.

Field, R. (2010). "Fundamentals of fouling." Membranes for Water Treatment **4**: 1-23.

Flemming, H.-C. (1997). "Reverse osmosis membrane biofouling." Experimental Thermal and Fluid Science **14**(4): 382-391.

Fouilland, E. and B. Mostajir (2010). "Revisited phytoplanktonic carbon dependency of heterotrophic bacteria in freshwaters, transitional, coastal and oceanic waters." FEMS microbiology ecology **73**(3): 419-429.

Gómez-Ordóñez, E. and P. Rupérez (2011). "FTIR-ATR spectroscopy as a tool for polysaccharide identification in edible brown and red seaweeds." Food Hydrocolloids **25**(6): 1514-1520.

Gasia-Bruch, E., P. Sehn, V. García-Molina, M. Busch, O. Raize and M. Negrin (2011). "Field experience with a 20,000 m3/d integrated membrane seawater desalination plant in Cyprus." Desalination and Water Treatment **31**(1-3): 178-189.

Goosen, M. F. A., S. S. Sablani, H. Al-Hinai, S. Al-Obeidani, R. Al-Belushi and D. Jackson (2005). "Fouling of Reverse Osmosis and Ultrafiltration Membranes: A Critical Review." Separation Science and Technology **39**(10): 2261-2297.

Grant, G. T., E. R. Morris, D. A. Rees, P. J. C. Smith and D. Thom (1973). "Biological interactions between polysaccharides and divalent cations: The egg-box model." FEBS Letters **32**(1): 195-198.

Guezennec, J., J. M. Herry, A. Kouzayha, E. Bachere, M. W. Mittelman and M. N. Bellon Fontaine (2012). "Exopolysaccharides from unusual marine environments inhibit early stages of biofouling." International Biodeterioration & Biodegradation **66**(1): 1-7.

Habib, M., U. Habib, A. R. Memon, U. Amin, Z. Karim, A. U. Khan, S. Naveed and S. Ali (2013). "Predicting colloidal fouling of tap water by silt density index (SDI): Pore blocking in a membrane process." Journal of Environmental Chemical Engineering **1**(1): 33-37.

Hao, Y., A. Moriya, Y. Ohmukai, H. Matsuyama and T. Maruyama (2013). "Effect of metal ions on the protein fouling of hollow-fiber ultrafiltration membranes." Separation and Purification Technology **111**(0): 137-144.

Hayat, M. A. (1993). Stains and cytochemical methods, Springer Science & Business Media.

Hermia, J. (1985). Blocking Filtration. Application to Non-Newtonian Fluids. Mathematical Models and Design Methods in Solid-Liquid Separation. A. Rushton, Springer Netherlands. **88:** 83-89.

Herzberg, M. and M. Elimelech (2007). "Biofouling of reverse osmosis membranes: Role of biofilm-enhanced osmotic pressure." Journal of Membrane Science **295**(1–2): 11-20.

Hogg, R., T. W. Healy and D. W. Fuerstenau (1966). "Mutual coagulation of colloidal dispersions." Transactions of the Faraday Society **62**(0): 1638-1651.

Hong, S. and M. Elimelech (1997). "Chemical and physical aspects of natural organic matter (NOM) fouling of nanofiltration membranes." Journal of Membrane Science **132**(2): 159-181.

Jin, X., X. Huang and E. M. Hoek (2009). "Role of specific ion interactions in seawater RO membrane fouling by alginic acid." Environmental science & technology **43**(10): 3580-3587.

José Juan, B.-A., M. Gleyci Aparecida Oliveira and S.-C. Marisa Prado (2012). "Role of Transparent Exopolymer Particles on Phytoplankton Dynamics in a Subtropical Estuary, Cananéia-Iguape (SP, Brazil)." Open Journal of Marine Science **2012**.

Kanani, D. M., X. Sun and R. Ghosh (2008). "Reversible and irreversible membrane fouling during in-line microfiltration of concentrated protein solutions." Journal of Membrane Science **315**(1–2): 1-10.

Katsoufidou, K., S. G. Yiantsios and A. J. Karabelas (2007). "Experimental study of ultrafiltration membrane fouling by sodium alginate and flux recovery by backwashing." Journal of Membrane Science **300**(1–2): 137-146.

Katsoufidou, K. S., D. C. Sioutopoulos, S. G. Yiantsios and A. J. Karabelas (2010). "UF membrane fouling by mixtures of humic acids and sodium alginate: Fouling mechanisms and reversibility." Desalination **264**(3): 220-227.

Kiørboe, T., L. Claus, O. Michael and J. L. S. Hansen (1994). "Aggregation and sedimentation processes during a spring phytoplankton bloom: A field experiment to test coagulation theory." Journal of Marine Research **52**(2): 297-323.

Kiørboe, T. and J. L. S. Hansen (1993). "Phytoplankton aggregate formation: observations of patterns and mechanisms of cell sticking and the significance of exopolymeric material." Journal of Plankton Research **15**(9): 993-1018.

Kim, A. S., H. Chen and R. Yuan (2006). "EPS biofouling in membrane filtration: An analytic modeling study." Journal of Colloid and Interface Science **303**(1): 243-249.

Kim, H.-J., A. J. Miller, J. McGowan and M. L. Carter (2009). "Coastal

phytoplankton blooms in the Southern California Bight." Progress in Oceanography **82**(2): 137-147.

Kimura, K., I. Tanaka, S.-I. Nishimura, R. Miyoshi, T. Miyoshi and Y. Watanabe (2012). "Further examination of polysaccharides causing membrane fouling in membrane bioreactors (MBRs): Application of lectin affinity chromatography and MALDI-TOF/MS." Water Research **46**(17): 5725-5734.

Klein, C., P. Claquin, A. Pannard, C. Napoléon, B. Le Roy and B. Véron (2011). "Dynamics of soluble extracellular polymeric substances and transparent exopolymer particle pools in coastal ecosystems." Marine Ecology Progress Series **427**: 13-27.

Komlenic, R. (2010). "Rethinking the causes of membrane biofouling." Filtration & Separation **47**(5): 26-28.

Koros, W. J., Y. H. Ma and T. Shimidzu (1996). "Terminology for membranes and membrane processes (IUPAC Recommendations 1996)." Journal of Membrane Science **120**(2): 149-159.

Leal, D., B. Matsuhiro, M. Rossi and F. Caruso (2008). "FT-IR spectra of alginic acid block fractions in three species of brown seaweeds." Carbohydrate Research **343**(2): 308-316.

Lee, J., W.-Y. Ahn and C.-H. Lee (2001). "Comparison of the filtration characteristics between attached and suspended growth microorganisms in submerged membrane bioreactor." Water Research **35**(10): 2435-2445.

Lee, K. Y. and D. J. Mooney (2012). "Alginate: properties and biomedical applications." Prog Polym Sci **37**(1): 106-126.

Lee, K. Y. and D. J. Mooney (2012). "Alginate: properties and biomedical applications." Progress in Polymer Science **37**(1): 106-126.

Lee, S. and M. Elimelech (2006). "Relating Organic Fouling of Reverse Osmosis

Membranes to Intermolecular Adhesion Forces." Environmental Science & Technology **40**(3): 980-987.

Leppard, G. G., A. Massalski and D. R. S. Lean (1977). "Electron-opaque microscopic fibrils in lakes: Their demonstration, their biological derivation and their potential significance in the redistribution of cations." Protoplasma **92**(3-4): 289-309.

Li, H., Y. Lin, P. Yu, Y. Luo and L. Hou (2011). "FTIR study of fatty acid fouling of reverse osmosis membranes: Effects of pH, ionic strength, calcium, magnesium and temperature." Separation and Purification Technology **77**(1): 171-178.

Li, Q., Z. Xu and I. Pinnau (2007). "Fouling of reverse osmosis membranes by biopolymers in wastewater secondary effluent: Role of membrane surface properties and initial permeate flux." Journal of Membrane Science **290**(1–2): 173-181.

Lin, H. J., K. Xie, B. Mahendran, D. M. Bagley, K. T. Leung, S. N. Liss and B. Q. Liao (2009). "Sludge properties and their effects on membrane fouling in submerged anaerobic membrane bioreactors (SAnMBRs)." Water Research **43**(15): 3827-3837.

Lin, Y., M. de Kreuk, M. C. van Loosdrecht and A. Adin (2010). "Characterization of alginate-like exopolysaccharides isolated from aerobic granular sludge in pilot-plant." Water Res **44**(11): 3355-3364.

Listiarini, K., W. Chun, D. D. Sun and J. O. Leckie (2009). "Fouling mechanism and resistance analyses of systems containing sodium alginate, calcium, alum and their combination in dead-end fouling of nanofiltration membranes." Journal of Membrane Science **344**(1–2): 244-251.

Liu, Y.-J. and D. D. Sun (2012). "Particles size-associated membrane fouling in microfiltration of denitrifying granules supernatant." Chemical Engineering Journal **181-182**: 494-500.

Liu, Y. and Z.-W. Wang (2008). "Uncertainty of preset-order kinetic equations in description of biosorption data." Bioresource Technology **99**(8): 3309-3312.

Logan, B. E., H. P. Grossart and M. Simon (1994). "Direct observation of phytoplankton, TEP and aggregates on polycarbonate filters using brightfield microscopy." Journal of Plankton Research **16**(12): 1811-1815.

Long, R. A. and F. Azam (1996). "Abundant protein-containing particles in the sea." Aquatic Microbial Ecology **10**: 213.

M. Greiveldinger and M. Shanahan (1999). "A Critique of the Mathematical Coherence of Acid/Base Interfacial Free Energy Theory." Journal of Colloid and Interface Science **215**(1): 170-178.

Mallevialle, J., P. E. Odendaal and M. R. Wiesner (1996). Water treatment membrane processes, American Water Works Association.

Mari, X. and T. Kiørboe (1996). "Abundance, size distribution and bacterial colonization of transparent exopolymeric particles (TEP) during spring in the Kattegat." Journal of Plankton Research **18**(6): 969-986.

Meng, F., F. Yang, B. Shi and H. Zhang (2008). "A comprehensive study on membrane fouling in submerged membrane bioreactors operated under different aeration intensities." Separation and Purification Technology **59**(1): 91-100.

Meng, S. and Y. Liu (2013). "Alginate block fractions and their effects on membrane fouling." Water Research **47**(17): 6618-6627.

Meng, S., M. Rzechowicz, H. Winters, A. Fane and Y. Liu (2013). "Transparent exopolymer particles (TEP) and their potential effect on membrane biofouling." Applied Microbiology and Biotechnology **97**(13): 5705-5710.

Meng, S., M. Rzechowicz, H. Winters, A. G. Fane and Y. Liu (2013). "Transparent exopolymer particles (TEP) and their potential effect on membrane biofouling." Applied Microbiology and Biotechnology **97**(13): 5705-5710.

Mi, B. and M. Elimelech (2010). "Organic fouling of forward osmosis membranes: Fouling reversibility and cleaning without chemical reagents." Journal of Membrane Science **348**(1–2): 337-345.

Montgomery, D. C. and G. C. Runger (2003). Applied statistics and probability for engineers, John Wiley & Sons.

Mopper, K., K. S. Ramana and D. T. Drapeau (1995). "The role of surface-active carbohydrates in the flocculation of a diatom bloom in a mesocosm." Deep Sea Research Part II: Topical Studies in Oceanography **42**(1): 47-73.

Oss, C. J. and R. J. Good (1988). "Orientation of the water molecules of hydration of human serum albumin." Journal of Protein Chemistry **7**(2): 179-183.

Oss, C. J., R. J. Good and M. K. Chaudhury (1986). "Solubility of proteins." Journal of Protein Chemistry **5**(6): 385-405.

Ouwerx, C., N. Velings, M. M. Mestdagh and M. A. V. Axelos (1998). "Physico-chemical properties and rheology of alginate gel beads formed with various divalent cations." Polymer Gels and Networks **6**(5): 393-408.

Paerl, H. W. (1988). "Nuisance phytoplankton blooms in coastal, estuarine, and inland waters1." Limnology and Oceanography **33**(4part2): 823-843.

Parker, B. C. and A. G. Diboll (1966). "Alcian stains for histochemical localization of acid and sulfated polysaccharides in algae." Phycologia **6**(1): 37-46.

Passow, U. (2000). "Formation of Transparent Exopolymer Particles, TEP, from dissolved precursor material." Marine ecology-progress series **192**: 1-11.

Passow, U. (2002). "Transparent exopolymer particles (TEP) in aquatic environments." Progress in Oceanography **55**(3–4): 287-333.

Passow, U. and A. L. Alldredge (1994). "Distribution, size and bacterial colonization of transparent exopolymer particles (TEP) in the ocean." Marine ecology progress series **113**(1-2): 185-198.

Passow, U. and A. L. Alldredge (1995). "Aggregation of a diatom bloom in a mesocosm: The role of transparent exopolymer particles (TEP)." Deep Sea Research Part II: Topical Studies in Oceanography **42**(1): 99-109.

Passow, U. and A. L. Alldredge (1995). "A Dye-Binding Assay for the Spectrophotometric Measurement of Transparent Exopolymer Particles (TEP)." Limnology and Oceanography **40**(7): 1326-1335.

Peeva, P. D., A. E. Palupi and M. Ulbricht (2011). "Ultrafiltration of humic acid solutions through unmodified and surface functionalized low-fouling polyethersulfone membranes – Effects of feed properties, molecular weight cut-off and membrane chemistry on fouling behavior and cleanability." Separation and Purification Technology **81**(2): 124-133.

Peinemann, K. V. and S. P. Nunes (2010). Membranes for water treatment., Weinheim : Wiley-VCH ; [Chichester : John Wiley, distributor], c2010.

Pendarvis, R. (1998). "Essentials of Carbohydrate Chemistry by John F. Robyt." The Chemical Educator **3**(5): 1-2.

Qin, Y. (2004). "Gel swelling properties of alginate fibers." Journal of Applied Polymer Science **91**(3): 1641-1645.

Rabalais, N. N., R. E. Turner, R. J. Díaz and D. Justić (2009). "Global change and eutrophication of coastal waters." ICES Journal of Marine Science: Journal du Conseil **66**(7): 1528-1537.

Radmacher, M. (2002). "Measuring the Elastic Properties of Living Cells by the Atomic Force Microscope." Methods in Cell Biology **68**: 67-90.

Ramaiah, N. and K. Furuya (2002). "Seasonal variations in phytoplankton composition and transparent exopolymer particles in a eutrophicated coastal environment." Aquatic microbial ecology **30**(1): 69-82.

Ramus, J. (1977). "Alcian blue: A quantitative aequeous assay for algal acid and sulfated polysaccharides." Journal of Phycology **13**(4): 345-348.

Riemann, L., G. F. Steward and F. Azam (2000). "Dynamics of bacterial community composition and activity during a mesocosm diatom bloom." Applied and Environmental Microbiology **66**(2): 578-587.

Saha, N. K., M. Balakrishnan and M. Ulbricht (2007). "Sugarcane juice ultrafiltration: FTIR and SEM analysis of polysaccharide fouling." Journal of Membrane Science **306**(1–2): 287-297.

Sarma, V., S. Gupta, P. Babu, T. Acharya, N. Harikrishnachari, K. Vishnuvardhan, N. Rao, N. Reddy, V. Sarma and Y. Sadhuram (2009). "Influence of river discharge on plankton metabolic rates in the tropical monsoon driven Godavari estuary, India." Estuarine, Coastal and Shelf Science **85**(4): 515-524.

Schäfer, A. I., A. G. Fane and T. D. Waite (2005). Nanofiltration : principles and applications, Oxford ; New York : Elsevier Advanced Technology, c2005.

Schippers, J. C., G. L. Amy, M. D. Kennedy and L. O. Villacorte (2009). "Measuring transparent exopolymer particles (TEP) as indicator of the (bio)fouling potential of RO feed water." Desalination and Water Treatment: 207-212.

Schuster, S. and G. J. Herndl (1995). "Formation and significance of transparent exopolymeric particles in the northern Adriatic Sea." Marine ecology progress series. Oldendorf **124**(1): 227-236.

Scott, J. E. (1973). "Alcian dyes: I.C.I. cease manufacture and release details of composition." Histochemie **37**(4): 379-380.

Seidel, A. and M. Elimelech (2002). "Coupling between chemical and physical interactions in natural organic matter (NOM) fouling of nanofiltration membranes: implications for fouling control." Journal of Membrane Science **203**(1–2): 245-255.

Shannon, M. A., P. W. Bohn, M. Elimelech, J. G. Georgiadis, B. J. Marinas and A. M. Mayes (2008). "Science and technology for water purification in the

coming decades." Nature **452**(7185): 301-310.

Simpson, N. E., C. L. Stabler, C. P. Simpson, A. Sambanis and I. Constantinidis (2004). "The role of the CaCl2–guluronic acid interaction on alginate encapsulated βTC3 cells." Biomaterials **25**(13): 2603-2610.

Sintes, E., K. Stoderegger, V. Parada and G. J. Herndl (2010). "Seasonal dynamics of dissolved organic matter and microbial activity in the coastal North Sea." Aquatic Microbial Ecology **60**(1): 85.

Sioutopoulos, D. C., T. B. Goudoulas, E. G. Kastrinakis, S. G. Nychas and A. J. Karabelas (2013). "Rheological and permeability characteristics of alginate fouling layers developing on reverse osmosis membranes during desalination." Journal of Membrane Science **434**: 74-84.

Smidsrød, O. (1974). "Molecular basis for some physical properties of alginates in the gel state." Faraday Discussions of the Chemical Society **57**: 263.

Smidsrød, O. and K. Draget (1996). "Chemistry and physical properties of alginates." carbohydrate Europe **14**: 6-13.

Smidsrød, O. and G. Skja˚k-Br˛k (1990). "Alginate as immobilization matrix for cells." Trends in Biotechnology **8**(0): 71-78.

Steyermark, A. (1976). "Spectrometric identification of organic compounds. Third edition: By Robert M. Silverstein, G. Clayton Bassler, and Terence C. Morrill. Wiley, New York, 1974. 340 pp. $13.95." Microchemical Journal **21**(4): 496.

Susanto, H., H. Arafat, E. M. L. Janssen and M. Ulbricht (2008). "Ultrafiltration of polysaccharide–protein mixtures: Elucidation of fouling mechanisms and fouling control by membrane surface modification." Separation and Purification Technology **63**(3): 558-565.

Sweity, A., W. Ying, M. S. Ali-Shtayeh, F. Yang, A. Bick, G. Oron and M. Herzberg (2011). "Relation between EPS adherence, viscoelastic properties, and MBR

operation: Biofouling study with QCM-D." Water Research **45**(19): 6430-6440.

Synytsya, A., W.-J. Kim, S.-M. Kim, R. Pohl, A. Synytsya, F. Kvasnička, J. Čopíková and Y. I. Park (2010). "Structure and antitumour activity of fucoidan isolated from sporophyll of Korean brown seaweed Undaria pinnatifida." Carbohydrate Polymers **81**(1): 41-48.

Tønnesen, H. H. and J. Karlsen (2002). "Alginate in Drug Delivery Systems." Drug Development and Industrial Pharmacy **28**(6): 621-630.

Taimur Khan, M. M., S. Takizawa, Z. Lewandowski, M. Habibur Rahman, K. Komatsu, S. E. Nelson, F. Kurisu, A. K. Camper, H. Katayama and S. Ohgaki (2013). "Combined effects of EPS and HRT enhanced biofouling on a submerged and hybrid PAC-MF membrane bioreactor." Water Research **47**(2): 747-757.

Tang, C. Y., Y.-N. Kwon and J. O. Leckie (2007). "Fouling of reverse osmosis and nanofiltration membranes by humic acid—Effects of solution composition and hydrodynamic conditions." Journal of Membrane Science **290**(1–2): 86-94.

Tansel, B., J. Sager, J. Garland, S. Xu, L. Levine and P. Bisbee (2006). "Deposition of extracellular polymeric substances (EPS) and microtopographical changes on membrane surfaces during intermittent filtration conditions." Journal of Membrane Science **285**(1–2): 225-231.

Tchobanoglous, G., F. L. Burton and H. D. Stensel (2003). Wastewater engineering : treatment and reuse, Boston : McGraw-Hill, c2003.4th ed. / revised by George Tchobanoglous, Franklin L. Burton, H. David Stensel.

Thornton, D. C. O., E. M. Fejes, S. F. DiMarco and K. M. Clancy (2007). "Measurement of acid polysaccharides in marine and freshwater samples using alcian blue." Limnology and Oceanography: Methods **5**(2): 73-87.

Ulbricht, M., W. Ansorge, I. Danielzik, M. König and O. Schuster (2009). "Fouling

in microfiltration of wine: The influence of the membrane polymer on adsorption of polyphenols and polysaccharides." Separation and Purification Technology **68**(3): 335-342.

Valladares Linares, R., V. Yangali-Quintanilla, Z. Li and G. Amy (2012). "NOM and TEP fouling of a forward osmosis (FO) membrane: Foulant identification and cleaning." Journal of Membrane Science(0).

van de Lisdonk, C. A. C., J. A. M. van Paassen and J. C. Schippers (2000). "Monitoring scaling in nanofiltration and reverse osmosis membrane systems." Desalination **132**(1–3): 101-108.

van de Ven, W. J. C., K. v. t. Sant, I. G. M. Pünt, A. Zwijnenburg, A. J. B. Kemperman, W. G. J. van der Meer and M. Wessling (2008). "Hollow fiber dead-end ultrafiltration: Influence of ionic environment on filtration of alginates." Journal of Membrane Science **308**(1–2): 218-229.

van den Brink, P., A. Zwijnenburg, G. Smith, H. Temmink and M. van Loosdrecht (2009). "Effect of free calcium concentration and ionic strength on alginate fouling in cross-flow membrane filtration." Journal of Membrane Science **345**(1–2): 207-216.

Van Nevel, S., T. Hennebel, K. De Beuf, G. Du Laing, W. Verstraete and N. Boon (2012). "Transparent exopolymer particle removal in different drinking water production centers." Water Research **46**(11): 3603-3611.

van Oss, C. J. (1993). "Acid—base interfacial interactions in aqueous media." Colloids and Surfaces A: Physicochemical and Engineering Aspects **78**(0): 1-49.

Van Oss, C. J. (2006). Interfacial forces in aqueous media Boca Raton, Fla. : Taylor & Francis, 2006. 2nd ed.

Verdugo, P., A. L. Alldredge, F. Azam, D. L. Kirchman, U. Passow and P. H. Santschi (2004). "The oceanic gel phase: a bridge in the DOM–POM continuum." Marine Chemistry **92**(1–4): 67-85.

Verdugo, P. and P. H. Santschi (2010). "Polymer dynamics of DOC networks and gel formation in seawater." Deep Sea Research Part II: Topical Studies in Oceanography **57**(16): 1486-1493.

Villacorte, L. O., Y. Ekowati, H. N. Calix-Ponce, J. C. Schippers, G. L. Amy and M. D. Kennedy (2015). "Improved method for measuring transparent exopolymer particles (TEP) and their precursors in fresh and saline water." Water Research **70**(0): 300-312.

Villacorte, L. O., M. D. Kennedy, G. L. Amy and J. C. Schippers (2009). "The fate of Transparent Exopolymer Particles (TEP) in integrated membrane systems: Removal through pre-treatment processes and deposition on reverse osmosis membranes." Water Research **43**(20): 5039-5052.

Villacorte, L. O., M. D. Kennedy, G. L. Amy and J. C. Schippers (2009). "Measuring transparent exopolymer particles (TEP) as indicator of the (bio)fouling potential of RO feed water." Desalination and Water Treatment **5**(1-3): 207-212.

Villacorte, L. O., R. Schurer, M. D. Kennedy, G. L. Amy and J. C. Schippers (2010). "The fate of transparent exopolymer particles (TEP) in seawater UF-RO system: A pilot plant study in Zeeland, The Netherlands." Desalination and Water Treatment **13**(1-3): 109-119.

Villacorte, L. O., R. Schurer, M. D. Kennedy, G. L. Amy and J. C. Schippers (2010). "Removal and Deposition of Transparent Exopolymer Particles in a Seawater UF-RO System." IDA Journal of Desalination and Water Reuse **2**(1): 45-55.

Vold, I. M. N., K. A. Kristiansen and B. E. Christensen (2006). "A Study of the Chain Stiffness and Extension of Alginates, in Vitro Epimerized Alginates, and Periodate-Oxidized Alginates Using Size-Exclusion Chromatography Combined with Light Scattering and Viscosity Detectors." Biomacromolecules **7**(7): 2136-2146.

Wachinski, A. M. (2013). Membrane processes for water reuse, New York, NY : McGraw-Hill, [2013].

Watanabe, Y. and K. Kimura (2011). 4.02 - Membrane Filtration in Water and Wastewater Treatment. Treatise on Water Science. P. Wilderer. Oxford, Elsevier**:** 23-61.

Wei, C.-H., S. Laborie, R. Ben Aim and G. Amy (2012). "Full utilization of silt density index (SDI) measurements for seawater pre-treatment." Journal of Membrane Science **405–406**(0): 212-218.

Wells, M. L. and E. D. Goldberg (1993). "Colloid aggregation in seawater." Marine Chemistry **41**(4): 353-358.

Whiteman, P. (1973). "The quantitative determination of glycosaminoglycans in urine with Alcian Blue 8GX." Biochem. J **131**: 351-357.

Wurl, O. and M. Holmes (2008). "The gelatinous nature of the sea-surface microlayer." Marine Chemistry **110**(1): 89-97.

Xu, H. and Y. Liu (2011). "Control and cleaning of membrane biofouling by energy uncoupling and cellular communication." Environmental Science and Technology **45**(2): 595-601.

Yao, M., K. Zhang and L. Cui (2010). "Characterization of protein–polysaccharide ratios on membrane fouling." Desalination **259**(1–3): 11-16.

Zhang, W., Z. Zhu, M. Y. Jaffrin and L. Ding (2014). "Effects of Hydraulic Conditions on Effluent Quality, Flux Behavior, and Energy Consumption in a Shear-Enhanced Membrane Filtration Using Box-Behnken Response Surface Methodology." Industrial & Engineering Chemistry Research **53**(17): 7176-7185.